Investigation of Three Integrated Energy Systems with Desalination, Heat Storage, Thermochemical Cycles and Heat Upgrade

by

Yarkin Gevez

A thesis submitted to the
School of Graduate and Postdoctoral Studies in partial
fulfillment of the requirements for the degree of

Master of Applied Science in Mechanical Engineering

Faculty of Engineering and Applied Science

University of Ontario Institute of Technology (Ontario Tech University)

Oshawa, Ontario, Canada

September 2020

THESIS EXAMINATION INFORMATION

Submitted by: **Yarkin Gevez**

Master of Applied Science in Mechanical Engineering

Thesis title: Investigation of Three Integrated Energy Systems with Desalination, Heat Storage, Thermochemical Cycles and Heat Upgrade

An oral defense of this thesis study took place on 13 August, 2020 in front of the following examining committee:

Examining Committee:

Chair of Examining Committee	Prof. Dr. Martin Agelin-Chaab
Research Supervisor	Prof. Dr. Ibrahim Dincer
Examining Committee Member	Prof. Dr. Bekir Sami Yilbas
Examining Committee Member	Dr. Sayyed Ali Hosseini
Thesis Examiner	Dr. Ahmad Barari, FEAS - AMME

The above committee determined that the thesis is acceptable in form and content and that a satisfactory knowledge of the field covered by the thesis was demonstrated by the candidate during an oral examination. A signed copy of the Certificate of Approval is available from the School of Graduate and Postdoctoral Studies.

ABSTRACT

This thesis study proposes three different novel renewable energy-based multigeneration integrated systems with molten salt heat storage and desalination options where copper-chlorine (Cu-Cl) and magnesium-chlorine (Mg-Cl) thermochemical water-splitting cycles for hydrogen production are used. System 1 integrates the wind, solar and geothermal energies with high-temperature electrolysis, methanol synthesis and multi-effect desalination. Systems 2 and 3 have two variants such that the first variant considers integration of solar and geothermal-energies with multi-effect desalination and thermochemical hydrogen production through Cu-Cl and Mg-Cl cycles respectively. The second variant of systems 2 and 3 replaces the solar thermal energy with mercury-based heat pump system to provide the required heat for the respective thermochemical cycles. Systems are presented and analyzed thermodynamically through energy and exergy approaches to be compared with each other in terms of their energy and exergy efficiencies. A series of parametric studies have been conducted for all the systems in order to see the effects of different operating conditions on energy and exergy efficiencies and system outputs. Five case studies have been performed by considering Vancouver, Canada to produce five useful outputs to meet the needs of a community. These commodities are electricity, freshwater, space heating, hot water, hydrogen and methanol (only for the first system). According to thermodynamic analysis, the second variant of system 3 is capable of achieving an overall energy efficiency of 49.58% and an overall exergy efficiency of 59.23% for the system which uses heat upgrading options from geothermal energy to meet the high-temperature requirement of the thermochemical Mg-Cl cycle chosen as a hydrogen production method at 25 °C ambient temperature and 101 kPa ambient pressure. At the same time, the second variant of system 3 has 47012 kW exergy destruction rate which is the lowest one when compared to other evaluated systems.

Keywords: solar energy; desalination; geothermal energy; heat upgrade; heat storage; efficiency

AUTHOR'S DECLARATION

I hereby declare that this thesis study consists of original work of which I have authored. This is a true copy of the thesis, including any required final revisions, as accepted by my examiners.

I authorize the University of Ontario Institute of Technology (Ontario Tech University) to lend this thesis study to other institutions or individuals for the purpose of scholarly research. I further authorize University of Ontario Institute of Technology (Ontario Tech University) to reproduce this thesis study by photocopying or by other means, in total or in part, at the request of other institutions or individuals for the purpose of scholarly research. I understand that my thesis will be made electronically available to the public.

Yarkin Gevez

STATEMENT OF CONTRIBUTIONS

Part of the work described as System 1 will be published as:

Y. Gevez, I. Dincer, (Under Review) “The Development and Performance Assessment of An Integrated System with Desalination and Heat Storage Options”, International Journal of Energy Storage

Part of the work described as System 2 Version 1 will be published as:

Y. Gevez, I. Dincer, (Under Review) “Development and Investigation of An Integrated System with Cu-Cl Thermochemical Cycle and Desalination Options”, Journal of Desalination

ACKNOWLEDGEMENTS

I am so grateful to my supervisor Prof. Dr. Ibrahim Dincer who has always been guiding and supporting me in every sense of life besides being an excellent guide academically. I cannot express my appreciation for giving me the opportunity to study and work in this area.

I cannot pass the importance of the friendships and academic supports of all my colleagues in CERL and ACE 3030B. At the very beginning, I would like to thanks Mert Temiz who I have spent the most important part of my time together not only as a colleague but also as a brother, supporter and confidant.

Special thanks to Mehmet Ozkan who has the most important contribution to my career journey, and his precious family who always made me feel their support in every sense.

I would like to thank Atakan Onderoglu, Cagla Yilmaz and Ece Tavukcu to always made me feel their presence and supports, even if they are so far from me.

I feel fortunate to had Eren Dincer, Johannes Posch, Marcus Elbert, Sandra Aviles, Karla Carillo and Laura Rivera who are accompanying me in all wonderful stories in this journey and leaving unforgettable traces and moments in my life.

Special thanks to Unlu Dogan who has always given me significant insights about life, makes me always feel his support behind me and is now one of my family.

Last but not least, I would like to send my deepest and sincere gratitude to my mother Inci Gevez and my father Aslan Saim Gevez who are supporting me in every part of my life unconditionally and do not refrain their devotion and effort on me.

TABLE OF CONTENTS

LIST OF TABLES

LIST OF FIGURES

NOMENCLATURE

Comp	compressor
COP	coefficient of performance
C_p	power coefficient of the windmill
ex	specific exergy (kJ/kg)
$\dot{E}x$	exergy rate (kW)
F	Faraday constant (C/mol)
h	specific enthalpy (kJ/kg)
I	solar irradiation intensity (W/m^2)
HHV	higher heating value (kJ/kg)
LHV	lower heating value (kJ/kg)
m	mass (kg)
$\dot{m}$	mass flow rate (kg/s)
P	pressure (kPa)
Q	heat transfer (kJ)
$\dot{Q}$	heat rate (kW)
R	gas constant (kJ/kmol K)
s	specific entropy (kJ/kg K)
S	area (m^2)
$\dot{S}$	entropy rate (kW/K)
T	temperature (°C)
V	speed (m/s)
$\dot{W}$	power generation rate (kW)

Greek letters

η	efficiency
Δ	difference

ϕ	latitude
ρ	wind density

Subscripts

aq	aqueous
br	brine
c	compressor
chem	chemical
com	community
comp	compressor
cv	control volume
d, dest	destruction
distwater	distillated water
e	exit
en	energy, energetic
eva	evaporator
ex	exergy
f	fresh
g	gaseous
gen	generation
geot	geothermal
hf	heliostat field
i	inlet
k	k^{th}
kin	kinetic
l	liquid
mech	mechanical
out	outlet

P	pump
rec	received
s	solid
sys	system
turb	turbine
w	water
windt	wind tower

Acronyms

ORC	organic Rankine cycle
PEM	proton exchange membrane
CERL	Clean Energy Research Laboratory
CH_3OH	methanol
CHP	combined heat power
Cu Cl	cuprous chloride
Cu-Cl	copper chlorine
EES	Engineering Equation Solver
Fe-Cl	iron chlorine
H_2	hydrogen
H_2O	water
HCl	hydrochloric acid
Hg	mercury
HRSG	heat recovery steam generator
HTE	high temperature electrolyser
HX	heat exchanger
IGCC	integrated gasification combined cycle
Li	lithium

MED	multi-effect desalination
MC	mixing chamber
Mg-Cl	magnesium chlorine
MS	molten salt
OECD	Organisation for Economic Co-operation and Development
ORC	organic Rankine cycle
O_2	oxygen
PEM	proton exchange membrane
PV	photovoltaic
SOFC	solid oxide fuel cell

Superscripts

o	reference

Chapter 1 INTRODUCTION

1.1 Renewable Energy and Sustainable Development

Global warming and the elimination of the factors causing it has been the main aim for studies on renewable energy resources. Major environmental problems such as fossil fuel depletion, increase in air pollution and rise in the average global temperature are caused as the global energy demand is increasing [1]. The continuous exploitation of fossil fuels that make up the majority of the world's energy sources cause a reduction of oxygen content in the air and promotes the formation of greenhouse gases (GHG) which largely contribute towards global warming [2]. Studies on clean and green methods of energy production possess key significance in the new and developing world. However, the interminttant avaibility of the renewable energy sources such as solar and wind energies is a major challenge in achieving higher efficiencies in various energy systems.

The integration of the sources with the other promising renewable methods such as geothermal with its major utilization in heating, desalination and cooling is possible with the high-efficiency levels it brings [3]. A second key term which is sustainability appears in the integration and operation of these systems. The sustainable concept plays an important role in the reconsideration of traditional methods in the context of politics, economics and technology [1]. There are certain conditions in which the energy obtained can be sustained as a result of achieving sustainable development. One of the most essential requirements of sustainable development is the achievement of rich sustainable energy in terms of quantity and quality. As an inherent requirement of sustainable development, it is considered that the new green methods and sources are intended to replace the conventional ones such as natural gas, coal, gasoline and so on [4]. Sustainability adopts the optimum methods to prevent the energy needs of the future generations to be negatively affected, in addition to preventing the current energy to be met. This optimum point should be low cost as well as the location where the damage to nature and society will be minimized. Solar energy, which is a significant thermal energy source, could be considered as a prime candidate to achieve sustainibility. It emerges as the wind and waves indirect energy sources that are created due to the temperature and the pressure differences, the sun creates on the surface of the world. Hydrogen can be placed at the top of the sustainable energy resources with its high energy density, high efficiency and low environmental impact during production and use stages [5].

Energy production from renewable sources compared to the total energy use in Canada is 20% and is leading the world in this regard. Electricity generation by hydro energy sources is at the top with 60% share in Canada's renewable energy [6]. At the same time, this ratio makes it the world's third-largest producer in terms of hydroelectric power generation. Canada has implemented a program that is intended to reduce the GHG emissions by about 80% by 2050. The world's total energy production from renewable sources has exceeded 100,000 MW by 2015, which is about 20% of total energy production [7]. The share of total and renewable energy of Canada's use is represented in Figure 1.1. It is clear that the largest share among renewable energy sources is hydro energy. However, hydrogen which is a high energy carrier option should take its place in Canada's future green energy plans.

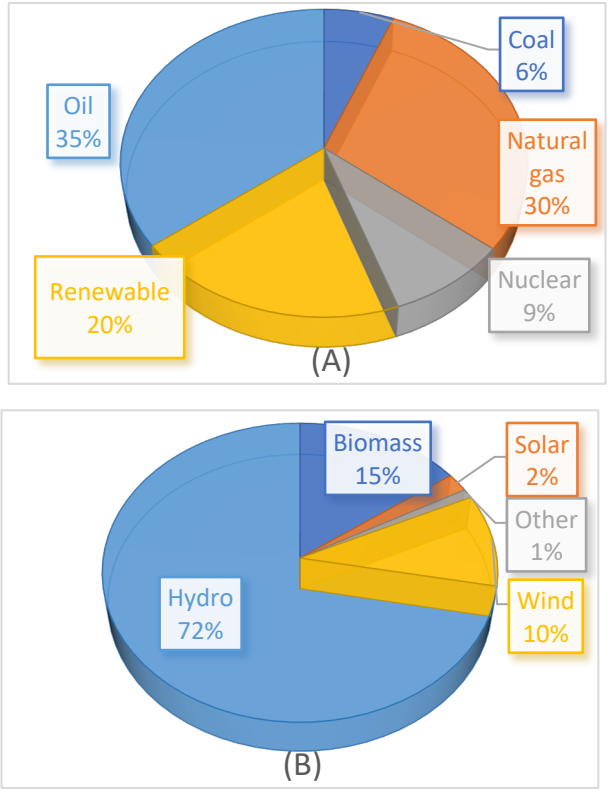

Figure 1.1 Total (A) and renewable (B) energy share of Canada (data from [7])

Hydrogen is an energy carrier that can be used to store, move, and deliver energy produced from other sources. Hydrogen can easily be converted to thermal energy by its combustion and electricity through utilizing fuel cells. The fact that it can easily be converted into electrical energy with minimum environmental impact provides the opportunity to be used in the transportation

sector. The most important reasons for being sustainable are the new hydrogen production and storage methods and the technology to allow cost reduction.

Another remarkable factor that makes hydrogen one of the most preferred fuels is its advantages in storage. For the seasonal energy sources that don't offer continuous production of renewable, hydrogen is a very efficient storage medium [8]. Stored hydrogen can be used at any time with fuel cell technologies. Hydrogen could have a significant place in production to meet the future nutritional needs of the exponentially increasing world population. For fertilizer production to be used in this area, the place of hydrogen will be important in the petrochemical industry [9].

The total amount of hydrogen globally produced per day is 50 million metric tons whereas that of oil is 4000 million metric tons. Approximately 95% of the daily hydrogen production meets the needs of the petrochemical industry. Based on the 2004-2013 data, the average hydrogen production and application rates can be seen in Figure 1.2 [10].

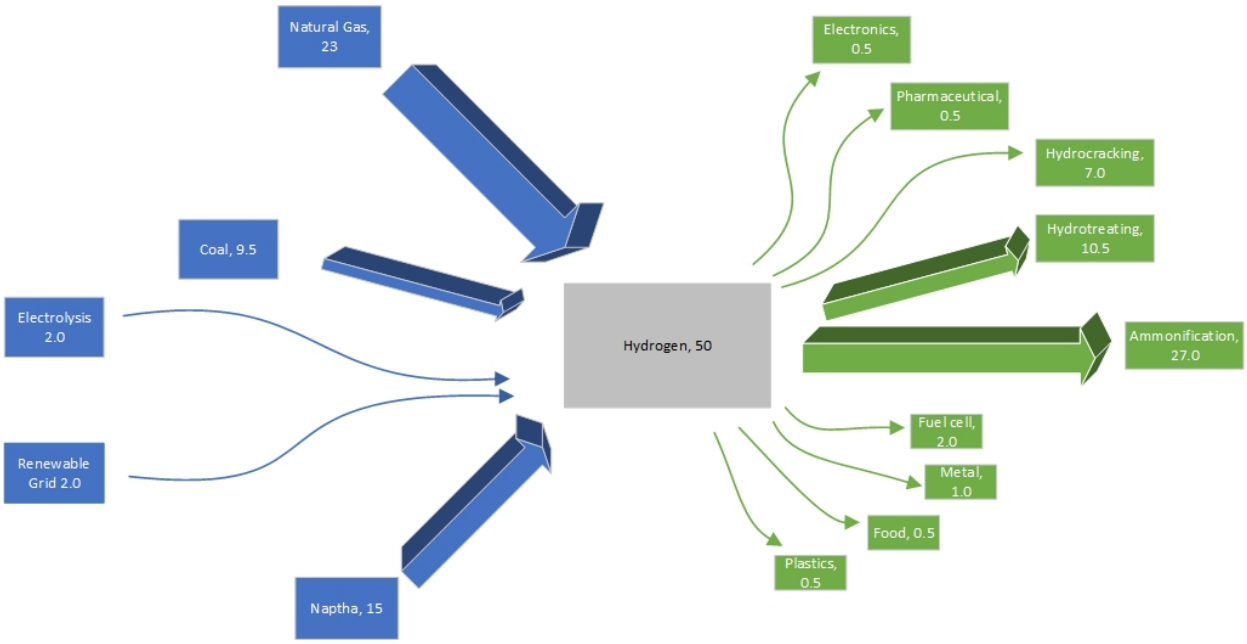

Figure 1.2 Average hydrogen production and application rates in million metric tons (data taken and modified from [10])

1.2 Hydrogen Production Methods

There are several hydrogen production methods based on various domestic sources such as nuclear power, biomass, renewable power and so on. These methods can be categorize into two groups as clean and green methods and conventional hydrocarbon-based methods. However, the only possible option for sustainable hydrogen production is renewable ones [11]. Green hydrogen production is possible with various solar-based hydrogen production methods. With photovoltaic cells, solar energy can be converted into electrical energy to be used for the electrolysis process. Steam or high-temperature electrolysis technology is more efficient and environmentally benign when compared with the photovoltaic method [12].

1.3 Renewable Production Methods

The use of renewable energy sources in the production of hydrogen gas is important in terms of creating sustainable processes and introducing environmentally friendly methods. The benefits include reductions in carbon and sulfur emissions [13]. It is observed that renewable energy sources have positive impacts compared to non-renewable ones when life cycle assessment is applied. Detailed schematic which shows the hydrogen production with renewable and green methods is illustrated in Figure 1.3. When compared with other production methods, thermochemical water-splitting process is the most environmentally friendly and economical method. Thermochemical processes can be defined as a heat-driven method in which various chemical reactions are used for hydrogen and oxygen production. Some thermochemical cycles are commercially appropriate due to economic, safety, financial factors such as copper-chlorine (Cu-Cl), magnesium-chlorine (Mg-Cl) and iron-chlorine (Fe-Cl) [14]. The Cu-Cl and the Mg-Cl cycles have lower thermal energy requirements (around 530 ℃) and lower maintenance costs which makes them attractive options for hydrogen production.

1.3.1 Copper-Chlorine (Cu-Cl) Thermochemical Cycle

Cu-Cl cycle is a method for hydrogen production which uses thermochemical water splitting. When compared with other thermochemical cycles, lower temperature requirements and lower maintenance costs make Cu-Cl cycle one of the most promising thermochemical water splitting methods. Heat recovery and waste heat use options for heat requirements of the cycle are possible [15].

The Cu-Cl hydrogen production cycles may consist of different components. The number of cycle steps vary between two and five. Orhan et al. studied the various configurations of Cu-Cl cycles on the basis of the number of cycle steps [16]. Apart from additional processes such as evaporation, dissolution and crystallization, there are three main reactions in the optimized thermochemical cycle. Table 1.1 shows the chemical reactions of each step of the four-step Cu-Cl cycle.

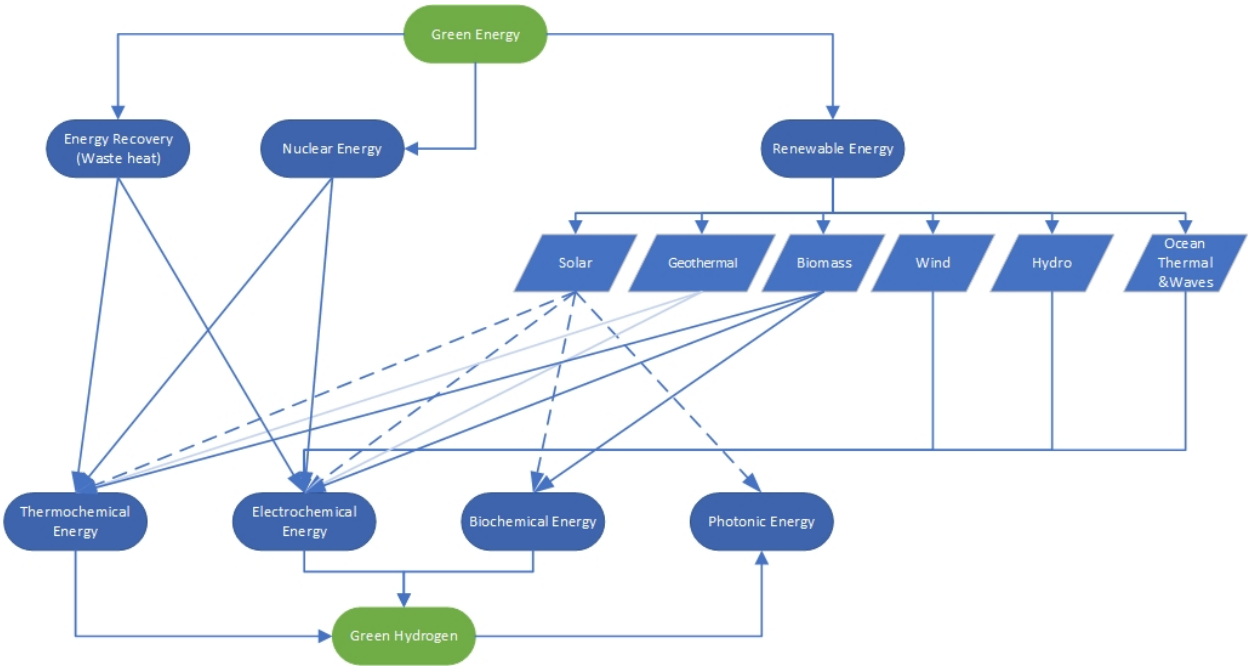

Figure 1.3 Schematic of various renewable methods for hydrogen production [1]

Table 1.1 Reactions of 4-step Cu-Cl cycle

Stage – Temperature	**Reaction**
Hydrolysis Reaction ≈ 400 °C	$2CuCl_2 + H_2O \leftrightarrow 2Cu_2OCl_2 + 2HCl$
Thermolysis Reaction ≈ 500 °C *(Oxygen Production)*	$Cu_2OCl_2 \leftrightarrow 2CuCl + \frac{1}{2}O_2$
Electrolysis Reaction < 100 °C *(Hydrogen Production)*	$2CuCl + 2HCl \leftrightarrow 2CuCl_2 + H_2$ $2Cu^+ \leftrightarrow 2Cu^{2+} + 2e^-$ $2H^+ + 2e^- \leftrightarrow H_2$
Drying Process < 400 °C	$CuCl_{2(aq)} \leftrightarrow \ CuCl_{2(s)}$

The most important factor in the Cu-Cl cycle is to provide the necessary thermal energy and to reach the required temperature level. The thermolysis process or otherwise called the "decomposition" step, is the process in which cuprous chloride (CuCl) and oxygen (O_2) are produced as a result of the thermal dissociation of copper-oxychloride (Cu_2OCl_2) during the most energy intensive step in all Cu-Cl configurations. Nuclear reactor temperatures can be used to meet this temperature level requirement.

1.3.2 Magnesium-Chlorine (Mg-Cl) Thermochemical Cycle

Mg-Cl cycle is a thermochemical process used to separate water into hydrogen and oxygen. In the separation process of the water into its components, a hybrid process consisting of electricity and heat is applied. There are two thermochemical steps of chlorination and hydrolysis, in a three-step Mg-Cl cycle. Likewise in the Cu-Cl cycle, waste heat recovery can be used to reach the required temperature levels of around 530 ℃ in the Mg-Cl cycle. This temperature level is required for the hydrolysis step where water and $MgCl_2$ reacts into HCl and MgO. Hydrogen is produced at the chlorination step as a result of the electrochemical decomposition of HCl. Table 1.2 shows the chemical reaction steps of the Mg-Cl cycle. Also, a detailed schematic of the cycle is shown in Figure 1.5.

Table 1.2 Reactions of 3-step Mg-Cl cycle

Stage – Temperature	**Reaction**
Hydrolysis Reaction ≈ *450-550* ℃	$MgCl_{2_{(s)}} + H_2O_{(g)} \leftrightarrow MgO_{(s)} + 2HCl_{(g)}$
Chlorination Reaction ≈ *450-500* ℃ *(Oxygen Production)*	$MgO_{(s)} + Cl_{2_{(g)}} \leftrightarrow MgCl_{2_{(s)}} + \frac{1}{2}O_{2(g)}$
Electrolysis Reaction < *100* ℃ *(Hydrogen Production)*	$2HCl_{(g)} \leftrightarrow Cl_{2_{(g)}} + H_{2_{(g)}}$

1.4 Motivation

Undoubtedly, most of these processes serve as alternates for the existing carbon-based fossil fuels that are considered as one of the main reasons of global warming, with renewable and green solutions. According to the results of the International Energy Agency's research in OECD countries, the percentage distribution in the use of energy sources has experienced a change from 1975 to 2015 as in Figure 1.6.

As a result of the various studies signifying the detrimental implications of the currently used fuels and the associated by-products such as GHGs like CO_2, CO, HC etc., there is a need to investigate new and environmentally benign fuels. At present, hydrogen is as a promising alternate fuel, due to its sustainability and suitability of being produced through green methods.

Hydrogen carries a solution value in this area with the availability of technologies that can easily be used in different fields, its ability to be easily converted into mechanical energy and high energy density per kilogram.

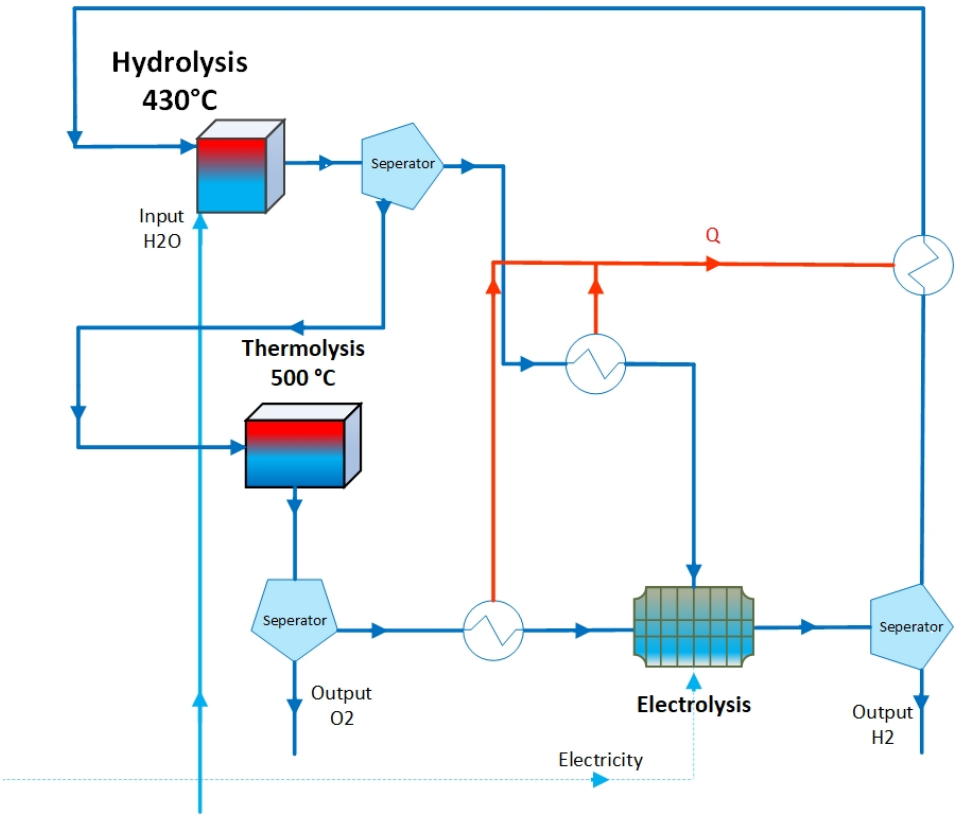

Figure 1.4 Schematic diagram of 4-step Cu-Cl cycle

A comparison of energy density per kilogram of hydrogen and other energy sources can be seen in Figure 1.7. Hydrogen can also be produced with many different renewable technologies. With the integrated use of renewable energy sources of hydrogen, the high-efficiency opportunity plays an important role in green energy production targets. The integration of renewable energy sources and the development of different working principals in various combinations for high efficiency is the main motivation for this study.

1.5 Objectives

This thesis study focuses primarily on developing production methods by integrating renewable sources. It is also among the objectives to create useful outputs that meet the basic needs of a community. The main aim of this thesis is to examine the feasibility of integrating sustainable hydrogen production methods such as the high-temperature electrolysis and thermochemical water-splitting processes with various other processes driven by renewable energy sources. These processes create a requirement for achieving high temperatures in the system. The thesis also has the aim of producing various solutions to meet these temperature needs and to compare them with each other.

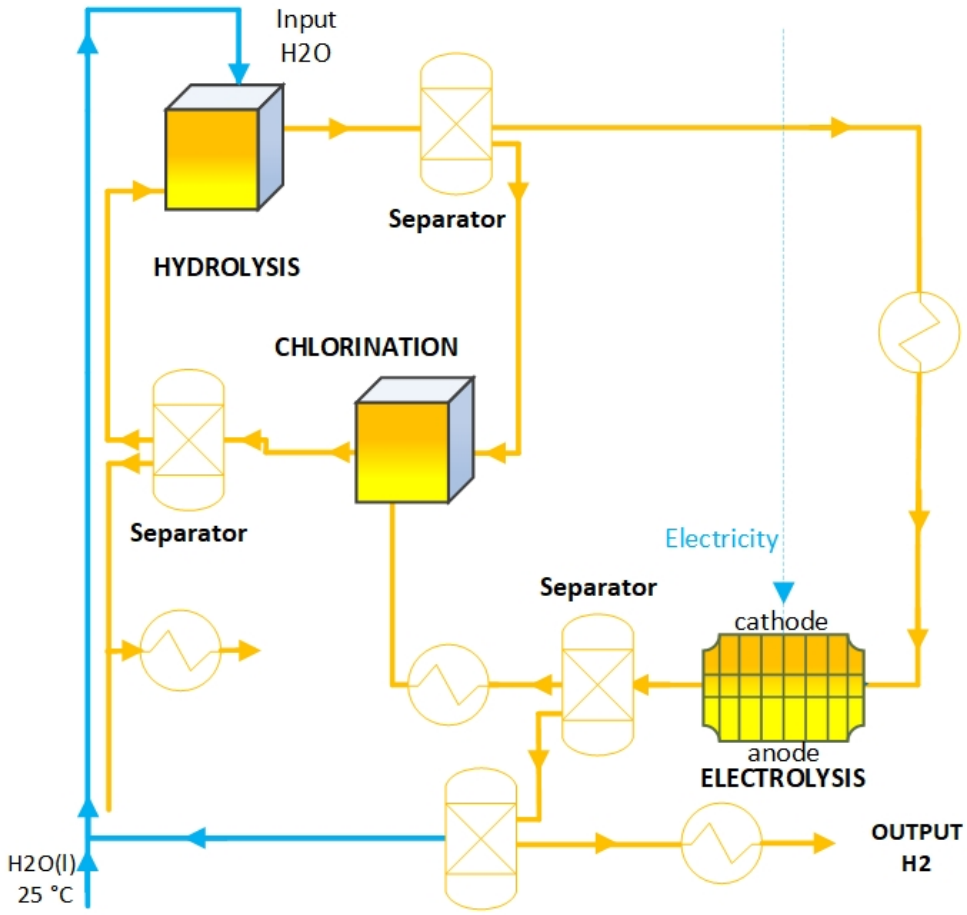

Figure 1.5 Schematic diagram of Mg-Cl cycle

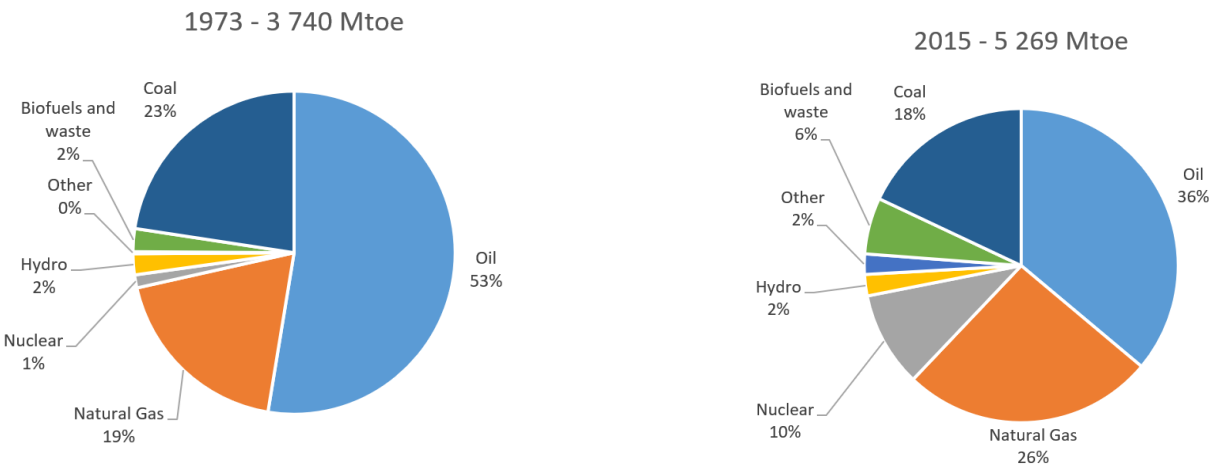

Figure 1.6 Total primary energy supply from 1973 to 2015 for OECD countries (data from [17])

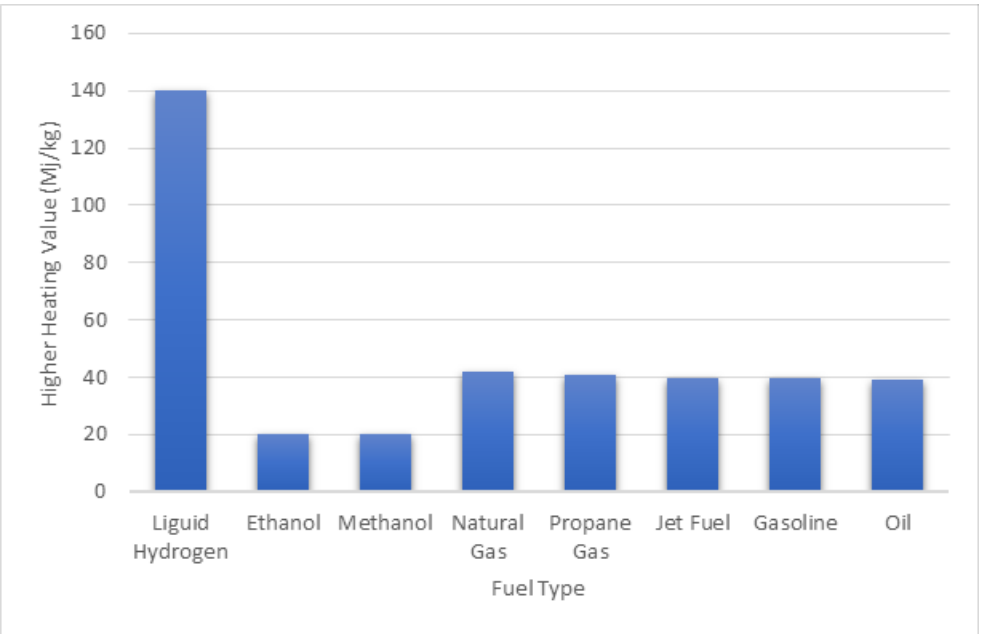

Figure 1.7 Energy densities for various energy sources (data from [18])

The methods of obtaining high-temperatures with solar energy and thermal energy storage have been investigated in this study. The cascaded Cu-Cl heat pump proposed by Zamfirescu et al. [17] is also studied and integrated into the system. In this way, the heat requirement of high-temperature electrolysis, thermolysis and hydrolysis stages of Cu-Cl and Mg-Cl thermochemical cycles is met. In addition, hydrogenation of carbon dioxide with hydrogen has been studied and the industrial released gases have been evaluated in the production of methanol.

The specific objectives of this thesis study are as follows:

- To develop and study three novel renewable energy-based integrated systems and two other versions of two of them with electricity, fresh-water, hot water, space heating, hydrogen or methanol commodities.
- To perform the thermodynamic analyses of presently developed systems through energy and exergy approaches.
- To integrate the solar power with geothermal and molten salt heat storage for the first versions of all three systems.
- To develop an efficient process for hydrogen production by benefiting from thermochemical cycles.
- To incorporate a high efficient heat pump configuration to the second versions of system 2 and system 3 to reach the required temperature levels in
- To assess the performance of the system using variations in operational and ambient conditions in addition to different energy sources and system configurations.
- To compare the systems with each other and adopting the most ideal working principle.

1.6 Thesis Outline

This section guides to understand how the thesis study is proposed. This thesis study consists of five main chapters including an introduction. In the first chapter of the thesis, the environmental problems that can be shown as a result of this study, sources of these problems and some numerical data are mentioned. In the second chapter, a detailed literature review has been conducted by considering the various studies performed on the thermochemical Cu-Cl and Mg-Cl cycles, high-temperature electrolysis, heat pumps, thermal energy storage and methanol synthesis. The third chapter proposes the development process and a detailed explanation of each system and their versions separately. Chapter four explains the detailed thermodynamic analyses of the proposed integrated systems based on the first and second laws of thermodynamics. Chapter five provide the details of the results obtained as a consequence of the thermodynamic analyses. This chapter contains separate sections for each system and its versions. In each section, there are results according to the main assumptions of the study, and then parametric studies where environmental factors and state properties are changed to observe their effects on the systems.

Chapter 2 LITERATURE REVIEW

A literature review has been conducted on both the industry and the academia-based studies about the systems used and the working areas prior to this thesis study. As a result of this literature review, new ideas about integrated systems have been obtained and the results of experimental studies have been used in order to obtain more efficient results.

Various useful outputs are provided in three different systems and their versions. In two of these systems, hydrogen is used as a direct output, while the first system uses it for methanol synthesis. In this context, various hydrogen production methods have been adopted. In the first system, high-temperature electrolysis has been incorported for hydrogen production (instead of a conventional electrolysis system) for which the required thermal energy has been harnessed from the solar tower. In other systems, Cu-Cl and Mg-Cl cycles, which are thermochemical processes that provide an advantage in terms of costs and sustainability for hydrogen production, have been used. As a result of the studies conducted in these fields, they have more reasonable temperature ranges although they still have endothermic processes with high temperatures and fewer maintenance costs when compared with other cycles, which is why they are used in this study.

Heat pump configurations are examined to reach the required temperature levels which are ranging from 500 ℃ to 530 ℃ for thermochemical cycles from geothermal sources where solar energy is not used. Storage of thermal energy is vital in integrated systems using solar energy technologies due to limited exposure or complete absence solar energy. There are various technologies available for storing thermal energy. For the systems considered in this study, the molten salt heat storage option, which is currenlty one of the most promising methods, has been taken into consideration for storing the high temperatures obtained from the solar towers. A literature review has been conducted to determine the working fluid used. On the other hand, for methanol production, carbon dioxide hydro generation methanol synthesis reactor technology has been used, where hydrogen produced from high-temperature electrolysis is used as input.

Therefore, the literature review is mainly focused on the following areas that are critical to the system:

- Cu-Cl Thermochemical cycles
- Mg-Cl Thermochemical cycles
- High-temperature electrolysis

- Mechanical heat pumps
- Chemical heat pumps
- Molten salt heat storage
- Methanol synthesis reactors

2.1 Cu-Cl Thermochemical Cycles

Several studies on the Cu-Cl thermochemical cycle, including experimental and theoretical ones, have been carried out. These studies have been observed in the ways in which the integration of other systems has been examined and its efficiency is sought, as well as overcoming the difficulties encountered.

Ratlamwala et al. [18] analyzed an integrated system containing the Cu-Cl thermochemical cycle, Kalina cycle and the electrolysis unit used in hydrogen production. This study examines a series of heat exchanger systems to be used for heat recovery in order to achieve the highest possible efficiency as well as the layout of the integration of the Cu-Cl cycle with a new system. It has been observed that the improved cycle performance in the temperature of the electrolysis unit up to 326 $°K$ has reached a negative acceleration after this temperature.

Aghahosseini et al. [19] developed a multigeneration system for producing electricity, steam and hydrogen where Cu-Cl thermochemical and Integrated Gasification Combined Cycle (IGCC) were integrated. It was observed that when oxygen was used instead of air for the gasification process to be integrated with the Cu-Cl cycle, the hydrogen combustion efficiency experienced an increase by about 20% alongwith reduction in the GHG emissions. The integration of IGCC with thermochemical cycles of hydrogen production provides remarkable improvements for the production of useful outputs which include hydrogen, steam and electricity.

Natarer et al. [20] discussed and reviewed the advances in the Cu-Cl cycle in hydrogen production. Recent developments of the consortium Cu-Cl cycle, especially in terms of hydrogen production with Canada's Belt IV reactor, SCWR (Super Critical Water Reactor) are the focus points of this study. System modeling with Aspen has studied in the second complementary article as well as thermochemistry, safety and reliability features of the Cu-Cl cycle.

Aghaghosseinni et al. [21] studied the integration of hydrolysis and electrolysis unit which is one of the most important issues in hydrogen production from the Cu-Cl cycle. This study shows that the amount of steam produced in the heat recovery steam generator (HRSG) unit meets the steam

requirement of the hydrolysis reaction by up to 14 times the stoichiometric value and separation effectively provides up to 22 mol% concentration of HCl acid for electrolysis reaction.

Gabriel et al. [22] developed a lab-scale Cu-Cl cycle in the Clean Energy Research Laboratory (CERL). The reagent conversion rates for the used parameters ranged from 7 to 10%. The maximum HCl ratio in the hydrolysis reactor was determined as 7.5 mol/kg according to the equilibrium condition of the system. PH values of reaction products were observed to affect the system efficiency and to control the $CuCl_2$ pumping to the system. It was concluded that the heat transfer process should be improved in order to minimize the amount of unreacted $CuCl_2$. An atomizing nozzle was used to ensure the regular and fine-grained droplets while providing $CuCl_2$ to the system. Thus, the heat transfer surface was increased for the $CuCl_2$ injected and the heat transfer process was improved.

2.2 Mg-Cl Thermochemical Cycle

Ozcan et al. [23] developed a four-step Mg-Cl cycle integrated with nuclear energy in order to achieve hydrogen production. The nuclear energy source is used for the energy requirements of the Mg-Cl cycle as well as the Rankine cycle which produces electricity required for electrolysis and system compressors. The thermodynamic analysis which is conducted through energy and exergy concept indicated that the system energy and exergy efficiencies are 18.7 and 31.3% respectively. When all subsystems were examined according to the exergy destruction concept, it was observed that the highest irreversibility belongs to the Mg-Cl cycle with 41%. It is also observed that an electrical gain of 6.7% was achieved compared to the conventional electrolysis units were the Mg-Cl cycle is used.

Balta et al. [24] developed a new Mg-Cl cycle system integrated with solar energy to be examined through energy and exergy approach. Their system consisted of five main sections which include heliostat or central receiver solar collectors, steam production providers and thermochemical processes. The study showed that the highest exergy losses occurred in the power cycle and in the central solar energy receiver. Energy and exergy efficiencies were obtained respectively as 58.4% and 64.99%. These efficiencies are 18.18% and 19.15% when the overall system is analyzed. This study demonstrated the importance of the integrated use of solar energy with thermochemical processes for the future of green energy. The rate of hydrogen production is achieved as 1 kmol per second. As a result of this study, it was demonstrated that for the hydrolysis reactor operating

at 500 ℃, the $MgCl_2$ to steam ratio was found to be 3.1 which should be increased to achieve higher yield from reactants. Molten salt is used for the storage of thermal energy obtained from solar energy. To increase molten salt storage output temperature and concentration ratio but to decrease the solar receiver area plays an important role to improve solar field efficiency. This study showed that the difficulties encountered that must be overcome are high power demand and challenges on the separation process of O_2 and Cl_2 at the chlorination reactor. Heat recovery from nuclear or waste energy could be a solution to these issues.

2.3 High-Temperature Electrolysis

Patyk et al. [25] studied an integrated system based on five high-temperature electrolysis (HTE) configurations. They performed the life cycle assessment (LCA) and conducted performance analysis to monitor the impact on the environment. The examined processes include steam generation from a nuclear power plant, intermittent operation with wind and water energy, intermittent operation with natural gas and include biogas reform as a backup. The results of the study have shown that the highest level of the harmful effect that occured was observed in the construction process of the high-temperature electrolysis plant. For the effects during the hydrogen production phase, the strongest impact was due to the search for power supply. Large scale natural gas reform (NGR) was taken as a reference in the performance analysis for their study. Only the HTE configurations where wind energy was used showed less energy consumption in comparison with NGR.

2.4 Mechanical Heat Pumps

Many vapor compression based heat pump configurations are available to reach high-temperature levels. These are methods used in integrated systems for thermochemical cycles which often require high temperature.

Zamfirescu et al. [26] examined heat pump systems consisting of four different configurations. Bethe-zel'dovich-Thompson (BZT) fluids were used as working fluids. It was observed that the heat pump configuration working with BZT fluid had a very high COP value compared to other heat pump systems. In the another study, Zamfirescu et al. [27] compared heat pump options using two organic and two titanium-based working fluids. The highest COP was achieved from the use of titanium tetraiodide with 7.3 for energy and 4.3 for exergy. One of the most significant problems encountered in titanium-based working fluids was the requirement of two-phase compression heat

pumps in the decomposition reactor of Cu_2OCl_2 . The decomposition reactor system with vapor compression option for that type of working fluid was studied by Zamfirescu et al. [17]. The study of Powles [28] concluded that CuCl can be used as a working fluid in the multi-stage compression system in order to feed the decomposition reactor and to meet the temperature needs of endothermic reactions.

2.5 Chemical Heat Pumps

Many heat upgrading methods with chemical processes were proposed and reviewed by Wongsuwan et al. [29]. These processes include a series of endothermic and exothermic thermal stages. Odukoya et al. [30] studied a hydrogen production process from industrial waste heat by heat upgrade via a calcium steam/oxide heat pump system. A combined heat and power compression plant (CHP) was used to upgrade heat to meet the high level of temperature requirements in the decomposition stage of the Cu-Cl thermochemical cycle. Where the optimal pressure was determined as 3.6 bar at the decomposition reactor, a COP of 4.6 was achieved. These results showed that a higher efficiency could be achieved with the CHP cycle when compared to other thermochemical processes and conventional electrolysis units.

Oduyaka and Natarer [31] also presented a numerical study where the CHP cycle was used to upgrade heat for thermochemical hydrogen production. Cement plant was selected as a heat source fo heat recovery and upgrading by CHP. The maximum temperature of 600 ℃ was achieved where the CaO to steam ratio was 2 by using the CHP cycle. The hydrogen production rate was achieved as 12.28 mol/kg Ca (OH) in their study where Cu-Cl and CHP cycles were integrated.

2.5.1 Mercury Heat Pump

M Almahdi [32] performed a comprehensive study on Mercury and Bihelyn heat pumps as two options for heat upgrading to be used in the thermochemical CuCl cycle on hydrogen production. By utilizing the heat released as waste energy in the industry, these configurations increased the temperature at 300 °C levels to 500 °C levels required in the thermochemical cycles.

Heat upgrading with Mercury heat pump configuration with 1.93, energetic coefficient of performance (COP_{en}) and with 1.25 energetic performance (COP_{ex}) is provided to be used in CuCl thermochemical cycle. In addition to the thermodynamic analysis that evaluates the energy and exergy performance in the system, an exergoeconomic analysis is also conducted. Mercury heat pump configuration has been more advantageous than Biheplyn, with an exergy destruction rate

of $ 2000 per hour when Biheplyn has $ 5000 per hour, although it has an initial installation cost of approximately 550,000 more.

2.6 Molten Salt Heat Storage

Wang et al. [33] studied an integrated solar power system with molten salt heat storage where $S-CO_2$ Brayton cycle was used. Molten salt heat storage was integrated with solar power tower receiver. Genetic algorithm, an optimization tool used to find optimum parameters to reach the highest level of efficiency, were applied for optimization purposes. The optimum temperature for the molten salt storage and pressure for the cycle reported to be 560 ℃ and ranging from 7.8 to 10 MPa respectively.

Sorgulu and Dincer [34] proposed a study where a solar power tower system and thermal energy storage option were combined in order to achieve useful outputs which are electricity distilled water. The molten salt heat storage was used to store solar energy for 12 hours a day to be used in the absence of sun. Where 16.1% and 12.25% overall energy and exergy efficiency was achieved, more than 180 MW electricity generation was obtained.

2.7 Methanol Synthesis

Kiss et al. [35] conducted a novel study to improve the carbon dioxide hydrogenation process using hydrogen which was recovered as a by-product of the chloralkali production process. The method developed has two positive effects on the process. First, it helped to separate carbon mono oxide and carbon dioxide from a mixture of methanol and water. So, carbon dioxide natural conversion is allowed. As a second positive effect, an efficient method was provided by removing the water from the wet hydrogen. By using this novel system, it was possible to produce one ton of methanol wit 550 kWh electricity and 0.48-1.16 ton steam.

Chapter 3 SYSTEM DESCRIPTION

This study proposes three novel integrated energy systems with desalination, thermal energy storage, Cu-Cl and Mg-Cl based hydrogen production cycles and heat upgrade options. These three systems are intended to produce five different useful outputs such as electricity, hot water, space heating, fresh-water and hydrogen or methanol as fuel. Each of these three systems benefit from the geothermal energy source and freshwater is obtained from seawater by the multistage distillation process. Three different options are adopted for hydrogen production. In the first system, high-temperature electrolysis is used instead of conventional electrolysis systems. The hydrogen produced here goes to the CO_2 hydro generation methanol synthesis reactor to be converted to methanol. The energy source required to meet the need for high temperature or to produce other system outputs has been determined as a solar power tower receiver to be a supplement to the wind and geothermal. These options constitute the basis of the first system.

In both versions of the second and the third systems, thermochemical processes are used for hydrogen production. Two different thermochemical cycles are used. The Cu-Cl and the Mg-Cl cycles have been incorporated respectively in the second and the third systems. If both cycles are compared with the other thermochemical processes, it is clear that they are advantageous in terms of low-temperature requirements and low maintenance costs. In the first versions of both the systems, it can be seen tat the use of solar tower technology continues as a source, but the wind energy is removed from the integrated system.

In the second version of the second and the third systems, solar power tower technology is not proposed. Instead, the high-temperature requirement, which is around 530 ℃ in the thermochemical processes, is met through a combination of geothermal energy source and the heat pump technology. In accordance with the results from the literature review carried out at this stage, the mercury heat pump cascaded heat pump technology is selected. Hydrogen production is also provided in this system and thermochemical processes are used. For this reason, two different systems consisting of Cu-Cl and Mg-Cl configurations are also the subject of this version. In order to store the thermal energy, a molten salt thermal storage option is offered. The molten salt is stored in two different storage tanks as hot and cold tanks.

The detailed specifications that belong to the systems and their versions are given in Table 3.1.

Table 3.1 System specifications

	SYSTEM 1		SYSTEM 2				SYSTEM 3			
			Version 1		Version 2		Version 1		Version 2	
Energy Sources	1. Geothermal		1. Geothermal		1. Geothermal		1. Geothermal		1. Geothermal	
	2. Sea Water		2. Sea Water		2. Sea Water		2. Sea Water		2. Sea Water	
	3. Solar Tower		3. Solar Tower				3. Solar Tower			
	4. Wind Tower									
Hydrogen Production	High Temperature Electrolyser		Cu-Cl Thermochemical Cycle		Cu-Cl Thermochemical Cycle		Mg-Cl Thermochemical Cycle		Mg-Cl Thermochemical Cycle	
Hydrogen Production Method Specifications	**Electrode Type**	*Ni-doped Ceramic*	**Step Number**		*3*		**Step Number**		*3*	
	Cell Temperature °C	*700-1000*	**Simulation Software**		*Aspen-Plus*		**Simulation Software**		*Aspen-Plus*	
	Typical Pressure (bar)	*1-15*	**Method**		*IDEAL*		**Method**		*ELECNRTL*	
	Efficiency	*1*	**Electrolysis Temperature**		*70*		**Electrolysis Temperature**		*70*	
	Nominal System Efficiency	*76-81%*	**Hydrolysis Temperature**		*400*		**Hydrolysis Temperature**		*537*	
	Specific energy consumption rate (kWh/m^3)	*3*	**Thermolysis Temperature**		*500*		**Chlorination Temperature**		*537*	
	Investment costs ($/kW)	*2200*								
Thermal Storage	Molten Salt Storage - 650 °C for cold tank and 910 °C for hot tank		Molten Salt Storage - 600 °C for cold tank and 910 °C for hot tank				Molten Salt Storage - 600 °C for cold tank and 910 °C for hot tank			
Heat Upgrade					CuCl-Mercury Cascaded Heat Pump				CuCl-Mercury Cascaded Heat Pump	
System Outputs	**Net Power Outlet (kW)**	*16828*	**Net Power Outlet (kW)**	*4182*	**Net Power Outlet (kW)**	*8277*	**Net Power Outlet (kW)**	*8519*	**Net Power Outlet (kW)**	*16096*
	Heating Condenser (kW)	*25873*	**Electrolysis input (kW)**	*173.3*	**Electrolysis input (kW)**	*173.3*	**Electrolysis input (kW)**	*261.7*	**Electrolysis input (kW)**	*261.7*
	Hot Water (kW)	*21949*	**Heating Condenser (kW)**	*25873*	**Heating Condenser (kW)**	*8080*	**Heating Condenser (kW)**	*25873*	**Heating Condenser (kW)**	*8080*
	Solar Power Tower Outlet (kW)	*93323*	**Hot Water (kW)**	*21949*	**Hot Water (kW)**	*10450*	**Hot Water (kW)**	*21949*	**Hot Water (kW)**	*10450*
	Wind Power Towers Outlet (kW)	*12088*	**Solar Power Tower Outlet (kW)**	*93323*	**Fresh-water production (kg/s)**	*47.887*	**Solar Power Tower Outlet (kW)**	*93323*	**Fresh-water Production (kg/s)**	*48.0212*
	Fresh-water production (kg/s)	*48.23*	**Fresh-water production (kg/s)**	*47.887*	**Hydrogen output by Cu-Cl cycle (kg/hr)**	*7.2517*	**Fresh-water Production (kg/s)**	*48.0212*	**Hydrogen output by Mg-Cl cycle (kg/hr)**	*8.7088*
	Methanol production (kg/s)	*1.326*	**Hydrogen output by Cu-Cl cycle (kg/hr)**	*7.2517*			**Hydrogen output by Mg-Cl cycle (kg/hr)**	*8.7088*		

The present system proposes direct discharge of brine disposal into oceans, surface water or deep well injection. Future studies should be performed for new methods to eliminate the environmental problems of brine discharge. Salt disposed of desalination can be used in various processes. First of all, it should be subjected to dehydration and the appropriate process for brine should be developed for this process. The salt obtained can be used in chlorine production. Chlorine can be manufactured by the Chloralkali process which is the electrolysis of a sodium chloride solution. The production of chlorine results in the co-product's caustic soda and hydrogen gas. These two products are highly reactive as well as chlorine. Chlorine can also be produced by the electrolysis of a solution of potassium chloride, in which case the co-products are hydrogen and potassium hydroxide. There are three industrial methods for the extraction of chlorine by electrolysis of chloride solutions; Mercury Cell Electrolysis, Diaphragm Cell Electrolysis, Membrane Cell Electrolysis.

3.1 System 1: An Integrated System with Desalination and Heat Storage Options

In system 1, carbon dioxide is selected as the working fluid for the organic Rankine cycle. The remaining heat from the geothermal is transferred to the R134a refrigerant cycle for use in space heating and hot water production by heat exchanger 2. And geothermal water is re-injected to the ground at state 24. Heat exchanger 9 performs heat transfer from this cycle for use in hot water production. The thermal energy collected from the solar tower receiver is transferred to the hot molten salt storage. Here a by-pass option is provided by using heat exchanger 8. Thus, in the absence of solar energy, the cycle is completed so that thermal energy stored in molten salt storage can be used to achieve useful outputs. Heat exchanger 7, transfers the thermal energy stored in the tanks to heat exchanger 4 to use in high-temperature electrolysis. The remaining afterward is transferred to another organic Rankine cycle by heat exchanger 5 and 6 before returning to the storage tanks.

In the production of hydrogen, high-temperature electrolysis is preferred instead of the conventional electrolysis unit. Here, the temperature requirement of 700 ℃ is met by the thermal energy gained by the solar tower. Produced hydrogen is transferred to carbon dioxide hydro generation methanol synthesis reactor at state 33 and methanol production is achieved at state 34. Here, the release of carbon dioxide from the industry is prevented and the use of this carbon dioxide is also benefited in the synthesis of methanol. Energy production from wind turbine towers that are integrated into the system can also be countered into the general energy calculations. Surplus

energy produced can be added to the national grid on demand. In addition, the system offers a desalination option for freshwater production. Multistage or in another name muti-flash desalination unit option is preferred. The multi-stage desalination option is a preferred distillation process with its low energy consumption and low-temperature operation features. The fresh-water produced here is used for both meeting the domestic needs and to produce hydrogen in the electrolysis unit.

3.2 System 2: Cu-Cl Cycle Hydrogen Production

System 2 consists of two different versions due to the different configuration of the integrated system. The most important difference that distinguishes the two versions is the use of a solar energy receiver tower. In version two, heat pump configuration is used to reach the desired temperature levels while the first version has a power generation Rankine cycle in addition to the system one. Cu-Cl cycle, which is the thermochemical process for hydrogen production in both versions, has been adopted. In this system, wind energy will not be used as an energy source.

3.2.1 Version 1: Solar and Geothermal Based

Figure 3.2 shows the layout of the first version of the second system. Heat exchangers 4 and 9 are used to transfer the thermal energy received from solar power tower to the Cu-Cl cycle through the power generation Rankine cycle. At this stage, electricity production is obtained from the turbine 4. At the same time, the need for freshwater requirements for the hydrolysis unit is met by the production of the multistage desalination unit. On the other side, electricity production by turbine 1 from the geothermal energy source and by turbine 2 from stored thermal energy in the thermal energy storage also continues as well as system 1. Hot water supply continues with heat exchanger 9 as in system 1.

3.2.2 Version 2: Geothermal and Mercury Cascaded Heat Pump (Cu-Cl)

In this version of the second system, the solar tower is removed from the integrated system. Therefore the required temperature levels are met by geothermal energy. Production of system outputs is provided by the heat recovered at 200 ℃ levels. A cascaded heat pump configuration constituting two-stages is used to achieve this heat upgrading.

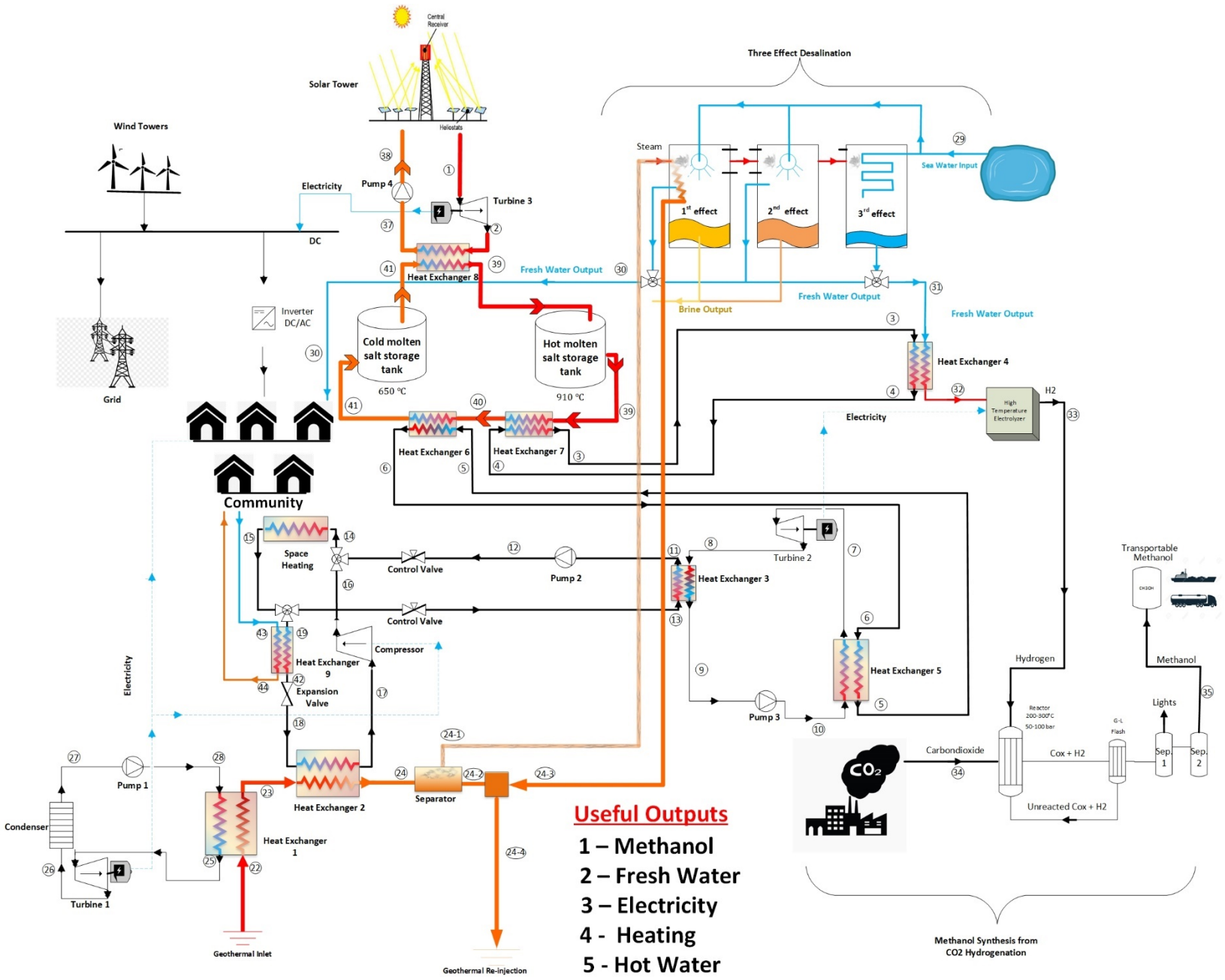

Figure 3.1 Layout of system 1

Table 3.2 State point information for system 1

State Points	Mass Flow Rate (kg/s)	Temperature (°C)	Pressure (kPa)
1	400	1176	1900
2	400	1116	1300
3	400	700	1000
4	400	600	700
5	300	445	550
6	300	475	700
7	300	310	1000
8	300	195	300
9	300	145	350
10	300	210	700
11	200	110	122
12	200	200	137
13	200	85	125
14	400	150	137
15	400	85	125
16	200	140	137
17	200	80	87
18	200	20	90
19	200	85	125
20	80	140	130
21	80	95	130
22	300	260	960
23	300	190	940
24	300	105	920
24-1	15	105	920
24-2	285	105	920
24-3	15	105	920
24-4	300	105	920
25	300	185	265
26	300	150	160
27	300	25	150
28	300	30	220
29	116.23	21	100
30	40	21	100
31	0.4825	21	100
32	0.4825	600	300
36	40	21	5
37	400	910	1280
38	400	920	1900
39	400	910	1000
40	400	750	1000
41	400	650	1000
42	200	70	100
43	150	25	100
44	150	60	100

The heat pump configuration, which is called the Mercury heat pump in Figure 3.3 consists of two different cycles as Mercury cascaded heat pumps at the bottom and Cu-Cl heat pump at the top.

Mercury heat pump cycle recovers heat at 320 ℃ from source by using heat exchanger 9. Mercury which is the working fluid of the Mercury heat pump cycle enters heat exchanger 9 as two at state 28 and leaves as a saturated vapor. Then. Mercury is compressed in 3 stages by 3 compressors into the two-phase fluid which has vapor quality. Between each compressing stage, intercooling takes places in heat exchangers. Heat exchangers 5, 6 and 7 ensure that the heat is transferred to the Cu-Cl cycle at the top as well as decrease the increasing temperature while in the compressing process due to decrease mechanic power consumption.

Then the Cu-Cl obtained in state 8 as a saturated vapor, enters a multistage compression configuration. Compressed CuCl to by compressor 1, compressor 2 and compressor 3 is intercooled by heat exchanger 4 and heat exchanger 3 between each compression stage. Each compression level of compressors is equal ($\Delta P_{comp1} = \Delta P_{comp2} = \Delta P_{comp3}$) and steam exits the compressor 3 with the same pressure level with steam in state 16 which is the outlet of the thermolysis unit at approximately 1 bar to be mixed with steam in state 16. Decomposition reaction occurs in the thermolysis unit at 530 ℃ levels. Steam in the state 15 which enters the thermolysis unit is higher than this temperature level. On the other hand, from the oxygen produced in state CS-2 and steam 4 which is Cu-Cl produced from the thermolysis reactor which has the same temperature level, sensible heat is transferred to the steam 7 by using heat exchanger 1 and heat exchanger 2. The produced Cu-Cl is transferred to the Cu-Cl cycle in the state 4 to produce hydrogen. State information which consists state temperature, pressure and mass flow rates for version 2 of system 2 can be found in Table 3.4.

3.3 System 3: Mg-Cl Cycle Hydrogen Production

Both system 2 and system 3 benefit from thermochemical processes with similar temperature requirements. Mg-Cl cycle is used in this system as a thermochemical process. The distinctive feature that distinguishes the versions of this system is the use of solar tower technology as in system 2. In version two of system 3, as in the second system, heat pump configuration is used.

3.3.1 Version 1: Solar and Geothermal Based

The reason for distinguishing the second version of the third system from the second system is the choice of the thermochemical cycle. With the same temperature requirement, Mg-Cl is also preferred for this system version. The temperature requirement of around 530 ℃ for the hydrolysis unit is met with heating the fresh-water supply by heat exchanger 8.

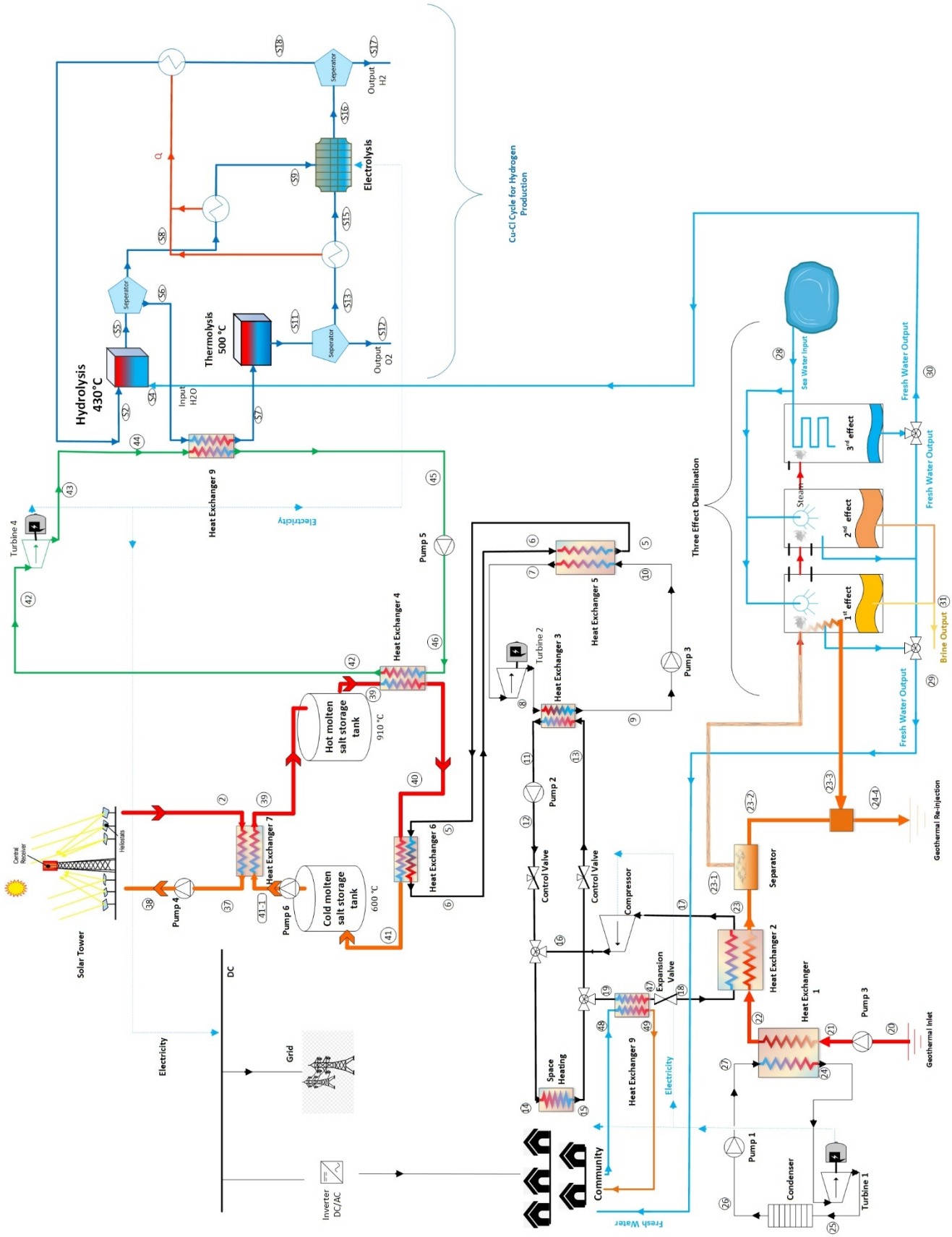

Figure 3.2 Layout of system 2, version 1

Table 3.3 State point information for the first versions of system 2 and 3 including Cu-Cl and Mg-Cl cycles

Version 1 of System 2 and System 3			
State Points	**Mass Flow Rate (kg/s)**	**Temperature (°C)**	**Pressure (kPa)**
2	400	1176	1300
5	300	400	550
6	300	500	700
7	300	370	1000
8	300	250	300
9	300	180	350
10	300	210	700
11	200	110	122
12	200	200	137
13	200	85	125
14	400	150	137
15	400	85	125
16	200	140	137
17	200	80	87
18	200	20	90
19	200	85	125
20	300	200	900
21	300	260	920
22	300	190	920
23	300	105	900
24	300	137	265
25	300	98	160
26	300	60	150
27	300	90	220
28	40.306	21	100
29	40	21	100
37	400	920	1300
38	400	940	1350
39	300	910	800
40	300	820	780
41	300	600	760
41-1	300	660	790
42	300	690	370
46	300	600	370
43-Sys 2	300	600	250
44-Sys 2	300	570	250
45-Sys 2	300	570	250
46-Sys 2	300	600	250
47-Sys 2	300	600	250

48-Sys 2	300	580	250
23-1	15	580	200
23-2	285	580	200
23-3	15	580	200
23-4	300	580	200
30- CuCl	0.186	21	100
S3 - Cu-Cl Cycle	64.855	25	100
S4 - Cu-Cl Cycle	64.855	400	100
S5 - Cu-Cl Cycle	1032.92	400	100
S6 - Cu-Cl Cycle	770.4	400	100
S7 - Cu-Cl Cycle	770.4	500	100
S8 - Cu-Cl Cycle	262.517	400	100
S9 - Cu-Cl Cycle	262.517	25	100
S11 - Cu-Cl Cycle	770.388	500	100
S12 - Cu-Cl Cycle	57.5978	500	100
S13 - Cu-Cl Cycle	712.791	500	100
S15 - Cu-Cl Cycle	712.791	430	100
S16 - Cu-Cl Cycle	975.307	25	100
S17 - Cu-Cl Cycle	7.25717	25	100
S18 - Cu-Cl Cycle	968.05	25	100
S19 - Cu-Cl Cycle	968.05	80	100
S1 - Mg-Cl Cycle	64.855008	25	100
S2 - Mg-Cl Cycle	1102.535136	70	100
S3 - Mg-Cl Cycle	1102.535136	537	100
S4 - Mg-Cl Cycle	411.308928	537	100
S5 - Mg-Cl Cycle	1513.844064	537	100
S6 - Mg-Cl Cycle	1339.729056	537	100
S7 - Mg-Cl Cycle	1339.729056	70	100
S8 - Mg-Cl Cycle	1339.729056	70	100
S9 - Mg-Cl Cycle	1033.417728	70	100
S10 - Mg-Cl	1024.709126	70	100
S11 - Mg-Cl	8.7086016	70	100
S12 - Mg-Cl	8.7086016	25	100
S13 - Mg-Cl	174.115008	537	100
S14 - Mg-Cl	306.311328	70	100
S15 - Mg-Cl	306.311328	537	100
S16 - Mg-Cl	480.426336	537	100
S17 - Mg-Cl	69.117408	537	100
S18 - Mg-Cl	69.117408	25	100

3.3.2 Version 2: Geothermal and Mercury Cascaded Heat Pump (Mg-Cl)

In this version of the third system, as in the second version of the second system, the required temperature levels for the system are provided only by geothermal energy sources. For this temperature requirement, Mercury heat pump configuration is used.

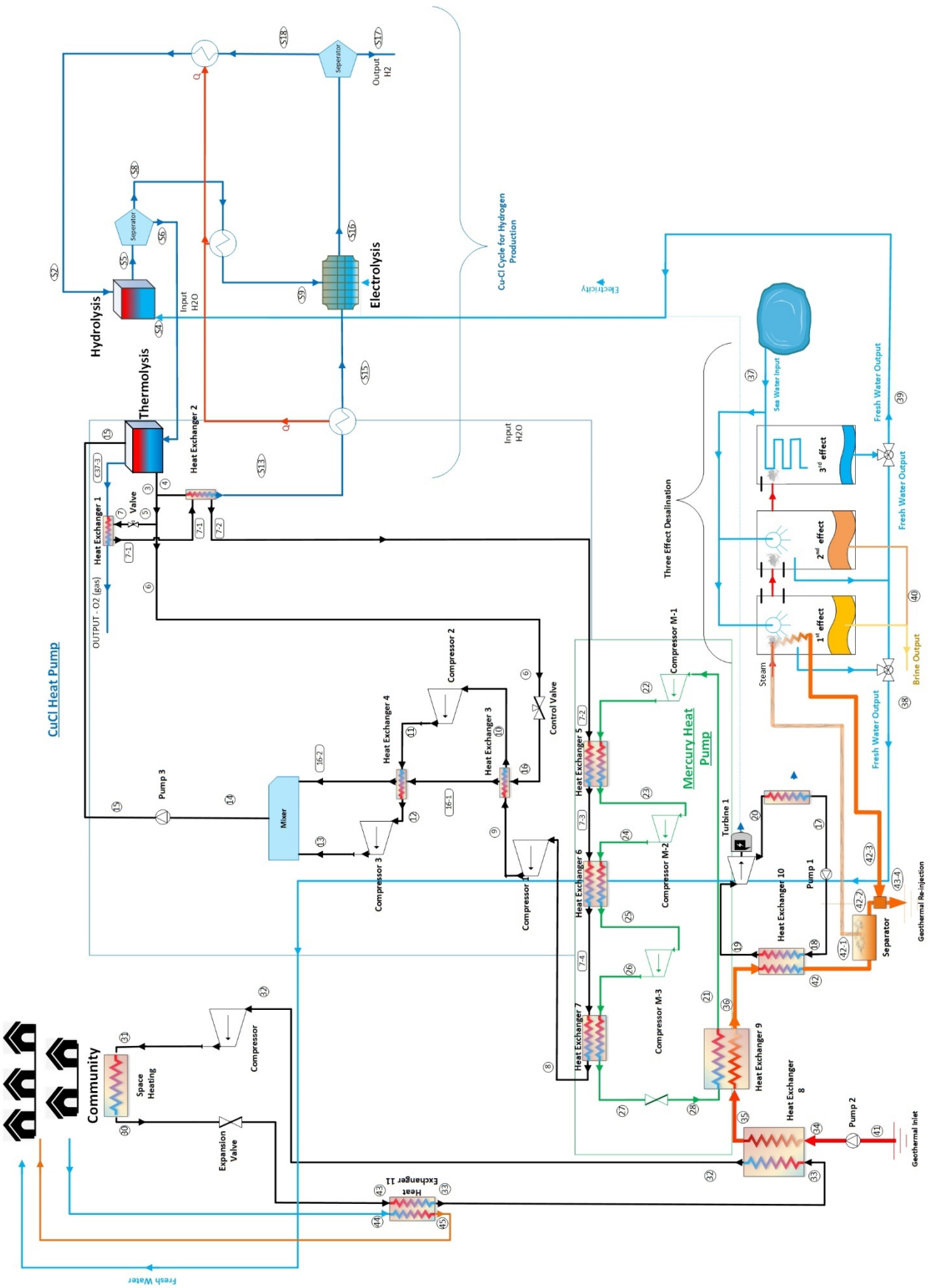

Figure 3.3 Layout of system 2, version 2

Table 3.4 State point information for the seond version of system 2

State Points	Mass Flow Rate (kg/s)	Temperature (°C)	Pressure (kPa)
0		25	101
3	19.08	576	102
4	1.58	576	102
5	0.39	576	102
6	17.11	576	102
7	0.39	480.993	0.03
7-1	0.39	480.993	0.03
7-2	0.39	480.993	0.03
7-3	0.39	480.993	0.03
7-4	0.39	480.993	0.03
8	0.39	480.993	0.03
9	0.39	1275.78	0.44
10	0.39	676.26	0.44
11	0.39	853.75	0.81
12	0.39	676.26	0.81
13	0.39	779.17	1.03
14	17.5	676.26	1.03
15	17.5	676.26	102
16	17.11	576	1.05
16-1	17.11	584	1.05
16-2	17.11	587	1.05
21-Mercury HP	0.916	296.86	30
22-Mercury HP	0.916	1292.89	290
23-Mercury HP	0.916	485.89	290
24-Mercury HP	0.916	748.1	565
25-Mercury HP	0.916	485.89	565
26-Mercury HP	0.916	638.43	818
27-Mercury HP	0.916	485.89	818
28-Mercury HP	0.916	296.86	30
29	300	200	960
30	150	85	125
31	150	135	137
32	150	125	102
33	150	70	102
34	300	325	960
35	300	320	960
36	300	300	960
37	120	21	100
38	40	21	100
39	40	21	100
40	40	21	5
41	300	320	940
42	300	125	920
42-1	15	125	920
42-2	285	125	920
43-3	15	125	920
44-4	300	125	920
43	150	80	100
44	100	25	100
45	100	50	100

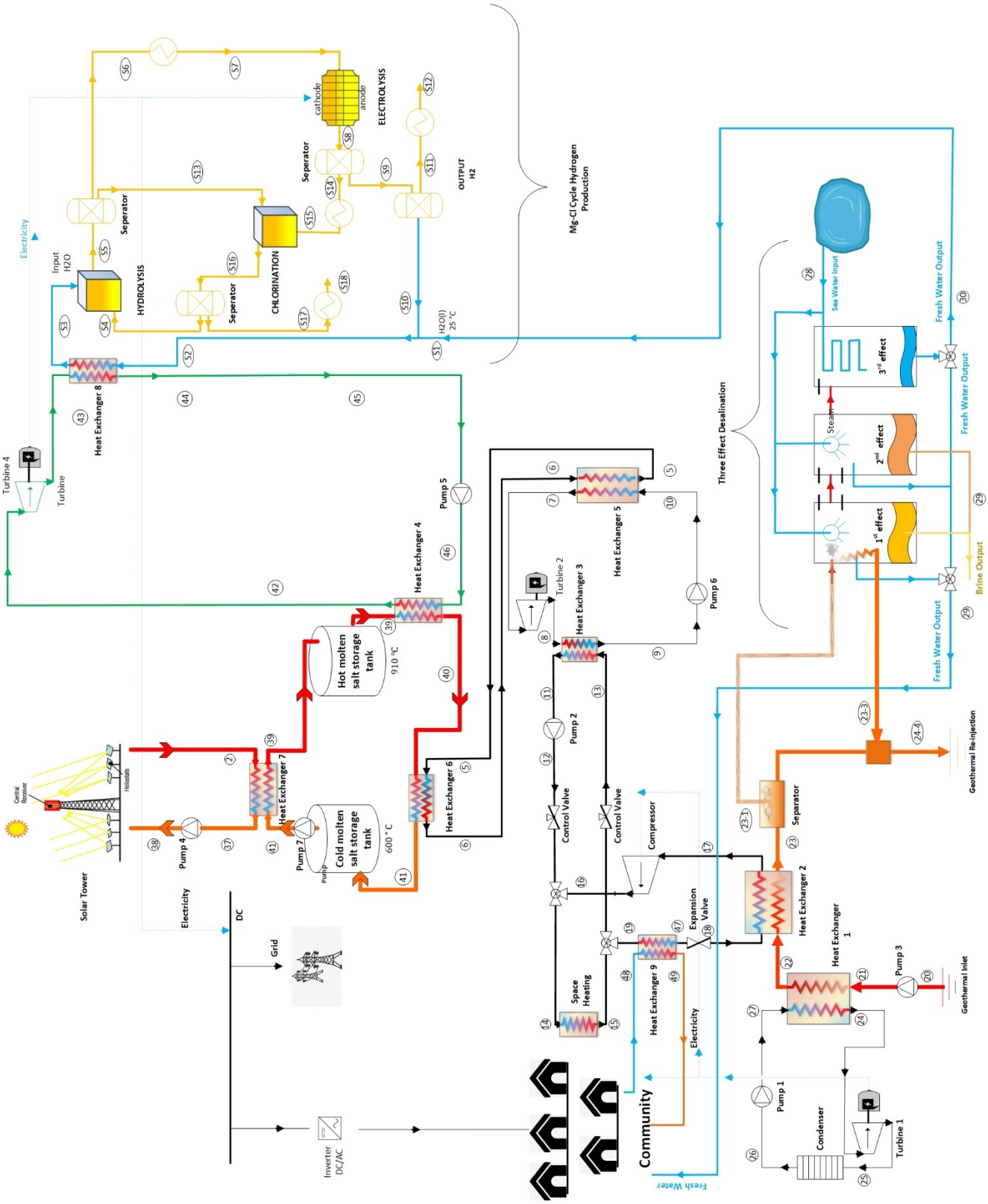

Figure 3.4 Layout of system 3, version 1

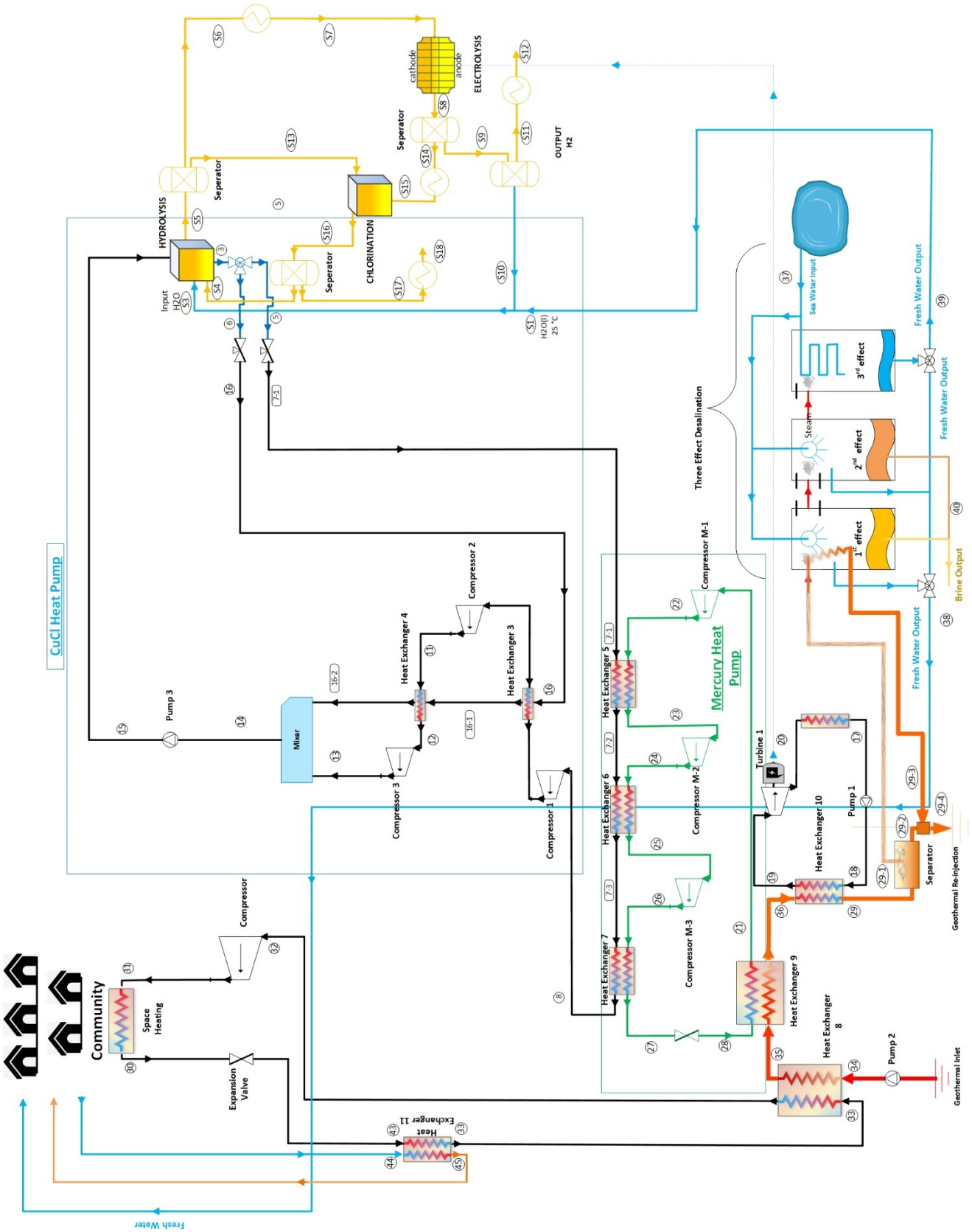

Figure 3.5 Layout of system 3, version 2

Chapter 4 SYSTEM DEVELOPMENT AND THERMODYNAMIC ANALYSIS

This chapter conducts a comprehensive thermodynamic analysis of the systems studied in the thesis through energy and exergy concepts and discusses the pure substances used as working fluids in terms of thermodynamic properties. Moreover, it provides the information about the development of the balance equations used as a tool in the thermodynamic analysis of the systems and explains these concepts according to the first and second law of thermodynamics.

To conduct thermodynamic analysis, Engineering Equation Software (EES) is used. The property database of EES allowed the evaluation of state properties of working fluids at various state points of the considered systems.

4.1 Properties of Working Substances

The pure substances used in these systems as working fluids include Mercury (Hg), copper chloride (CuCl), Magnesium-Chloride (MgCl). The information for these substances is also important in terms of revealing the differences by comparing them with experimental studies and giving the reader an idea about the realities of simulations. The Mercury cascaded heat pump configuration is simulated using Engineering Equation Solver (EES) under ideal gas conditions. Besides, the Cu-Cl cycle and Mg-Cl cycle are simulated using Aspen-Plus.

4.1.2 Mercury

Two-stage heat pump configurations are used to reach required temperature levels for thermochemical cycles at version 2 of the systems 2 and 3. The bottom cycle of this two-stage heat pump has Mercury as a working fluid. In reference to ambient temperature and pressure which are 25 °C and 101 kPa, Mercury is in the liquid phase. The boiling point, critical temperature and pressure are 357 °C, 1477 °C and 1720 kPa respectively. The thermodynamic analysis of the bottom cycle where the working fluid is Mercury has been conducted by using EES Software. Steady-state conditions and other general assumptions are used for this cycle as well. The study belongs to Sugawara et al. [36] has been used for reference values in order to compare the thermodynamical processes with experimental results. Table 4.2 provides a comparison of the results obtained through experimental and theoretical studies.

There is no experimental study that Mercury is used as a working fluid in heat pump configuration in literature due to health risks. Mercury is a heavy metal that is very harmful to human health.

Mercury can evaporate immediately at ambient pressure and temperature and has the ability to remain in ambient air for up to one year. Mercury is highly toxic which may be fatal if inhaled and harmful if absorbed through the skin. The inhaling of mercury vapor causes absorbing 80% of the vapor into the blood through the lungs. Therefore the use of mercury requires a variety of health procedures and serious precautions. The world health organization has announced a number of precautionary procedures for health care organizations where mercury is used for medical purposes. Similar procedures are available for the experimental processes. Developing a set of procedures for stages of clean up, waste handling and storage of mercury is crucial in creating a healthy working environment [37]. Developed procedures must cover staff training with educational programs, required protective gear, engineered storage facilities and appropriate waste storage containment.

On the other hand, Gutstein et al. [38] developed a Rankine cycle where Mercury is working fluid. The turbine process which exists in Gutsein's study is chosen as a reference process to compare our theoretical study. Table 4.1 shows the comparison between the experimental and theoretical values of the operating conditions and the power outputs of the Turbine. In a theoretical study that is performed by using EES Software, 68.09 kW power output is achieved although the experimental result is 64 kW. The difference obtained from theoretical and experimental data is 6.006% as can be seen in Table 4.1.

Table 4.1 Turbine power output comparison of EES and experimental data

	Experimental data taken from [38]	**EES Software - Own Database**	**Error %**
Mass Flow Rate	1.5 kg/s	1.5 kg/s	N/A
Intet Temperature	677 °C	678 °C	N/A
Outlet Temperature	1724 kPa	1725 kPa	N/A
Intel Pressure	354 °C	355 °C	N/A
Outlet Pressure	96.5 kPa	96.5 kPa	N/A
Power	64 kW	68.09	6.006

4.2 Thermodynamic Analysis

In this section of the fourth chapter, thermodynamic analysis of the studied systems through energy and exergy concept is provided. The mass balance equations are developed by the first and second laws of thermodynamics. The mass and energy balance equations are derived respectively according to the mass and energy conservation principles of the first law. The entropy balance equation comes from being non-conversible of entropy which is proved by the second law of

thermodynamics. To identify the principle that exergy could not be conserved, the exergy balance equation is used.

Table 4.2 Saturation pressure comparison of EES and experimental data

	Saturation Pressure		
T	**Data taken from Sugawara et al.** [36]	**Present EES Model**	**Error**
°C	kPa	kPa	%
200	2.353587259	2.325	1.214625
250	9.904679716	9.97	0.659489109
300	32.95022163	33	0.151071429
350	89.82858039	89.84	0.012712664
400	210.6460597	210.2	0.211757914
450	438.4536932	436.5	0.445587117
500	829.3453105	823.6	0.692752513
550	1451.37881	1438	0.9218
600	2382.026439	2354	1.176579662
650	3706.899933	3652	1.481020106
700	5517.2008	5419	1.779902595
750	7908.053191	7739	2.137734623
800	10983.40721	10685	2.716891071

4.2.1 Mass Balance Equation

The mass balance equation which identifies the conversation of mass can be derived as the form follows,

$$\sum \dot{m}_\iota = \sum \dot{m}_e \tag{4.1}$$

This balance equation shows that the inlet mass is equal to outlet mass at any time and mass flow is constant volume. This concept can be applied for any device when the steady-state assumption is conducted. Then, the change in the rate of mass flow is zero.

4.2.2 Energy Balance Equation

The energy balance of any steady-state device can be derived from the first law of thermodynamics as shown as follows:

$$\sum \dot{m}_\iota \times \left(h_i + gZ_i + \frac{v_i^2}{2} \right) = \sum \dot{m}_e \times \left(h_e + gZ_e + \frac{v_e^2}{2} \right) \pm \dot{W} \pm \dot{Q} \tag{4.2}$$

This equality proves that the entering energy in constant volume is equal to the leaving energy at any time. In steady-state assumption, any device can be modeled in constant volume with this

equality. The potential and kinetic energy changes that are related to the mass flow conditions are mostly negligible and can be assumed as zero in any thermodynamic analysis.

4.2.3 Entropy Balance Equation

The entropy balance equation can be expressed as follows:

$$\sum \dot{m}_\iota \times s_i + \dot{S}_{gen} = \sum \frac{\dot{Q}_n}{T_n} + \sum \dot{m}_e \times s_e \tag{4.3}$$

The energy balance equation is expressed from the second law of thermodynamic and identifies entropy generation exists in any process.

4.2.4 Exergy Balance Equation

The exergy balance equation is stated as flows for any process at the steady-state condition.

$$\sum \dot{m}_i \times ex_i = \sum \dot{m}_e \times ex_e \pm \dot{W} \pm \dot{E}x^Q + \dot{E}x_{dest} \tag{4.4}$$

According to the exergy balance equation at any time, the exergy change rate is equal to zero where mass flow is in the control volume.

Here, ex denotes the specific exergy and can be calculated which consist of four different exergy value which is physical exergy, chemical exergy, kinetic exergy and potential exergy as can be seen as follows:

$$ex_k = ex_k^{phys} + ex_k^{chem} + ex_k^{kin} + ex_k^{pot} \tag{4.5}$$

The kinetic and potential exergy values can be neglected as stated in the energy balance assumption. Also, chemical exergy can be neglected if the stream doesn't chemically change and described as follows:

$$ex^{chem} = \sum x_k \times ex_{chem}^k + R \times T_o \times \sum x_k \times \ln(x_n) \tag{4.6}$$

where x_k is the mole flow of stream and ex_{chem}^k is the specific definite value for species and R is the gas constant which is 8314.472 $\frac{kJ}{mol\,K}$.

$$ex^{phys} = (h_i - h_o) - T_o(s_i - s_o) \tag{4.7}$$

where h_i and s_i are the enthalpy and entropy values respectively for inlet and h_o and s_o are the enthalpy ad entropy values for ambient conditions.

4.2.5 Exergy Destruction and Exergy for Thermal Flow

In the analysis of any process where the system is assumed as steady-state, the exergy of thermal flow can be expressed as follow:

$$Ex^{Q} = (1 - \frac{T_o}{T_{amb}}) \times \dot{Q} \tag{4.8}$$

The exergy of thermal flow is equal to the multiplication of the Carnot factor and the rate of thermal flow.

The exergy destruction can be calculated by multiply the ambient temperature with entropy generation as can be seen as follows:

$$\dot{E}x_{dest} = T_o \times \dot{S}_{gen} \tag{4.9}$$

4.3 System Assumptions and Thermodynamic Analysis of Major Components

In this study, some assumptions which are generally accepted are used in the thermodynamic analysis. Thermodynamic analyses in this study address developing thermodynamic models to simulate the steady-state operation of the proposed systems. Dynamic responses of the system on system energy and exergy results because of solar irradiation and wind speed variations or ambient conditions changes are not included. Except for the assumptions for specific processes which are denoted in relevant sections, system assumptions for all five systems are as follows:

- All kinetic and potential energy and exergy changes are negligible.
- All chemical and nuclear reactions are ignored.
- All turbines, heat exchangers, pumps and compressors used in these five systems are assumed as adiabatic devices.
- Pressure losses through system devices are assumed pretty small and negligible
- System thermodynamic analysis is performed where processes are under steady-state conditions and constant volume flow. Ambient conditions are assumed as temperature and pressures are 25 °C and 101 kPa.

4.3.1 Turbine

The turbine is a mechanical device that is used to expand fluid and generate electricity. The work is an output of the turbine process. During the process, there is a decrease in the temperature of the fluid and it is also used for this purpose. The balance equations for mass, entropy, energy and exergy balance equations in a turbine as shown in Figure 4.1 are written as follows:

$$\dot{m}_1 = \dot{m}_2 \tag{4.10}$$

$$\dot{m}_1 \times h_1 = \dot{m}_2 \times h_2 + \tag{4.11}$$

$$\dot{m}_1 \times s_1 + \dot{S}_{gen} = \dot{m}_2 \times s_2 \tag{4.12}$$

$$\dot{m}_1 \times ex_1 = \dot{m}_2 \times ex_2 + \dot{W} + \dot{E}x_{dest} \tag{4.13}$$

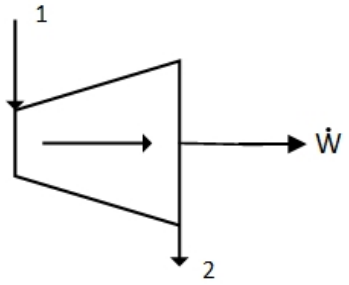

Figure 4.1 Turbine as a system component

Exergetic efficiency for a compressor can be denoted as follows:

$$\eta_{exerg,turbine} = \frac{\dot{W}_{turbine}}{\dot{m} \times (\dot{ex}_{in} - \dot{ex}_{out})}$$

4.3.2 Compressor

The compressor is a device to be used for compressing fluid. This process causes an increase in temperature and it is also used for this purpose. In order to perform this process, work must be applied to the device. The balance equations for mass, entropy, energy and exergy balance equations in a compressor as shown in Figure 4.2 are written as follows:

$$\dot{m}_1 = \dot{m}_2 \tag{4.14}$$

$$\dot{m}_1 \times h_1 + \dot{W} = \dot{m}_2 \times h_2 \tag{4.15}$$

$$\dot{m}_1 \times s_1 + \dot{S}_{gen} = \dot{m}_2 \times s_2 \tag{4.16}$$

$$\dot{m}_1 \times ex_1 + \dot{W} = \dot{m}_2 \times ex_2 + \dot{E}x_{dest} \tag{4.17}$$

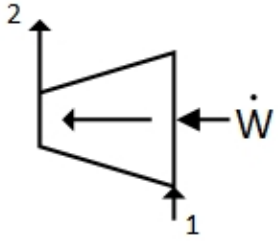

Figure 4.2 Compressor as a system component

Exergetic efficiency for a compressor can be denoted as follows:

$$\eta_{exerg,compressor} = \frac{\dot{m} \times (\dot{ex}_{out} - \dot{ex}_{in})}{\dot{W}_{compressor}}$$

4.3.3 Expansion Valve

The expansion valve is a device where inlet and outlet specific enthalpy values are equal, so an isenthalpic device. In addition to the absence of temperature change, it provides pressure reduction and allows fluid to recover more heat from the source, especially in the heating system. Any work input or output doesn't exist. The balance equations for mass, entropy, energy and exergy balance equations in an expansion valve as shown in Figure 4.3 are written as follows:

$$\dot{m}_1 = \dot{m}_2 \tag{4.18}$$

$$\dot{m}_1 \times h_1 = \dot{m}_2 \times h_2 \tag{4.19}$$

$$h_1 = h_2 \tag{4.20}$$

$$\dot{m}_1 \times s_1 + \dot{S}_{gen} = \dot{m}_2 \times s_2 \tag{4.21}$$

$$\dot{m}_1 \times ex_1 = \dot{m}_2 \times ex_2 + \dot{E}x_{dest} \tag{4.22}$$

Figure 4.3 Expansion valve as a system component

4.3.4 Heat Exchanger

The balance equations for mass, entropy, energy and exergy balance equations in a closed type heat exchanger as shown in Figure 4.4 are written as follows:

$$\dot{m}_1 + \dot{m}_2 = \dot{m}_3 + \dot{m}_4 \tag{4.23}$$

$$\dot{m}_1 \times h_1 + \dot{m}_2 \times h_2 = \dot{m}_3 \times h_3 + \dot{m}_4 \times h_4 \tag{4.24}$$

$$\dot{m}_1 \times s_1 + \dot{m}_2 \times s_2 + \dot{S}_{gen,hx} = \dot{m}_3 \times s_3 + \dot{m}_4 \times s_4 \tag{4.25}$$

$$\dot{m}_1 \times ex_1 + \dot{m}_2 \times ex_2 = \dot{m}_3 \times ex_3 + \dot{m}_4 \times \dot{ex}_4 + ExD_{hx} \tag{4.26}$$

Figure 4.4 Heat exchanger as a system component

4.3.5 Pump

The pump is the device that provides pressure to the fluid to be moved in the system. The balance equations for mass, entropy, energy and exergy balance equations in a pump as shown in Figure 4.5 are written as follows:

$$\dot{m}_1 = \dot{m}_2 \tag{4.27}$$

$$\dot{m}_1 \times h_1 + \dot{W}_{pump} = \dot{m}_2 \times h_2 \tag{4.28}$$

$$\dot{m}_1 \times s_1 + \dot{S}_{gen} = \dot{m}_2 \times s_2 \tag{4.29}$$

$$\dot{m}_1 \times ex_1 + \dot{W}_{pump} = \dot{m}_2 \times ex_2 + \dot{E}x_{dest} \tag{4.30}$$

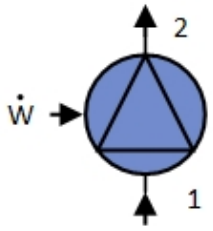

Figure 4.5 Pump as a system component

4.4 Thermodynamic Analysis of Studied Sytems

The section examines the detailed thermodynamic analysis of systems and subunits. The state numbers of each system used are organized in accordance with the system layouts introduced in Chapter 2.

4.4.1 Solar Power Tower

The solar power tower is used to receive solar irradiation and transfer the energy to the system. Solar irradiation data is retrieved for the city of Vancouver, Canada (North: 49.25, West: 123.12) for June 2020 [39]. The average radiation level for June is 200 W/m^2 .

The heat recovered by the tower can be denoted as follows,

$$\dot{Q}_{receiver} = \eta_{hel} \times \dot{Q}_{sol} \tag{4.31}$$

where η_{hel} is the heliostat efficiency for a solar power tower. It is assumed 0.89 for this study. $\dot{Q}_{sol}$ is the heat comes from solar irradiation and can be calculated as follows:

$$\dot{Q}_{solar} = I \times A_{hel,field} \tag{4.32}$$

where I is the solar irradiation can be received from the sun for this region and $A_{hel,field}$ is the heliostat field which is selected as 524.2 meter square while the width is 26.21 m and the height is 20 m.

Figure 4.6 illustrates the irradiation data recorded for Vancouver, Canada in June 2020

Exergetic efficiency of the solar tower is calculated in this study as follows,

$$\eta_{exerg,solartower} = \frac{\dot{m} \times (\dot{ex}_{in} - \dot{ex}_{out})}{\dot{Q}_{solar} \times (1 - \frac{T_{solar}}{T_o})}$$

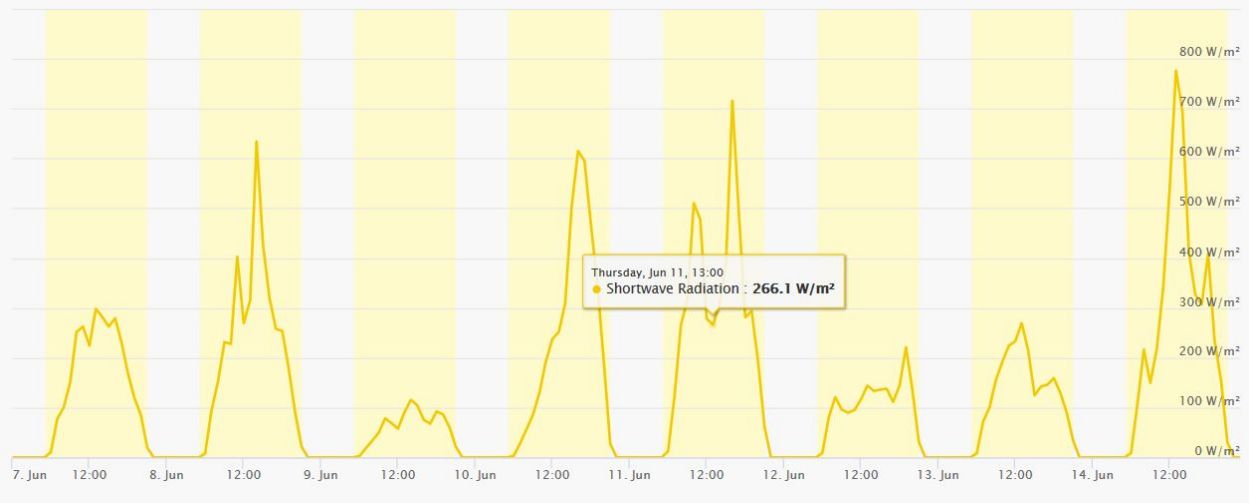

Figure 4.6 Solar irradiation data taken for Vancouver, Canada from [42]

The specifications of the solar power tower are listed in Table 4.3

Table 4.3 Solar power tower parameters

Parameters	**Values**
Average Solar Irradiance	200.00 W/m^2.
Heliostat Field Efficiency	0.89
Heliostat Field Dimensions	26.21 m × 20 m

4.4.2 Wind Power Tower

The 10 wind power towers are integrated into the first system to generate. This section contains detailed explanations of the capacity calculations of the wind power. Daily and hourly wind speed data recorded for Vancouver, Canada (North: 49.25, West: 123.12) in June, is used in this study.

The average wind speed for this period is 2.7 m/s [40]. In this context, the power output for wind power tower can be calculated as follows,

$$\dot{W}_{output} = \frac{1}{2} \times \rho \times A \times V_i^2 \times C_p \times \eta_{mech} \quad (4.33)$$

where ρ is the density for the wind for the relevant region, A is the area of a wind tower, C_p is the power factor for a windmill of power tower which identifies the maximum power that can be extracted which is assumed as 0.593 [41] for this study. V_i is the avarege power which is 2.7 m/s in our study for Vancouver.

The power which is received to be converted to electricity is calculated as follow,

$$P_{rec} = \frac{1}{2} \times \rho \times A \times V_i^3 \quad (4.34)$$

The induction factor which donates the aerodynamic performance of wind turbine is defined as follows,

$$a = \frac{(V_i - V_o)}{V_i} \quad (4.35)$$

where V_o is the output wind speed. To calculate the electric energy which is generated by wind power tower, the conversation of energy principle is used. The power which is generated by the tower rotor is denoted as follows,

$$P_{rot} = \frac{1}{2} \times \rho \times A \times V_i^3 \times 4a(1-a)^2 \quad (4.36)$$

The power coefficient (C_p) of the wind rotor is calculated [42] as follows,

$$C_p = \frac{Power\ of\ Rotor}{Power\ of\ Wind} = 4a(1-a)^2 \quad (4.37)$$

Parameters which are used at the calculation for wind power tower are listed in Table 4.4 and the recorded wind speed data is retrieved for Vancouver, Canada in June 2020 as can be seen in Figure 4.7

Exergy destruction of wind power tower is calculated as below,

$$Ex_{D,windt} = \left(\frac{1}{C_p}\right) \times P_{rot} \quad (4.38)$$

Figure 4.7 Wind speed data taken for Vancouver, Canada from [42]

Table 4.4 Information for wind power tower

Parameter	**Value**
a	0.33
V_i	2.7 m/s
η_{mech}	0.96
Diameter for blades (m)	109
C_p	0.593

4.4.3 Multistage Desalination

The multistage desalination process is an efficient operation when compared with other types of desalination systems due to its advantages of low energy consumption and low operation temperature option [43]. Distilllate water from seawater can be shown with proportion in follows,

$$\frac{\dot{m}_{distwater}}{\dot{m}_{seawater}} = \frac{L_{H,v}}{c \times \Delta F} + \frac{N-1}{2N} \tag{4.39}$$

where $\dot{m}_{seawater}$ and $\dot{m}_{distwater}$ denote the mass flow of seawater and distilled water in terms of kg/s, $L_{H,v}$ is the parameter for latent heat to be requested for evaporation process of water in terms of kJ/kmol, c is the specific heat value for water in constant pressure condition, ΔF denotes the

change in flashing temperatures of highest and lowest ones for stages in term of Kelvin (K). The detailed specifications for multi-stage desalination unit are shown in Table 4.5

Table 4.5 Specifications form multi-stage desalination unit

Parameters	**Values**
$L_{H,v}$ (kJ/mol)	2.38
c (kJ/kg ℃)	1.99
N (number of stages)	3
Mass Flow for Sea-water (kg/s)	116.23 (For the system 1)

4.4.4 Rankine Cycles

Three different Rankine cycle are used in all five systems for heat recovery and electricity generation.

- 1st Rankine Cycle :

The fist Rankine cycle is the Organic Rankine cycle where the working fluid is carbon dioxide which is used to recover heat from the geothermal source and generate electricity. The energy and exergy efficiencies of the cycle can be calculated as follows,

$$\eta_{en,Rankine1} = \frac{\dot{W}_{net,Rankine1}}{\dot{Q}_{Geot}} \tag{4.40}$$

$$\psi_{ex,Rankine1} = \frac{\dot{W}_{net,Rankine1}}{\dot{E}x^{Q_{Geot}}} \tag{4.41}$$

where the $\dot{W}_{net,Rankine1}$ is the work net output which can be evaluated as follow

$$\dot{W}_{net,Rankine1} = \dot{W}_{tur_1} - \dot{W}_{pump1} \tag{4.42}$$

- 2nd Rankine Cycle:

The second Rankine cycle is the organic Rankine cycle and uses carbon dioxide as a working fluid. The energy and exergy efficiencies of this cycle can be found as follows,

$$\eta_{en,Rankine2} = \frac{\dot{W}_{net,Rankine2}}{\dot{Q}_{eva}} \tag{4.40}$$

$$\psi_{ex,Rankine2} = \frac{\dot{W}_{net,Rankine2}}{\dot{E}x^{Q_{eva}}} \tag{4.41}$$

where the $\dot{Q}_{eva}$ is the heat recovered from the molten salt heat storage and the net work output of the cycle $\dot{W}_{net,Rankine2}$ is evaluated as follows,

$$\dot{W}_{net,Rankine2} = \dot{W}_{tur_2} - \dot{W}_{pump3} \tag{4.42}$$

- 3rd Rankine Cycle :

The third Rankine cycle is the steam Rankine cycle to recover heat from the molten salt heat storage and to transfer to the thermochemical hydrogen production cycle. The energy and exergy efficiencies of the system can be found as follows,

$$\eta_{en,Rankine3} = \frac{\dot{W}_{net,Rankine3}}{\dot{Q}_{MS}} \tag{4.43}$$

$$\psi_{ex,Rankine3} = \frac{\dot{W}_{net,Rankine3}}{\dot{E}x^{Q_{MS}}} \tag{4.44}$$

where the $\dot{Q}_{MS}$ is the heat recovered from the molten salt heat storage and the work net output $\dot{W}_{net,Rankine3}$ is calculated as follows,

4.4.6 System 2 Version 2

In version 2 of the system 2, the cascaded heat pump configuration is used to reach required temperature levels for the thermochemical cycle which is used to produce hydrogen. In this version of the system, the solar power tower is removed and the geothermal energy source is the only heat source for the system. The net work output must be calculated to find overall system energy and exergy efficiency. The net work output definition is conducted as follows,

$$\dot{W}_{net} = \dot{W}_{tur_1} - (\dot{W}_{comp1} + \dot{W}_{comp2} + \dot{W}_{comp3} + \dot{W}_{comp4} + \dot{W}_{compM1} + \dot{W}_{compM1} + \dot{W}_{compM2} + \dot{W}_{pumpM3} + \dot{W}_{pump1}) \tag{4.58}$$

The energy and exergy efficiency definitions for version 2 of the system 2 can be found as follows respectively,

$$\eta_{\text{en,overall}} = \frac{\dot{W}_{net} + \dot{Q}_{spaceheating} + \dot{Q}_{Hydrogen} + \dot{Q}_{FreshWater} + \dot{Q}_{HotWater}}{\dot{Q}_{geothermal} + \dot{Q}_{SeaWater}} \tag{4.59}$$

$$\eta_{\text{ex,overall}} = \frac{\dot{W}_{net} + \dot{E}x^{Qspace_{heating}} + \dot{Q}^{Ex_{hydrogen}} + \dot{Q}^{Ex_{Freshwater}} + \dot{Q}^{Ex_{Hotwater}}}{\dot{E}x^{Q_{geothermal}} + + \dot{Q}^{Ex_{Seahwater}}} \tag{4.60}$$

Coefficient of performances parameters COP which is generally denoted through energetic and exergetic approach as follows

$$COP_{energy} = \frac{\sum \dot{Q}_{con}}{\sum \dot{W}_{input}} \tag{4.61}$$

$$COP_{exergy} = \frac{\sum \dot{Q}_{con} \times (1 - \frac{T_o}{T_{con}})}{\sum \dot{W}_{input}} \tag{4.62}$$

where T_{con} is assumed as reaction temperature because of being temperature of the reactor where heat recovery from the CuCl heat pump occurs. The Carnot factor which comes from the finite temperature difference approach is $(1 - \frac{T_o}{T_{con}})$. $\sum \dot{W}_{input}$ is the total input power to the cascaded heat pump.

For CuCl heat pump for CuCl cycle and MgCl cycle COP can be calculated by using $\dot{Q}_{con}$definition as follows respectively,

$$\dot{Q}_{con,CuCl} = h_{CuCl} \times \dot{m}_{CuCl} + h_{O_2} \times \dot{m}_{O_2} - h_{Cu_2OCl_2} \times \dot{m}_{Cu_2OCl_2} \tag{4.62}$$

$$\dot{Q}_{con,MgCl_2} = h_{H_2O} \times \dot{m}_{H_2O} + h_{O_{MgCl_2}} \times \dot{m}_{MgCl_2} - h_{MgO} \times \dot{m}_{MgO} \tag{4.63}$$

$\dot{Q}_{con}$ is the heat recovery from CuCl heat pump to the CuCl and MgCl thermochemical cycles.

The balance equations evaluated for the system can be found in Table 4.10.

Table 4.6 Balance equations for version 2 of the system 2

Heat Exchanger 1	MBE: $\dot{m}_7 + \dot{m}_{37-3} = \dot{m}_{7-1} + \dot{m}_{37-31}$ EBE: $\dot{m}_7 \times h_7 + \dot{m}_{37-3} \times h_{37-3} = \dot{m}_{7-1} \times h_{7-1} + \dot{m}_{37-31} \times h_{37-31}$ EnBE: $\dot{m}_7 \times s_7 + \dot{m}_{27} \times s_{27} + \dot{S}_{gen,hx1} = \dot{m}_{7-1} \times s_{7-1} + \dot{m}_{37-31} \times s_{37-31}$ ExBE: $\dot{m}_7 \times ex_7 + \dot{m}_{37-3} \times ex_{37-3} = \dot{m}_{7-1} \times ex_{7-1} +$ $\dot{m}_{37-31} \times \dot{ex}_{37-31} + ExD_{hx1}$
Heat Exchanger 2	MBE: $\dot{m}_{7-1} + \dot{m}_4 = \dot{m}_{7-2} + \dot{m}_{4-1}$ EBE: $\dot{m}_{7-1} \times h_{7-1} + \dot{m}_4 \times h_4 = \dot{m}_{7-2} \times h_{7-2} + \dot{m}_{4-1} \times h_{4-1}$ EnBE: $\dot{m}_{7-1} \times s_{7-1} + \dot{m}_4 \times s_4 + \dot{S}_{gen,hx2} = \dot{m}_{7-2} \times s_{7-2} + \dot{m}_{4-1} \times s_{4-1}$ ExBE: $\dot{m}_{7-1} \times ex_{7-1} + \dot{m}_4 \times ex_4 = \dot{m}_{7-2} \times ex_{7-2} +$ $\dot{m}_{4-1} \times \dot{ex}_{4-1} + ExD_{hx2}$
Heat Exchanger 3	MBE: $\dot{m}_{16} + \dot{m}_9 = \dot{m}_{10} + \dot{m}_{16-1}$ EBE: $\dot{m}_{16} \times h_{16} + \dot{m}_9 \times h_9 = \dot{m}_{10} \times h_{10} + \dot{m}_{16-1} \times h_{16-1}$ EnBE: $\dot{m}_{16} \times s_{16} + \dot{m}_9 \times s_9 + \dot{S}_{gen,hx3} = \dot{m}_{10} \times s_{10} + \dot{m}_{16-1} \times s_{16-1}$ ExBE: $\dot{m}_{16} \times ex_{16} + \dot{m}_9 \times ex_9 = \dot{m}_{10} \times ex_{10} +$ $\dot{m}_{16-1} \times \dot{ex}_{16-1} + ExD_{hx3}$
Heat Exchanger 4	MBE: $\dot{m}_{16-1} + \dot{m}_{11} = \dot{m}_{16-2} + \dot{m}_{12}$ EBE: $\dot{m}_{16-1} \times h_{16-1} + \dot{m}_{11} \times h_{11} = \dot{m}_{16-2} \times h_{16-2} + \dot{m}_{12} \times h_{12}$ EnBE: $\dot{m}_{16-1} \times s_{16-1} + \dot{m}_{11} \times s_{11} + \dot{S}_{gen,hx4} = \dot{m}_{16-2} \times s_{16-2} +$ $\dot{m}_{12} \times s_{12}$

	ExBE: $\dot{m}_{16-1} \times ex_{16-1} + \dot{m}_{11} \times ex_{11} = \dot{m}_{16-2} \times ex_{16-2} + \dot{m}_{12} \times \dot{e}x_{12} + ExD_{hx4}$
Heat Exchanger 5	MBE: $\dot{m}_{22} + \dot{m}_{7-2} = \dot{m}_{7-3} + \dot{m}_{23}$ EBE: $\dot{m}_{22} \times h_{22} + \dot{m}_{7-2} \times h_{7-2} = \dot{m}_{7-3} \times h_{7-3} + \dot{m}_{23} \times h_{23}$ EnBE: $\dot{m}_{22} \times s_{22} + \dot{m}_{7-2} \times s_{7-2} + \dot{S}_{gen,hx5} = \dot{m}_{7-3} \times s_{7-3} + \dot{m}_{23} \times s_{23}$ ExBE: $\dot{m}_{22} \times ex_{22} + \dot{m}_{7-2} \times ex_{7-2} = \dot{m}_{7-3} \times ex_{7-3} + \dot{m}_{23} \times \dot{e}x_{23} + ExD_{hx5}$
Heat Exchanger 6	MBE: $\dot{m}_{7-3} + \dot{m}_{24} = \dot{m}_{25} + \dot{m}_{7-4}$ EBE: $\dot{m}_{7-3} \times h_{7-3} + \dot{m}_{24} \times h_{24} = \dot{m}_{25} \times h_{25} + \dot{m}_{7-4} \times h_{7-4}$ EnBE: $\dot{m}_{7-3} \times s_{7-3} + \dot{m}_{24} \times s_{24} + \dot{S}_{gen,hx6} = \dot{m}_{25} \times s_{25} + \dot{m}_{7-4} \times s_{7-4}$ ExBE: $\dot{m}_{7-3} \times ex_{7-3} + \dot{m}_{24} \times ex_{24} = \dot{m}_{25} \times ex_{25} + \dot{m}_{7-4} \times \dot{e}x_{7-4} + ExD_{hx6}$
Heat Exchanger 7	MBE: $\dot{m}_{7-4} + \dot{m}_{26} = \dot{m}_{8} + \dot{m}_{27}$ EBE: $\dot{m}_{7-4} \times h_{7-4} + \dot{m}_{26} \times h_{26} = \dot{m}_{8} \times h_{8} + \dot{m}_{27} \times h_{27}$ EnBE: $\dot{m}_{7-4} \times s_{7-4} + \dot{m}_{26} \times s_{26} + \dot{S}_{gen,hx7} = \dot{m}_{8} \times s_{8} + \dot{m}_{27} \times s_{27}$ ExBE: $\dot{m}_{7-4} \times ex_{7-4} + \dot{m}_{26} \times ex_{26} = \dot{m}_{8} \times ex_{8} + \dot{m}_{27} \times \dot{e}x_{27} + ExD_{hx7}$
Heat Exchanger 8	MBE: $\dot{m}_{34} + \dot{m}_{33} = \dot{m}_{35} + \dot{m}_{32}$ EBE: $\dot{m}_{34} \times h_{34} + \dot{m}_{33} \times h_{33} = \dot{m}_{35} \times h_{35} + \dot{m}_{32} \times h_{32}$ EnBE: $\dot{m}_{34} \times s_{34} + \dot{m}_{33} \times s_{33} + \dot{S}_{gen,hx8} = \dot{m}_{35} \times s_{35} + \dot{m}_{32} \times s_{32}$ ExBE: $\dot{m}_{34} \times ex_{34} + \dot{m}_{33} \times ex_{33} = \dot{m}_{35} \times ex_{35} + \dot{m}_{32} \times \dot{e}x_{32} + ExD_{hx8}$
Heat Exchanger 9	MBE: $\dot{m}_{35} + \dot{m}_{28} = \dot{m}_{21} + \dot{m}_{36}$ EBE: $\dot{m}_{35} \times h_{35} + \dot{m}_{28} \times h_{28} = \dot{m}_{21} \times h_{21} + \dot{m}_{36} \times h_{36}$ EnBE: $\dot{m}_{35} \times s_{35} + \dot{m}_{28} \times s_{28} + \dot{S}_{gen,hx9} = \dot{m}_{21} \times s_{21} + \dot{m}_{36} \times s_{36}$ ExBE: $\dot{m}_{35} \times ex_{35} + \dot{m}_{28} \times ex_{28} = \dot{m}_{21} \times ex_{21} + \dot{m}_{36} \times \dot{e}x_{36} + ExD_{hx9}$
Heat Exchanger 10	MBE: $\dot{m}_{36} + \dot{m}_{18} = \dot{m}_{19} + \dot{m}_{42}$ EBE: $\dot{m}_{36} \times h_{36} + \dot{m}_{18} \times h_{18} = \dot{m}_{19} \times h_{19} + \dot{m}_{42} \times h_{42}$ EnBE: $\dot{m}_{36} \times s_{36} + \dot{m}_{18} \times s_{18} + \dot{S}_{gen,hx10} = \dot{m}_{19} \times s_{19} + \dot{m}_{42} \times s_{42}$ ExBE: $\dot{m}_{36} \times ex_{36} + \dot{m}_{18} \times ex_{18} = \dot{m}_{19} \times ex_{19} + \dot{m}_{42} \times \dot{e}x_{42} + ExD_{hx10}$
Heat Exchanger 11	MBE: $\dot{m}_{43} + \dot{m}_{44} = \dot{m}_{33} + \dot{m}_{45}$ EBE: $\dot{m}_{43} \times h_{43} + \dot{m}_{44} \times h_{44} = \dot{m}_{33} \times h_{33} + \dot{m}_{45} \times h_{45}$ EnBE: $\dot{m}_{43} \times s_{43} + \dot{m}_{44} \times s_{44} + \dot{S}_{gen,hx11} = \dot{m}_{33} \times s_{21} + \dot{m}_{45} \times s_{45}$ ExBE: $\dot{m}_{43} \times ex_{43} + \dot{m}_{44} \times ex_{44} = \dot{m}_{33} \times ex_{33} + \dot{m}_{45} \times \dot{e}x_{45} + ExD_{hx11}$
Compressor 1	MBE: $\dot{m}_{8} = \dot{m}_{9}$ EBE: $\dot{m}_{8} \times h_{8} + \dot{W}_{comp1} = \dot{m}_{9} \times h_{9}$ EnBE: $\dot{m}_{8} \times s_{8} + \dot{S}_{gen,comp1} = \dot{m}_{9} \times s_{9}$ ExBE: $\dot{m}_{8} \times ex_{8} + \dot{E}x_{Q_{comp1}} = \dot{m}_{9} \times ex_{9} + \dot{E}xD_{comp1}$
Compressor 2	MBE: $\dot{m}_{10} = \dot{m}_{11}$ EBE: $\dot{m}_{10} \times h_{10} + \dot{W}_{comp2} = \dot{m}_{11} \times h_{11}$ EnBE: $\dot{m}_{10} \times s_{10} + \dot{S}_{gen,comp2} = \dot{m}_{11} \times s_{11}$ ExBE: $\dot{m}_{10} \times ex_{10} + \dot{E}x_{Q_{comp2}} = \dot{m}_{11} \times ex_{11} + \dot{E}xD_{comp2}$
Compressor 3	MBE: $\dot{m}_{12} = \dot{m}_{13}$ EBE: $\dot{m}_{12} \times h_{12} + \dot{W}_{comp3} = \dot{m}_{13} \times h_{13}$ EnBE: $\dot{m}_{12} \times s_{12} + \dot{S}_{gen,comp3} = \dot{m}_{13} \times s_{13}$ ExBE: $\dot{m}_{12} \times ex_{12} + \dot{E}x_{Q_{comp3}} = \dot{m}_{13} \times ex_{13} + \dot{E}xD_{comp3}$
Compressor 4	MBE: $\dot{m}_{32} = \dot{m}_{31}$ EBE: $\dot{m}_{32} \times h_{32} + \dot{W}_{comp4} = \dot{m}_{31} \times h_{31}$

	EnBE: $\dot{m}_{32} \times s_{32} + \dot{S}_{gen,comp4} = \dot{m}_{31} \times s_{31}$ ExBE: $\dot{m}_{32} \times ex_{32} + \dot{E}x_{Q_{comp4}} = \dot{m}_{31} \times ex_{31} + \dot{E}xD_{comp4}$
Turbine 1	MBE: $\dot{m}_{19} = \dot{m}_{20}$ EBE: $\dot{m}_{19} \times h_{19} = \dot{m}_{20} \times h_{20} + \dot{W}_{tur1}$ EnBE: $\dot{m}_{19} \times s_{19} + \dot{S}_{gen,tur1} = \dot{m}_{20} \times s_{20}$ ExBE: $\dot{m}_{19} \times ex_{19} + \dot{E}x_{Q_{tur1}} = \dot{m}_{20} \times ex_{20} + \dot{E}xD_{tur1}$
Pump 1	MBE: $\dot{m}_{17} = \dot{m}_{18}$ EBE: $\dot{m}_{17} \times h_{17} + \dot{W}_{Pump1} = \dot{m}_{18} \times h_{18}$ EnBE: $\dot{m}_{17} \times s_{17} + \dot{S}_{gen,Pump1} = \dot{m}_{18} \times s_{18}$ ExBE: $\dot{m}_{17} \times ex_{17} + \dot{W}_{Pump1} = \dot{m}_{18} \times ex_{18} + \dot{E}xD_{Pump1}$
Pump 2	MBE: $\dot{m}_{41} = \dot{m}_{34}$ EBE: $\dot{m}_{41} \times h_{41} + \dot{W}_{Pump2} = \dot{m}_{34} \times h_{34}$ EnBE: $\dot{m}_{41} \times s_{41} + \dot{S}_{gen,Pump2} = \dot{m}_{34} \times s_{34}$ ExBE: $\dot{m}_{41} \times ex_{41} + \dot{W}_{Pump1} = \dot{m}_{34} \times ex_{34} + \dot{E}xD_{Pump2}$
Pump 3	MBE: $\dot{m}_{14} = \dot{m}_{15}$ EBE: $\dot{m}_{14} \times h_{14} + \dot{W}_{Pump3} = \dot{m}_{15} \times h_{15}$ EnBE: $\dot{m}_{14} \times s_{14} + \dot{S}_{gen,Pump3} = \dot{m}_{15} \times s_{15}$ ExBE: $\dot{m}_{14} \times ex_{14} + \dot{W}_{Pump1} = \dot{m}_{15} \times ex_{15} + \dot{E}xD_{Pump3}$
Pump 4	MBE: $\dot{m}_{37} = \dot{m}_{38}$ EBE: $\dot{m}_{37} \times h_{37} + \dot{W}_{Pump4} = \dot{m}_{38} \times h_{38}$ EnBE: $\dot{m}_{37} \times s_{37} + \dot{S}_{gen,Pump4} = \dot{m}_{38} \times s_{38}$ ExBE: $\dot{m}_{37} \times ex_{37} + \dot{W}_{Pump1} = \dot{m}_{38} \times ex_{38} + \dot{E}xD_{Pump4}$
Expansion Valve	MBE: $\dot{m}_{30} = \dot{m}_{33}$ EBE: $\dot{m}_{30} \times h_{30} = \dot{m}_{33} \times h_{33}$ EnBE: $\dot{m}_{30} \times s_{30} + \dot{S}_{gen,exp} = \dot{m}_{33} \times s_{33}$ ExBE: $\dot{m}_{30} \times ex_{30} = \dot{m}_{33} \times ex_{33} + \dot{E}xD_{exp}$

4.4 System 1: Thermodynamic Analysis

In the first integrated system, carbon dioxide hydrogenation methanol synthesis reactor is used to produce methanol from hydrogen. The high-temperature electrolyzer (HTE) is used to produce hydrogen to be used in the methanol synthesis reactor due to a couple of advantages. The specifications of high-temperature electrolyzer are shown as listed in Table 4.6

In this study, higher heating values (HHV) are used in the systems, as well as in the energetic value calculations of methanol which is produced from the methanol synthesis reactor. Energetic and exergetic parameters are denoted in Table 4.7 for all five systems. In this context, energy and exergy efficiency calculations can be conducted through the methanol synthesis reactor.

$$\eta_{energy,MethanolSR} = \frac{\dot{m}_{CH_3OH} \times \mathrm{H}HV_{methanol}}{E_{input}} \tag{4.46}$$

$$\eta_{exergy,MethanolSR} = \frac{\dot{m}_{CH_3OH} \times \mathrm{ex}_{\mathrm{CH_3OH}}}{E_{input}} \quad (4.47)$$

Table 4.7 Specifications of HTE

High-Temperature Electrolysis Specifications	
Electrode Type	Ni-doped Ceramic
Cell Temperature (°C)	700-1000
Typical Pressure (bar)	1-15
Nominal Stack Efficiency	100%
Nominal System Efficiency	76-81%
Specific energy consumption rate (kWh/m^3)	3
Investment costs ($/kW)	2200

where $\dot{m}_{CH_3OH}$ is the production of methanol synthesis reactor and E_{input} is the required energy for the methanol synthesis process. On the other hand, another useful output produced in the system is the freshwater. Freshwater provided from the desalination unit is used both to feed the high-temperature electrolyzer and to meet the community's need for fresh water. The specific energy and chemical exergy values are used to calculate the energy values in the inclusion of the efficiency calculations of the freshwater produced. The energy and exergy values for produced freshwater is calculated in this study as follows,

$$\dot{Q}_{\mathrm{water}} = h_{\mathrm{water}} \times \dot{m}_{\mathrm{Water}} \quad (4.48)$$

$$\dot{Q}^{Ex_{\mathrm{Water}}} = \overline{ex}_{ch_{Water}} \times \dot{m}_{Water} \quad (4.49)$$

where h_{water} is the specific enthalpy of water in terms of kJ/kg and $\overline{ex}_{ch_{Water}}$ is the chemical exergy value.

In order to calculate the overall system efficiency, the net work is calculated. The work output which can be achieved from the first system can be evaluated as follows,

$$\dot{W}_{net} = \dot{W}_{tur_1} + \dot{W}_{tur_2} + \dot{W}_{tur_3} + \dot{W}_{wind_{out}} - (\dot{W}_{comp} + \dot{W}_{pump1} + \dot{W}_{pump2} + \dot{W}_{pump3} + \dot{W}_{pump4}) \quad (4.50)$$

The overall efficiencies through energy and exergy for the first system are evaluated in equation 4.51 and 4.52 respectively,

$$\eta_{\text{en,overall}} = \frac{\dot{W}_{net} + \dot{Q}_{spaceheating} + \dot{Q}_{Methanol} + \dot{Q}_{FreshWater} + \dot{Q}_{HotWater}}{\dot{Q}_{solar} + \dot{Q}_{geothermal} + \dot{W}_{Wind_{input}}} \quad (4.51)$$

$$\eta_{\text{ex,overall}} = \frac{\dot{W}_{net} + \dot{E}x^{Q_{heating}} + \dot{Q}^{Ex_{methanol}} + \dot{Q}^{Ex_{Freshwater}} + \dot{Q}^{Ex_{Hotwater}}}{\dot{E}x^{Q_{solar}} + \dot{E}x^{Q_{geothermal}} + \dot{W}_{Wind_{input}}} \quad (4.52)$$

The mass balance (MBE), energy balance (EBE), entropy balance (EnBE) and exergy balance (ExBE) are defined in Table 4.8 for major system components as well as exergy destruction definitions.

Table 4.8 Energetic and exergetic parameters

Parameters	**Values**
Higher Heating Value for Methanol ($HHV_{methanol}$)	23 MJ/kg
Chemical Exergy of the Liquid Methanol (Ex_{chMeOH})	718 kJ/mol
Higher Heating Value for Hydrogen ($HHV_{hydrogen}$)	141.7 MJ/kg
Chemical Exergy of the Hydrogen (Ex_{ch_2})	118 MJ/mol
Chemical Exergy of the Liquid Water	1.3 kJ/mol

Table 4.9 Balance equations for system 1

Heat Exchanger 1	MBE: $\dot{m}_{28} + \dot{m}_{22} = \dot{m}_{23} + \dot{m}_{25}$ EBE: $\dot{m}_{28} \times h_{28} + \dot{m}_{22} \times h_{22} = \dot{m}_{23} \times h_{23} + \dot{m}_{25} \times h_{25}$ EnBE: $\dot{m}_{28} \times s_{28} + \dot{m}_{22} \times s_{22} + \dot{S}_{gen,hx1} = \dot{m}_{23} \times s_{23} + \dot{m}_{25} \times s_{25}$ ExBE: $\dot{m}_{28} \times ex_{28} + \dot{m}_{22} \times ex_{22} = \dot{m}_{23} \times ex_{23} + \dot{m}_{25} \times \dot{ex}_{25} + ExD_{hx1}$
Heat Exchanger 2	MBE: $\dot{m}_{21} + \dot{m}_{23} = \dot{m}_{20} + \dot{m}_{24}$ EBE: $\dot{m}_{21} \times h_{21} + \dot{m}_{23} \times h_{23} = \dot{m}_{20} \times h_{20} + \dot{m}_{24} \times h_{24}$ EnBE: $\dot{m}_{21} \times s_{21} + \dot{m}_{23} \times s_{23} + \dot{S}_{gen,hx2} = \dot{m}_{20} \times s_{20} + \dot{m}_{24} \times s_{24}$ ExBE: $\dot{m}_{21} \times ex_{10} + \dot{m}_{23} \times ex_{23} = \dot{m}_{20} \times ex_{20} + \dot{m}_{24} \times \dot{ex}_{24} + ExD_{hx2}$
Heat Exchanger 3	MBE: $\dot{m}_8 + \dot{m}_{13} = \dot{m}_9 + \dot{m}_{11}$ EBE: $\dot{m}_8 \times h_8 + \dot{m}_{13} \times h_{13} = \dot{m}_9 \times h_9 + \dot{m}_{11} \times h_{11}$ EnBE: $\dot{m}_8 \times s_8 + \dot{m}_{13} \times s_{13} + \dot{S}_{gen,hx3} = \dot{m}_9 \times s_9 + \dot{m}_{11} \times s_{11}$ ExBE: $\dot{m}_8 \times ex_8 + \dot{m}_{13} \times ex_{13} = \dot{m}_9 \times ex_9 + \dot{m}_{11} \times \dot{ex}_{11} + ExD_{hx3}$

Heat Exchanger 4	MBE: $\dot{m}_{31} + \dot{m}_3 = \dot{m}_4 + \dot{m}_{32}$ EBE: $\dot{m}_{31} \times h_{31} + \dot{m}_3 \times h_3 = \dot{m}_4 \times h_4 + \dot{m}_{32} \times h_{32}$ EnBE: $\dot{m}_{31} \times s_{31} + \dot{m}_3 \times s_3 + \dot{S}_{gen,hx4} = \dot{m}_4 \times s_4 + \dot{m}_{32} \times s_{32}$ ExBE: $\dot{m}_{31} \times ex_{31} + \dot{m}_3 \times ex_3 = \dot{m}_4 \times ex_4 + \dot{m}_{32} \times \dot{ex}_{32} + ExD_{hx4}$
Heat Exchanger 5	MBE: $\dot{m}_{10} + \dot{m}_6 = \dot{m}_5 + \dot{m}_7$ EBE: $\dot{m}_{10} \times h_{10} + \dot{m}_6 \times h_6 = \dot{m}_5 \times h_5 + \dot{m}_7 \times h_7$ EnBE: $\dot{m}_{10} \times s_{10} + \dot{m}_6 \times s_6 + \dot{S}_{gen,hx5} = \dot{m}_5 \times s_5 + \dot{m}_7 \times s_7$ ExBE: $\dot{m}_{10} \times ex_{10} + \dot{m}_6 \times ex_6 = \dot{m}_5 \times ex_5 + \dot{m}_7 \times \dot{ex}_7 + ExD_{hx5}$
Heat Exchanger 6	MBE: $\dot{m}_5 + \dot{m}_{40} = \dot{m}_6 + \dot{m}_{41}$ EBE: $\dot{m}_5 \times h_5 + \dot{m}_{40} \times h_{40} = \dot{m}_6 \times h_6 + \dot{m}_{41} \times h_{41}$ EnBE: $\dot{m}_5 \times s_5 + \dot{m}_{40} \times s_{40} + \dot{S}_{gen,hx6} = \dot{m}_6 \times s_6 + \dot{m}_{41} \times s_{41}$ ExBE: $\dot{m}_5 \times ex_5 + \dot{m}_{40} \times ex_{40} = \dot{m}_6 \times ex_6 + \dot{m}_{41} \times \dot{ex}_{41} + ExD_{hx6}$
Heat Exchanger 7	MBE: $\dot{m}_4 + \dot{m}_{39} = \dot{m}_{40} + \dot{m}_3$ EBE: $\dot{m}_4 \times h_4 + \dot{m}_{39} \times h_{39} = \dot{m}_{40} \times h_{40} + \dot{m}_3 \times h_3$ EnBE: $\dot{m}_4 \times s_4 + \dot{m}_{39} \times s_{39} + \dot{S}_{gen,hx7} = \dot{m}_{40} \times s_{40} + \dot{m}_3 \times s_3$ ExBE: $\dot{m}_4 \times ex_4 + \dot{m}_{39} \times ex_{39} = \dot{m}_{40} \times ex_{40} + \dot{m}_3 \times \dot{ex}_3 + ExD_{hx7}$
Heat Exchanger 8	*MBE:* $\dot{m}_2 + \dot{m}_{41} = \dot{m}_{39} + \dot{m}_{37}$ *EBE:* $\dot{m}_2 \times h_2 + \dot{m}_{41} \times h_{41} = \dot{m}_{39} \times h_{39} + \dot{m}_{37} \times h_{37}$ *EnBE:* $\dot{m}_2 \times s_2 + \dot{m}_{41} \times s_{41} + \dot{S}_{gen,HX8} = \dot{m}_{39} \times s_{39} + \dot{m}_{37} \times s_{37}$ *ExBE:* $\dot{m}_2 \times ex_2 + \dot{m}_{41} \times ex_{41} + \dot{E}x_{HX8} = \dot{m}_{39} \times ex_{39} + \dot{m}_{37} \times ex_{37} + \dot{E}xD_{HX9}$
Heat Exchanger 9	*MBE:* $\dot{m}_{19} + \dot{m}_{43} = \dot{m}_{42} + \dot{m}_{44}$ *EBE:* $\dot{m}_{19} \times h_{19} + \dot{m}_{43} \times h_{43} = \dot{m}_{42} \times h_{42} + \dot{m}_{44} \times h_{44}$ *EnBE:* $\dot{m}_{19} \times s_{19} + \dot{m}_{43} \times s_{43} + \dot{S}_{gen,HX9} = \dot{m}_{42} \times s_{42} + \dot{m}_{44} \times s_{44}$ *ExBE:* $\dot{m}_{19} \times ex_{19} + \dot{m}_{43} \times ex_{43} + \dot{E}x_{HX9} = \dot{m}_{42} \times ex_{42} + \dot{m}_{44} \times ex_{44} + \dot{E}xD_{HX9}$
Compressor	MBE: $\dot{m}_{17} = \dot{m}_{16}$ EBE: $\dot{m}_{17} \times h_{17} + \dot{W}_{comp} = \dot{m}_{16} \times h_{16}$ EnBE: $\dot{m}_{17} \times s_{17} + \dot{S}_{gen,comp} = \dot{m}_{16} \times s_{16}$ ExBE: $\dot{m}_{17} \times ex_{17} + \dot{E}x_{Q_{comp}} = \dot{m}_{16} \times ex_{16} + \dot{E}xD_{comp}$
Turbine 1	MBE: $\dot{m}_{25} = \dot{m}_{26}$ EBE: $\dot{m}_{25} \times h_{25} = \dot{m}_{26} \times h_{26} + \dot{W}_{tur1}$ EnBE: $\dot{m}_{25} \times s_{25} + \dot{S}_{gen,tur1} = \dot{m}_{26} \times s_{26}$ ExBE: $\dot{m}_{25} \times ex_{25} + \dot{E}x_{Q_{tur1}} = \dot{m}_{26} \times ex_{26} + \dot{E}xD_{tur1}$
Turbine 2	MBE: $\dot{m}_7 = \dot{m}_8$ EBE: $\dot{m}_7 \times h_7 = \dot{m}_8 \times h_8 + \dot{W}_{tur2}$ EnBE: $\dot{m}_7 \times s_7 + \dot{S}_{gen,tur2} = \dot{m}_8 \times s_8$ ExBE: $\dot{m}_7 \times ex_7 + \dot{E}x_{Q_{tur2}} = \dot{m}_8 \times ex_8 + \dot{E}xD_{tur2}$
Turbine 3	MBE: $\dot{m}_1 = \dot{m}_2$ EBE: $\dot{m}_1 \times h_1 = \dot{m}_2 \times h_2 + \dot{W}_{tur3}$ EnBE: $\dot{m}_1 \times s_1 + \dot{S}_{gen,tur3} = \dot{m}_2 \times s_2$ ExBE: $\dot{m}_1 \times ex_1 + \dot{E}x_{Q_{tur3}} = \dot{m}_2 \times ex_2 + \dot{E}xD_{tur3}$
Pump 1	MBE: $\dot{m}_{27} = \dot{m}_{28}$ EBE: $\dot{m}_{27} \times h_{27} + \dot{W}_{Pump1} = \dot{m}_{28} \times h_{28}$ EnBE: $\dot{m}_{27} \times s_{27} + \dot{S}_{gen,Pump1} = \dot{m}_{28} \times s_{28}$ ExBE: $\dot{m}_{27} \times ex_{27} + \dot{W}_{Pump1} = \dot{m}_{28} \times ex_{28} + \dot{E}xD_{Pump1}$

Pump 2	MBE: $\dot{m}_{11} = \dot{m}_{12}$ EBE: $\dot{m}_{11} \times h_{11} + \dot{W}_{Pump2} = \dot{m}_{12} \times h_{12}$ EnBE: $\dot{m}_{11} \times s_{11} + \dot{S}_{gen,Pump2} = \dot{m}_{12} \times s_{12}$ ExBE: $\dot{m}_{11} \times ex_{11} + \dot{W}_{Pump2} = \dot{m}_{12} \times ex_{12} + \dot{E}xD_{Pump2}$
Pump 3	MBE: $\dot{m}_{9} = \dot{m}_{10}$ EBE: $\dot{m}_{9} \times h_{9} + \dot{W}_{Pump3} = \dot{m}_{10} \times h_{10}$ EnBE: $\dot{m}_{9} \times s_{9} + \dot{S}_{gen,Pump3} = \dot{m}_{10} \times s_{10}$ ExBE: $\dot{m}_{9} \times ex_{9} + \dot{W}_{Pump3} = \dot{m}_{10} \times ex_{10} + \dot{E}xD_{Pump3}$
Space Heating	MBE: $\dot{m}_{14} = \dot{m}_{15}$ EBE: $\dot{m}_{14} \times h_{14} = \dot{m}_{15} \times h_{15} + \dot{Q}_{COM}$ EnBE: $\dot{m}_{14} \times s_{14} + \dot{S}_{gen,COM} = \dot{m}_{15} \times s_{15} + \frac{\dot{Q}_{COM}}{T_{COM}}$ ExBE: $\dot{m}_{14} \times ex_{14} = \dot{m}_{15} \times ex_{15} + \dot{E}x_{Q_{COM}} + \dot{E}xD_{COM}$
Desalination	MBE: $\dot{m}_{29} = \dot{m}_{30} + \dot{m}_{31} + \dot{m}_{29}$ EBE: $\dot{m}_{29} \times h_{29} + \dot{Q}_{DE} = \dot{m}_{30} \times h_{30} + \dot{m}_{31} \times h_{31}$ EnBE: $\dot{m}_{29} \times s_{29} + \frac{\dot{Q}_{DE}}{T_{DE}} + \dot{S}_{gen,hxDE} = \dot{m}_{30} \times s_{30} + \dot{m}_{31} \times s_{31}$ ExBE: $\dot{m}_{29} \times ex_{29} + \dot{E}x_{Q_{DE}} = \dot{m}_{30} \times ex_{30} + \dot{m}_{31} \times ex_{31} + ExD_{hxDE}$

4.4.5 System 2 Version 1

In version 1 of the system 2, hydrogen is one of the useful outlets of production instead of methanol at system 1. CuCl cycle which is the thermochemical process is used to produce hydrogen and Aspen Plus (software) is used to simulate this process. Energy and exergy efficiencies can be evaluated as follows in a wider perspective,

$$\eta_{energy,CuCl} = \frac{\dot{m}_{H_2} \times \mathrm{H}HV_{hydrogen}}{E_{input}} \tag{4.53}$$

$$\eta_{exergy,CuCl} = \frac{\dot{m}_{H_2} \times \mathrm{ex}_{H_2}}{E_{input}} \tag{4.54}$$

where the higher heating value is used for energetic calculation for hydrogen mass flow. Other subsystems for this system are examined in previous sections. The energetic and exergetic parameters for hydrogen can be found in Table 4.7.

The net work to be used in energy and exergy efficiency calculations are evaluated as follows,

$$\dot{W}_{net} = \dot{W}_{tur_1} + \dot{W}_{tur_2} + \dot{W}_{tur_4} - (\dot{W}_{comp} + \dot{W}_{pump1} + \dot{W}_{pump2} + \dot{W}_{pump3} + \dot{W}_{pump4} + \dot{W}_{pump5}) \tag{4.55}$$

Equation 4.56 and 4.57 denote the overall system energy and exergy efficiency for version 1 of the system 2,

$$\eta_{\text{en,overall}} = \frac{\dot{W}_{net} + \dot{Q}_{spaceheating} + \dot{Q}_{Hydrogen} + \dot{Q}_{FreshWater} + \dot{Q}_{HotWater}}{\dot{Q}_{solar} + \dot{Q}_{geothermal} + \dot{Q}_{SeaWater}} \quad (4.56)$$

$$\eta_{\text{ex,overall}} = \frac{\dot{W}_{net} + \dot{E}x^{Qspace_{heating}} + \dot{Q}^{Ex_{hydrogen}} + \dot{Q}^{Ex_{Freshwater}} + \dot{Q}^{Ex_{Hotwater}}}{\dot{E}x^{Q_{solar}} + \dot{E}x^{Q_{geothermal}} + +\dot{Q}^{Ex_{Seahwater}}} \quad (4.57)$$

Balance equations for major system components for version 1 of system 2 are listed in Table 4.9.

Table 4.10 Balance equations for version 1 of the system 2

Heat Exchanger 1	MBE: $\dot{m}_{21} + \dot{m}_{27} = \dot{m}_{24} + \dot{m}_{22}$ EBE: $\dot{m}_{21} \times h_{21} + \dot{m}_{27} \times h_{27} = \dot{m}_{24} \times h_{24} + \dot{m}_{22} \times h_{22}$ EnBE: $\dot{m}_{21} \times s_{21} + \dot{m}_{27} \times s_{27} + \dot{S}_{gen,hx1} = \dot{m}_{24} \times s_{24} + \dot{m}_{22} \times s_{22}$ ExBE: $\dot{m}_{21} \times ex_{21} + \dot{m}_{27} \times ex_{27} = \dot{m}_{24} \times ex_{24} + \dot{m}_{22} \times \dot{ex}_{22} + ExD_{hx1}$
Heat Exchanger 2	MBE: $\dot{m}_{22} + \dot{m}_{18} = \dot{m}_{17} + \dot{m}_{23}$ EBE: $\dot{m}_{22} \times h_{22} + \dot{m}_{18} \times h_{18} = \dot{m}_{17} \times h_{17} + \dot{m}_{23} \times h_{23}$ EnBE: $\dot{m}_{22} \times s_{22} + \dot{m}_{18} \times s_{18} + \dot{S}_{gen,hx2} = \dot{m}_{17} \times s_{17} + \dot{m}_{23} \times s_{23}$ ExBE: $\dot{m}_{22} \times ex_{22} + \dot{m}_{18} \times ex_{18} = \dot{m}_{24} \times ex_{24} + \dot{m}_{23} \times \dot{ex}_{23} + ExD_{hx2}$
Heat Exchanger 3	MBE: $\dot{m}_{13} + \dot{m}_{8} = \dot{m}_{11} + \dot{m}_{9}$ EBE: $\dot{m}_{13} \times h_{13} + \dot{m}_{8} \times h_{8} = \dot{m}_{11} \times h_{11} + \dot{m}_{9} \times h_{9}$ EnBE: $\dot{m}_{13} \times s_{13} + \dot{m}_{8} \times s_{8} + \dot{S}_{gen,hx3} = \dot{m}_{11} \times s_{11} + \dot{m}_{9} \times s_{9}$ ExBE: $\dot{m}_{13} \times ex_{13} + \dot{m}_{8} \times ex_{8} = \dot{m}_{11} \times ex_{11} + \dot{m}_{9} \times \dot{ex}_{9} + ExD_{hx3}$
Heat Exchanger 4	MBE: $\dot{m}_{39} + \dot{m}_{46} = \dot{m}_{40} + \dot{m}_{42}$ EBE: $\dot{m}_{39} \times h_{39} + \dot{m}_{46} \times h_{46} = \dot{m}_{40} \times h_{40} + \dot{m}_{42} \times h_{42}$ EnBE: $\dot{m}_{39} \times s_{39} + \dot{m}_{46} \times s_{46} + \dot{S}_{gen,hx4} = \dot{m}_{40} \times s_{40} + \dot{m}_{42} \times s_{42}$ ExBE: $\dot{m}_{39} \times ex_{39} + \dot{m}_{46} \times ex_{46} = \dot{m}_{40} \times ex_{40} + \dot{m}_{42} \times \dot{ex}_{42} + ExD_{hx4}$
Heat Exchanger 5	MBE: $\dot{m}_{6} + \dot{m}_{10} = \dot{m}_{7} + \dot{m}_{5}$ EBE: $\dot{m}_{6} \times h_{6} + \dot{m}_{10} \times h_{10} = \dot{m}_{7} \times h_{7} + \dot{m}_{5} \times h_{5}$ EnBE: $\dot{m}_{6} \times s_{6} + \dot{m}_{10} \times s_{10} + \dot{S}_{gen,hx5} = \dot{m}_{7} \times s_{7} + \dot{m}_{5} \times s_{5}$ ExBE: $\dot{m}_{6} \times ex_{6} + \dot{m}_{10} \times ex_{10} = \dot{m}_{7} \times ex_{7} + \dot{m}_{5} \times \dot{ex}_{5} + ExD_{hx5}$
Heat Exchanger 6	MBE: $\dot{m}_{5} + \dot{m}_{40} = \dot{m}_{6} + \dot{m}_{41}$ EBE: $\dot{m}_{5} \times h_{5} + \dot{m}_{40} \times h_{40} = \dot{m}_{6} \times h_{6} + \dot{m}_{41} \times h_{41}$ EnBE: $\dot{m}_{5} \times s_{5} + \dot{m}_{40} \times s_{40} + \dot{S}_{gen,hx6} = \dot{m}_{6} \times s_{6} + \dot{m}_{41} \times s_{41}$ ExBE: $\dot{m}_{5} \times ex_{5} + \dot{m}_{40} \times ex_{40} = \dot{m}_{6} \times ex_{6} + \dot{m}_{41} \times \dot{ex}_{41} + ExD_{hx6}$
Heat Exchanger 7	MBE: $\dot{m}_{2} + \dot{m}_{41-1} = \dot{m}_{39} + \dot{m}_{37}$ EBE: $\dot{m}_{2} \times h_{2} + \dot{m}_{41-1} \times h_{41-1} = \dot{m}_{39} \times h_{39} + \dot{m}_{37} \times h_{37}$ EnBE: $\dot{m}_{2} \times s_{2} + \dot{m}_{41-1} \times s_{41-1} + \dot{S}_{gen,hx7} = \dot{m}_{39} \times s_{39} + \dot{m}_{37} \times s_{37}$ ExBE: $\dot{m}_{2} \times ex_{2} + \dot{m}_{41-1} \times ex_{41-1} = \dot{m}_{39} \times ex_{39} + \dot{m}_{37} \times \dot{ex}_{37} + ExD_{hx7}$
Heat Exchanger 8	*MBE:* $\dot{m}_{48} + \dot{m}_{19} = \dot{m}_{49} + \dot{m}_{47}$ *EBE:* $\dot{m}_{48} \times h_{48} + \dot{m}_{19} \times h_{19} = \dot{m}_{49} \times h_{49} + \dot{m}_{47} \times h_{47}$ *EnBE:* $\dot{m}_{48} \times s_{48} + \dot{m}_{19} \times s_{19} + \dot{S}_{gen,HX8} = \dot{m}_{49} \times s_{49} + \dot{m}_{47} \times s_{47}$ *ExBE:* $\dot{m}_{43} \times ex_{43} + \dot{m}_{19} \times ex_{19} + \dot{E}x_{HX8} = \dot{m}_{49} \times ex_{49} + \dot{m}_{47} \times ex_{47} + \dot{E}xD_{HX9}$
Heat Exchanger 9	*MBE:* $\dot{m}_{44} + \dot{m}_{s2} = \dot{m}_{45} + \dot{m}_{s3}$ *EBE:* $\dot{m}_{44} \times h_{44} + \dot{m}_{s2} \times h_{s2} = \dot{m}_{45} \times h_{45} + \dot{m}_{s3} \times h_{s3}$ *EnBE:* $\dot{m}_{44} \times s_{44} + \dot{m}_{s2} \times s_{s2} + \dot{S}_{gen,HX9} = \dot{m}_{45} \times s_{45} + \dot{m}_{s3} \times s_{s3}$

	ExBE: $\dot{m}_{44} \times ex_{44} + \dot{m}_{s2} \times ex_{s2} + \dot{E}x_{HX9} = \dot{m}_{45} \times ex_{45} + \dot{m}_{s3} \times ex_{s3} + \dot{E}xD_{HX9}$
Compressor	MBE: $\dot{m}_{17} = \dot{m}_{16}$ EBE: $\dot{m}_{17} \times h_{17} + \dot{W}_{comp} = \dot{m}_{16} \times h_{16}$ EnBE: $\dot{m}_{17} \times s_{17} + \dot{S}_{gen,comp} = \dot{m}_{16} \times s_{16}$ ExBE: $\dot{m}_{17} \times ex_{17} + \dot{E}x_{Q_{comp}} = \dot{m}_{16} \times ex_{16} + \dot{E}xD_{comp}$
Turbine 1	MBE: $\dot{m}_{24} = \dot{m}_{25}$ EBE: $\dot{m}_{24} \times h_{24} = \dot{m}_{25} \times h_{25} + \dot{W}_{tur1}$ EnBE: $\dot{m}_{24} \times s_{24} + \dot{S}_{gen,tur1} = \dot{m}_{25} \times s_{25}$ ExBE: $\dot{m}_{24} \times ex_{24} + \dot{E}x_{Q_{tur1}} = \dot{m}_{25} \times ex_{25} + \dot{E}xD_{tur1}$
Turbine 2	MBE: $\dot{m}_{7} = \dot{m}_{8}$ EBE: $\dot{m}_{7} \times h_{7} = \dot{m}_{8} \times h_{8} + \dot{W}_{tur2}$ EnBE: $\dot{m}_{7} \times s_{7} + \dot{S}_{gen,tur2} = \dot{m}_{8} \times s_{8}$ ExBE: $\dot{m}_{7} \times ex_{7} + \dot{E}x_{Q_{tur2}} = \dot{m}_{8} \times ex_{8} + \dot{E}xD_{tur2}$
Turbine 3	MBE: $\dot{m}_{1} = \dot{m}_{2}$ EBE: $\dot{m}_{1} \times h_{1} = \dot{m}_{2} \times h_{2} + \dot{W}_{tur3}$ EnBE: $\dot{m}_{1} \times s_{1} + \dot{S}_{gen,tur3} = \dot{m}_{2} \times s_{2}$ ExBE: $\dot{m}_{1} \times ex_{1} + \dot{E}x_{Q_{tur3}} = \dot{m}_{2} \times ex_{2} + \dot{E}xD_{tur3}$
Turbine 4	MBE: $\dot{m}_{42} = \dot{m}_{43}$ EBE: $\dot{m}_{42} \times h_{42} = \dot{m}_{43} \times h_{43} + \dot{W}_{tur4}$ EnBE: $\dot{m}_{42} \times s_{42} + \dot{S}_{gen,tur4} = \dot{m}_{43} \times s_{43}$ ExBE: $\dot{m}_{42} \times ex_{42} + \dot{E}x_{Q_{tur4}} = \dot{m}_{43} \times ex_{43} + \dot{E}xD_{tur4}$
Pump 1	MBE: $\dot{m}_{26} = \dot{m}_{27}$ EBE: $\dot{m}_{26} \times h_{26} + \dot{W}_{Pump1} = \dot{m}_{27} \times h_{27}$ EnBE: $\dot{m}_{26} \times s_{26} + \dot{S}_{gen,Pump1} = \dot{m}_{27} \times s_{27}$ ExBE: $\dot{m}_{26} \times ex_{26} + \dot{W}_{Pump1} = \dot{m}_{27} \times ex_{27} + \dot{E}xD_{Pump1}$
Pump 2	MBE: $\dot{m}_{26} = \dot{m}_{27}$ EBE: $\dot{m}_{26} \times h_{26} + \dot{W}_{Pump1} = \dot{m}_{27} \times h_{27}$ EnBE: $\dot{m}_{26} \times s_{26} + \dot{S}_{gen,Pump1} = \dot{m}_{27} \times s_{27}$ ExBE: $\dot{m}_{26} \times ex_{26} + \dot{W}_{Pump1} = \dot{m}_{27} \times ex_{27} + \dot{E}xD_{Pump1}$
Pump 3	MBE: $\dot{m}_{20} = \dot{m}_{21}$ EBE: $\dot{m}_{20} \times h_{20} + \dot{W}_{Pump3} = \dot{m}_{21} \times h_{21}$ EnBE: $\dot{m}_{20} \times s_{20} + \dot{S}_{gen,Pump3} = \dot{m}_{21} \times s_{21}$ ExBE: $\dot{m}_{20} \times ex_{20} + \dot{W}_{Pump1} = \dot{m}_{21} \times ex_{21} + \dot{E}xD_{Pump3}$
Pump 4	MBE: $\dot{m}_{37} = \dot{m}_{38}$ EBE: $\dot{m}_{37} \times h_{37} + \dot{W}_{Pump4} = \dot{m}_{38} \times h_{38}$ EnBE: $\dot{m}_{37} \times s_{37} + \dot{S}_{gen,Pump4} = \dot{m}_{38} \times s_{38}$ ExBE: $\dot{m}_{37} \times ex_{37} + \dot{W}_{Pump1} = \dot{m}_{38} \times ex_{38} + \dot{E}xD_{Pump4}$
Pump 5	MBE: $\dot{m}_{45} = \dot{m}_{46}$ EBE: $\dot{m}_{45} \times h_{45} + \dot{W}_{Pump5} = \dot{m}_{46} \times h_{46}$ EnBE: $\dot{m}_{45} \times s_{45} + \dot{S}_{gen,Pump5} = \dot{m}_{46} \times s_{46}$ ExBE: $\dot{m}_{45} \times ex_{45} + \dot{W}_{Pump1} = \dot{m}_{46} \times ex_{46} + \dot{E}xD_{Pump5}$
Pump 6	MBE: $\dot{m}_{41} = \dot{m}_{41-1}$ EBE: $\dot{m}_{41} \times h_{41} + \dot{W}_{Pump6} = \dot{m}_{41-1} \times h_{41-1}$

	EnBE: $\dot{m}_{41} \times s_{41} + \dot{S}_{gen,Pump6} = \dot{m}_{41-1} \times s_{41-1}$ ExBE: $\dot{m}_{41} \times ex_{41} + \dot{W}_{Pump1} = \dot{m}_{41-1} \times ex_{41-1} + \dot{E}xD_{Pump6}$
Expansion Valve	MBE: $\dot{m}_{19} = \dot{m}_{18}$ EBE: $\dot{m}_{19} \times h_{19} = \dot{m}_{18} \times h_{18}$ EnBE: $\dot{m}_{19} \times s_{19} + \dot{S}_{gen,exp} = \dot{m}_{18} \times s_{18}$ ExBE: $\dot{m}_{19} \times ex_{19} = \dot{m}_{18} \times ex_{18} + \dot{E}xD_{exp}$

4.4.7 System 3 Version 1

In version 1 of the system 3, the thermochemical cycle is chosen as MgCl cycle and the heat required is met with both geothermal and solar power tower. The system net work output can be evaluated in Equation 4.64

$$\dot{W}_{net} = \dot{W}_{tur_1} + \dot{W}_{tur_2} + \dot{W}_{tur_4} - (\dot{W}_{comp} + \dot{W}_{pump1} + \dot{W}_{pump2} + \dot{W}_{pump3} + \dot{W}_{pump4} + \dot{W}_{pump5}) \quad (4.64)$$

The overall system efficiencies through energy and exergy concept are evaluated in Equation 4.65 and 4.66 for version 1 of the system 3

$$\eta_{en,overall} = \frac{\dot{W}_{net} + \dot{Q}_{spaceheating} + \dot{Q}_{Hydrogen} + \dot{Q}_{FreshWater} + \dot{Q}_{HotWater}}{\dot{Q}_{solar} + \dot{Q}_{geothermal} + \dot{Q}_{SeaWater}} \quad (4.65)$$

$$\eta_{ex,overall} = \frac{\dot{W}_{net} + \dot{E}x^{Qspace_{heating}} + \dot{Q}^{Ex_{hydrogen}} + \dot{Q}^{Ex_{Freshwater}} + \dot{Q}^{Ex_{Hotwater}}}{\dot{E}x^{Q_{solar}} + \dot{E}x^{Q_{geothermal}} + + \dot{Q}^{Ex_{Seahwater}}} \quad (4.66)$$

The balance equations for the system are evaluated in Table 4.11

Table 4.11 Balance equations for version 1 of the system 3

Heat Exchanger 1	MBE: $\dot{m}_{21} + \dot{m}_{27} = \dot{m}_{24} + \dot{m}_{22}$ EBE: $\dot{m}_{21} \times h_{21} + \dot{m}_{27} \times h_{27} = \dot{m}_{24} \times h_{24} + \dot{m}_{22} \times h_{22}$ EnBE: $\dot{m}_{21} \times s_{21} + \dot{m}_{27} \times s_{27} + \dot{S}_{gen,hx1} = \dot{m}_{24} \times s_{24} + \dot{m}_{22} \times s_{22}$ ExBE: $\dot{m}_{21} \times ex_{21} + \dot{m}_{27} \times ex_{27} = \dot{m}_{24} \times ex_{24} + \dot{m}_{22} \times \dot{ex}_{22} + ExD_{hx1}$
Heat Exchanger 2	MBE: $\dot{m}_{22} + \dot{m}_{18} = \dot{m}_{17} + \dot{m}_{23}$ EBE: $\dot{m}_{22} \times h_{22} + \dot{m}_{18} \times h_{18} = \dot{m}_{17} \times h_{17} + \dot{m}_{23} \times h_{23}$ EnBE: $\dot{m}_{22} \times s_{22} + \dot{m}_{18} \times s_{18} + \dot{S}_{gen,hx2} = \dot{m}_{17} \times s_{17} + \dot{m}_{23} \times s_{23}$ ExBE: $\dot{m}_{22} \times ex_{22} + \dot{m}_{18} \times ex_{18} = \dot{m}_{24} \times ex_{24} + \dot{m}_{23} \times \dot{ex}_{23} + ExD_{hx2}$
Heat Exchanger 3	MBE: $\dot{m}_{13} + \dot{m}_{8} = \dot{m}_{11} + \dot{m}_{9}$ EBE: $\dot{m}_{13} \times h_{13} + \dot{m}_{8} \times h_{8} = \dot{m}_{11} \times h_{11} + \dot{m}_{9} \times h_{9}$ EnBE: $\dot{m}_{13} \times s_{13} + \dot{m}_{8} \times s_{8} + \dot{S}_{gen,hx3} = \dot{m}_{11} \times s_{11} + \dot{m}_{9} \times s_{9}$ ExBE: $\dot{m}_{13} \times ex_{13} + \dot{m}_{8} \times ex_{8} = \dot{m}_{11} \times ex_{11} + \dot{m}_{9} \times \dot{ex}_{9} + ExD_{hx3}$
Heat Exchanger 4	MBE: $\dot{m}_{39} + \dot{m}_{46} = \dot{m}_{40} + \dot{m}_{42}$ EBE: $\dot{m}_{39} \times h_{39} + \dot{m}_{46} \times h_{46} = \dot{m}_{40} \times h_{40} + \dot{m}_{42} \times h_{42}$ EnBE: $\dot{m}_{39} \times s_{39} + \dot{m}_{46} \times s_{46} + \dot{S}_{gen,hx4} = \dot{m}_{40} \times s_{40} + \dot{m}_{42} \times s_{42}$ ExBE: $\dot{m}_{39} \times ex_{39} + \dot{m}_{46} \times ex_{46} = \dot{m}_{40} \times ex_{40} + \dot{m}_{42} \times \dot{ex}_{42} + ExD_{hx4}$

Heat Exchanger 5	MBE: $\dot{m}_6 + \dot{m}_{10} = \dot{m}_7 + \dot{m}_5$ EBE: $\dot{m}_6 \times h_6 + \dot{m}_{10} \times h_{10} = \dot{m}_7 \times h_7 + \dot{m}_5 \times h_5$ EnBE: $\dot{m}_6 \times s_6 + \dot{m}_{10} \times s_{10} + \dot{S}_{gen,hx5} = \dot{m}_7 \times s_7 + \dot{m}_5 \times s_5$ ExBE: $\dot{m}_6 \times ex_6 + \dot{m}_{10} \times ex_{10} = \dot{m}_7 \times ex_7 + \dot{m}_5 \times \dot{ex}_5 + ExD_{hx5}$
Heat Exchanger 6	MBE: $\dot{m}_5 + \dot{m}_{40} = \dot{m}_6 + \dot{m}_{41}$ EBE: $\dot{m}_5 \times h_5 + \dot{m}_{40} \times h_{40} = \dot{m}_6 \times h_6 + \dot{m}_{41} \times h_{41}$ EnBE: $\dot{m}_5 \times s_5 + \dot{m}_{40} \times s_{40} + \dot{S}_{gen,hx6} = \dot{m}_6 \times s_6 + \dot{m}_{41} \times s_{41}$ ExBE: $\dot{m}_5 \times ex_5 + \dot{m}_{40} \times ex_{40} = \dot{m}_6 \times ex_6 + \dot{m}_{41} \times \dot{ex}_{41} + ExD_{hx6}$
Heat Exchanger 7	MBE: $\dot{m}_2 + \dot{m}_{41} = \dot{m}_{39} + \dot{m}_{37}$ EBE: $\dot{m}_2 \times h_2 + \dot{m}_{41-1} \times h_{41-1} = \dot{m}_{39} \times h_{39} + \dot{m}_{37} \times h_{37}$ EnBE: $\dot{m}_2 \times s_2 + \dot{m}_{41-1} \times s_{41-1} + \dot{S}_{gen,hx7} = \dot{m}_{39} \times s_{39} + \dot{m}_{37} \times s_{37}$ ExBE: $\dot{m}_2 \times ex_2 + \dot{m}_{41-1} \times ex_{41-1} = \dot{m}_{39} \times ex_{39} +$ $\dot{m}_{37} \times \dot{ex}_{37} + ExD_{hx7}$
Heat Exchanger 8	*MBE:* $\dot{m}_{43} + \dot{m}_{s2} = \dot{m}_{44} + \dot{m}_{s3}$ *EBE:* $\dot{m}_{43} \times h_{43} + \dot{m}_{s2} \times h_{43} = \dot{m}_{44} \times h_{44} + \dot{m}_{s3} \times h_{s3}$ *EnBE:* $\dot{m}_{43} \times s_{43} + \dot{m}_{s2} \times h_{s2} + \dot{S}_{gen,HX8} = \dot{m}_{44} \times s_{44} + \dot{m}_{s3} \times h_{s3}$ *ExBE:* $\dot{m}_{43} \times ex_{43} + \dot{m}_{s2} \times h_{s2} = \dot{m}_{44} \times ex_{44} + \dot{m}_{s3} \times h_{s3} + \dot{E}xD_{HX8}$
Heat Exchanger 9	*MBE:* $\dot{m}_{19} + \dot{m}_{48} = \dot{m}_{47} + \dot{m}_{49}$ *EBE:* $\dot{m}_{19} \times h_{19} + \dot{m}_{48} \times h_{48} = \dot{m}_{47} \times h_{47} + \dot{m}_{49} \times h_{49}$ *EnBE:* $\dot{m}_{19} \times s_{19} + \dot{m}_{48} \times h_{48} + \dot{S}_{gen,HX9} = \dot{m}_{47} \times s_{47} + \dot{m}_{49} \times h_{49}$ *ExBE:* $\dot{m}_{19} \times ex_{19} + \dot{m}_{48} \times h_{48} = \dot{m}_{47} \times ex_{47} + \dot{m}_{49} \times h_{49} + \dot{E}xD_{HX9}$
Compressor	MBE: $\dot{m}_{17} = \dot{m}_{16}$ EBE: $\dot{m}_{17} \times h_{17} + \dot{W}_{comp} = \dot{m}_{16} \times h_{16}$ EnBE: $\dot{m}_{17} \times s_{17} + \dot{S}_{gen,comp} = \dot{m}_{16} \times s_{16}$ ExBE: $\dot{m}_{17} \times ex_{17} + \dot{E}x_{Q_{comp}} = \dot{m}_{16} \times ex_{16} + \dot{E}xD_{comp}$
Turbine 1	MBE: $\dot{m}_{24} = \dot{m}_{25}$ EBE: $\dot{m}_{24} \times h_{24} = \dot{m}_{25} \times h_{25} + \dot{W}_{tur1}$ EnBE: $\dot{m}_{24} \times s_{24} + \dot{S}_{gen,tur1} = \dot{m}_{25} \times s_{25}$ ExBE: $\dot{m}_{24} \times ex_{24} + \dot{E}x_{Q_{tur1}} = \dot{m}_{25} \times ex_{25} + \dot{E}xD_{tur1}$
Turbine 2	MBE: $\dot{m}_7 = \dot{m}_8$ EBE: $\dot{m}_7 \times h_7 = \dot{m}_8 \times h_8 + \dot{W}_{tur2}$ EnBE: $\dot{m}_7 \times s_7 + \dot{S}_{gen,tur2} = \dot{m}_8 \times s_8$ ExBE: $\dot{m}_7 \times ex_7 + \dot{E}x_{Q_{tur2}} = \dot{m}_8 \times ex_8 + \dot{E}xD_{tur2}$
Turbine 3	MBE: $\dot{m}_1 = \dot{m}_2$ EBE: $\dot{m}_1 \times h_1 = \dot{m}_2 \times h_2 + \dot{W}_{tur3}$ EnBE: $\dot{m}_1 \times s_1 + \dot{S}_{gen,tur3} = \dot{m}_2 \times s_2$ ExBE: $\dot{m}_1 \times ex_1 + \dot{E}x_{Q_{tur3}} = \dot{m}_2 \times ex_2 + \dot{E}xD_{tur3}$
Turbine 4	MBE: $\dot{m}_{42} = \dot{m}_{43}$ EBE: $\dot{m}_{42} \times h_{42} = \dot{m}_{43} \times h_{43} + \dot{W}_{tur4}$ EnBE: $\dot{m}_{42} \times s_{42} + \dot{S}_{gen,tur4} = \dot{m}_{43} \times s_{43}$ ExBE: $\dot{m}_{42} \times ex_{42} + \dot{E}x_{Q_{tur4}} = \dot{m}_{43} \times ex_{43} + \dot{E}xD_{tur4}$
Pump 1	MBE: $\dot{m}_{26} = \dot{m}_{27}$ EBE: $\dot{m}_{26} \times h_{26} + \dot{W}_{Pump1} = \dot{m}_{27} \times h_{27}$ EnBE: $\dot{m}_{26} \times s_{26} + \dot{S}_{gen,Pump1} = \dot{m}_{27} \times s_{27}$

	ExBE: $\dot{m}_{26} \times ex_{26} + \dot{W}_{Pump1} = \dot{m}_{27} \times ex_{27} + \dot{E}xD_{Pump1}$
Pump 2	MBE: $\dot{m}_{26} = \dot{m}_{27}$ EBE: $\dot{m}_{26} \times h_{26} + \dot{W}_{Pump1} = \dot{m}_{27} \times h_{27}$ EnBE: $\dot{m}_{26} \times s_{26} + \dot{S}_{gen,Pump1} = \dot{m}_{27} \times s_{27}$ ExBE: $\dot{m}_{26} \times ex_{26} + \dot{W}_{Pump1} = \dot{m}_{27} \times ex_{27} + \dot{E}xD_{Pump1}$
Pump 3	MBE: $\dot{m}_{20} = \dot{m}_{21}$ EBE: $\dot{m}_{20} \times h_{20} + \dot{W}_{Pump3} = \dot{m}_{21} \times h_{21}$ EnBE: $\dot{m}_{20} \times s_{20} + \dot{S}_{gen,Pump3} = \dot{m}_{21} \times s_{21}$ ExBE: $\dot{m}_{20} \times ex_{20} + \dot{W}_{Pump1} = \dot{m}_{21} \times ex_{21} + \dot{E}xD_{Pump3}$
Pump 4	MBE: $\dot{m}_{37} = \dot{m}_{38}$ EBE: $\dot{m}_{37} \times h_{37} + \dot{W}_{Pump4} = \dot{m}_{38} \times h_{38}$ EnBE: $\dot{m}_{37} \times s_{37} + \dot{S}_{gen,Pump4} = \dot{m}_{38} \times s_{38}$ ExBE: $\dot{m}_{37} \times ex_{37} + \dot{W}_{Pump1} = \dot{m}_{38} \times ex_{38} + \dot{E}xD_{Pump4}$
Expansion Valve	MBE: $\dot{m}_{47} = \dot{m}_{18}$ EBE: $\dot{m}_{47} \times h_{47} = \dot{m}_{18} \times h_{18}$ EnBE: $\dot{m}_{47} \times s_{47} + \dot{S}_{gen,exp} = \dot{m}_{18} \times s_{18}$ ExBE: $\dot{m}_{47} \times ex_{47} = \dot{m}_{18} \times ex_{18} + \dot{E}xD_{exp}$

4.4.8 System 3 Version 2

Version 2 of system 3 has the same principle with version 2 of system 2 but Mg-Cl cycle is chosen as a thermochemical cycle to produce hydrogen. Net work output can be evaluated as follows for this system,

$$\dot{W}_{net} = \dot{W}_{tur_1} - (\dot{W}_{comp1} + \dot{W}_{comp2} + \dot{W}_{comp3} + \dot{W}_{comp4} + \dot{W}_{compM1} + \dot{W}_{compM1} + \dot{W}_{compM2} + \dot{W}_{pumpM3} + \dot{W}_{pump1}) \quad (4.67)$$

The overall system energy and exergy efficiency are denoted as follows for this system,

$$\eta_{\text{en,overall}} = \frac{\dot{W}_{net} + \dot{Q}_{spaceheating} + \dot{Q}_{Hydrogen} + \dot{Q}_{FreshWater} + \dot{Q}_{HotWater}}{\dot{Q}_{geothermal} + \dot{Q}_{SeaWater}} \quad (4.68)$$

$$\eta_{\text{ex,overall}} = \frac{\dot{W}_{net} + \dot{E}x^{Qspace_{heating}} + \dot{Q}^{Ex_{hydrogen}} + \dot{Q}^{Ex_{Freshwater}} + \dot{Q}^{Ex_{Hotwater}}}{\dot{E}x^{Q_{geothermal}} + + \dot{Q}^{Ex_{Seahwater}}} \quad (4.69)$$

The balance equations for this system are listed in Table 4.12.

Table 4.12 Balance equations for version 2 of the system 3

Heat Exchanger 1	MBE: $\dot{m}_{21} + \dot{m}_{27} = \dot{m}_{24} + \dot{m}_{22}$ EBE: $\dot{m}_{21} \times h_{21} + \dot{m}_{27} \times h_{27} = \dot{m}_{24} \times h_{24} + \dot{m}_{22} \times h_{22}$ EnBE: $\dot{m}_{21} \times s_{21} + \dot{m}_{27} \times s_{27} + \dot{S}_{gen,hx1} = \dot{m}_{24} \times s_{24} + \dot{m}_{22} \times s_{22}$ ExBE: $\dot{m}_{21} \times ex_{21} + \dot{m}_{27} \times ex_{27} = \dot{m}_{24} \times ex_{24} + \dot{m}_{22} \times \dot{e}x_{22} + ExD_{hx1}$
Heat Exchanger 2	MBE: $\dot{m}_{22} + \dot{m}_{18} = \dot{m}_{17} + \dot{m}_{23}$

	EBE: $\dot{m}_{22} \times h_{22} + \dot{m}_{18} \times h_{18} = \dot{m}_{17} \times h_{17} + \dot{m}_{23} \times h_{23}$ EnBE: $\dot{m}_{22} \times s_{22} + \dot{m}_{18} \times s_{18} + \dot{S}_{gen,hx2} = \dot{m}_{17} \times s_{17} + \dot{m}_{23} \times s_{23}$ ExBE: $\dot{m}_{22} \times ex_{22} + \dot{m}_{18} \times ex_{18} = \dot{m}_{24} \times ex_{24} + \dot{m}_{23} \times \dot{e}x_{23} + ExD_{hx2}$
Heat Exchanger 3	MBE: $\dot{m}_{13} + \dot{m}_8 = \dot{m}_{11} + \dot{m}_9$ EBE: $\dot{m}_{13} \times h_{13} + \dot{m}_8 \times h_8 = \dot{m}_{11} \times h_{11} + \dot{m}_9 \times h_9$ EnBE: $\dot{m}_{13} \times s_{13} + \dot{m}_8 \times s_8 + \dot{S}_{gen,hx3} = \dot{m}_{11} \times s_{11} + \dot{m}_9 \times s_9$ ExBE: $\dot{m}_{13} \times ex_{13} + \dot{m}_8 \times ex_8 = \dot{m}_{11} \times ex_{11} + \dot{m}_9 \times \dot{e}x_9 + ExD_{hx3}$
Heat Exchanger 4	MBE: $\dot{m}_{39} + \dot{m}_{46} = \dot{m}_{40} + \dot{m}_{42}$ EBE: $\dot{m}_{39} \times h_{39} + \dot{m}_{46} \times h_{46} = \dot{m}_{40} \times h_{40} + \dot{m}_{42} \times h_{42}$ EnBE: $\dot{m}_{39} \times s_{39} + \dot{m}_{46} \times s_{46} + \dot{S}_{gen,hx4} = \dot{m}_{40} \times s_{40} + \dot{m}_{42} \times s_{42}$ ExBE: $\dot{m}_{39} \times ex_{39} + \dot{m}_{46} \times ex_{46} = \dot{m}_{40} \times ex_{40} + \dot{m}_{42} \times \dot{e}x_{42} + ExD_{hx4}$
Heat Exchanger 5	MBE: $\dot{m}_6 + \dot{m}_{10} = \dot{m}_7 + \dot{m}_5$ EBE: $\dot{m}_6 \times h_6 + \dot{m}_{10} \times h_{10} = \dot{m}_7 \times h_7 + \dot{m}_5 \times h_5$ EnBE: $\dot{m}_6 \times s_6 + \dot{m}_{10} \times s_{10} + \dot{S}_{gen,hx5} = \dot{m}_7 \times s_7 + \dot{m}_5 \times s_5$ ExBE: $\dot{m}_6 \times ex_6 + \dot{m}_{10} \times ex_{10} = \dot{m}_7 \times ex_7 + \dot{m}_5 \times \dot{e}x_5 + ExD_{hx5}$
Heat Exchanger 6	MBE: $\dot{m}_5 + \dot{m}_{40} = \dot{m}_6 + \dot{m}_{41}$ EBE: $\dot{m}_5 \times h_5 + \dot{m}_{40} \times h_{40} = \dot{m}_6 \times h_6 + \dot{m}_{41} \times h_{41}$ EnBE: $\dot{m}_5 \times s_5 + \dot{m}_{40} \times s_{40} + \dot{S}_{gen,hx6} = \dot{m}_6 \times s_6 + \dot{m}_{41} \times s_{41}$ ExBE: $\dot{m}_5 \times ex_5 + \dot{m}_{40} \times ex_{40} = \dot{m}_6 \times ex_6 + \dot{m}_{41} \times \dot{e}x_{41} + ExD_{hx6}$
Heat Exchanger 7	MBE: $\dot{m}_2 + \dot{m}_{41-1} = \dot{m}_{39} + \dot{m}_{37}$ EBE: $\dot{m}_2 \times h_2 + \dot{m}_{41-1} \times h_{41-1} = \dot{m}_{39} \times h_{39} + \dot{m}_{37} \times h_{37}$ EnBE: $\dot{m}_2 \times s_2 + \dot{m}_{41-1} \times s_{41-1} + \dot{S}_{gen,hx7} = \dot{m}_{39} \times s_{39} + \dot{m}_{37} \times s_{37}$ ExBE: $\dot{m}_2 \times ex_2 + \dot{m}_{41-1} \times ex_{41-1} = \dot{m}_{39} \times ex_{39} +$ $\dot{m}_{37} \times \dot{e}x_{37} + ExD_{hx7}$
Heat Exchanger 8	MBE: $\dot{m}_{34} + \dot{m}_{33} = \dot{m}_{35} + \dot{m}_{32}$ EBE: $\dot{m}_{34} \times h_{34} + \dot{m}_{33} \times h_{33} = \dot{m}_{35} \times h_{35} + \dot{m}_{32} \times h_{32}$ EnBE: $\dot{m}_{34} \times s_{34} + \dot{m}_{33} \times s_{33} + \dot{S}_{gen,hx8} = \dot{m}_{35} \times s_{35} + \dot{m}_{32} \times s_{32}$ ExBE: $\dot{m}_{34} \times ex_{34} + \dot{m}_{33} \times ex_{33} = \dot{m}_{35} \times ex_{35} + \dot{m}_{35} \times \dot{e}x_{35} + ExD_{hx8}$
Heat Exchanger 9	MBE: $\dot{m}_{28} + \dot{m}_{35} = \dot{m}_{21} + \dot{m}_{36}$ EBE: $\dot{m}_{28} \times h_{28} + \dot{m}_{35} \times h_{35} = \dot{m}_{21} \times h_{21} + \dot{m}_{36} \times h_{36}$ EnBE: $\dot{m}_{28} \times s_{28} + \dot{m}_{35} \times s_{35} + \dot{S}_{gen,hx9} = \dot{m}_{21} \times s_{21} + \dot{m}_{36} \times s_{36}$ ExBE: $\dot{m}_{28} \times ex_{28} + \dot{m}_{35} \times ex_{35} = \dot{m}_{21} \times ex_{21} + \dot{m}_{36} \times \dot{e}x_{36} + ExD_{hx9}$
Heat Exchanger 10	MBE: $\dot{m}_{36} + \dot{m}_{18} = \dot{m}_{19} + \dot{m}_{42}$ EBE: $\dot{m}_{36} \times h_{36} + \dot{m}_{18} \times h_{18} = \dot{m}_{19} \times h_{19} + \dot{m}_{42} \times h_{42}$ EnBE: $\dot{m}_{36} \times s_{36} + \dot{m}_{18} \times s_{18} + \dot{S}_{gen,hx10} = \dot{m}_{19} \times s_{19} + \dot{m}_{42} \times s_{42}$ ExBE: $\dot{m}_{36} \times ex_{36} + \dot{m}_{18} \times ex_{18} = \dot{m}_{19} \times ex_{19} + \dot{m}_{42} \times \dot{e}x_{42} + ExD_{hx10}$
Heat Exchanger 11	MBE: $\dot{m}_{43} + \dot{m}_{44} = \dot{m}_{33} + \dot{m}_{45}$ EBE: $\dot{m}_{43} \times h_{43} + \dot{m}_{44} \times h_{44} = \dot{m}_{33} \times h_{33} + \dot{m}_{45} \times h_{45}$ EnBE: $\dot{m}_{43} \times s_{43} + \dot{m}_{44} \times s_{44} + \dot{S}_{gen,hx11} = \dot{m}_{33} \times s_{21} + \dot{m}_{45} \times s_{45}$ ExBE: $\dot{m}_{43} \times ex_{43} + \dot{m}_{44} \times ex_{44} = \dot{m}_{33} \times ex_{33} + \dot{m}_{45} \times \dot{e}x_{45} + ExD_{hx11}$
Compressor 1	MBE: $\dot{m}_8 = \dot{m}_9$ EBE: $\dot{m}_8 \times h_8 + \dot{W}_{comp1} = \dot{m}_9 \times h_9$ EnBE: $\dot{m}_8 \times s_8 + \dot{S}_{gen,comp1} = \dot{m}_9 \times s_9$ ExBE: $\dot{m}_8 \times ex_8 + \dot{E}x_{Q_{comp1}} = \dot{m}_9 \times ex_9 + \dot{E}xD_{comp1}$

Compressor 2	MBE: $\dot{m}_{10} = \dot{m}_{11}$ EBE: $\dot{m}_{10} \times h_{10} + \dot{W}_{comp2} = \dot{m}_{11} \times h_{11}$ EnBE: $\dot{m}_{10} \times s_{10} + \dot{S}_{gen,comp2} = \dot{m}_{11} \times s_{11}$ ExBE: $\dot{m}_{10} \times ex_{10} + \dot{E}x_{Q_{comp2}} = \dot{m}_{11} \times ex_{11} + \dot{E}xD_{comp2}$
Compressor 3	MBE: $\dot{m}_{12} = \dot{m}_{13}$ EBE: $\dot{m}_{12} \times h_{12} + \dot{W}_{comp3} = \dot{m}_{13} \times h_{13}$ EnBE: $\dot{m}_{12} \times s_{12} + \dot{S}_{gen,comp3} = \dot{m}_{13} \times s_{13}$ ExBE: $\dot{m}_{12} \times ex_{12} + \dot{E}x_{Q_{comp3}} = \dot{m}_{13} \times ex_{13} + \dot{E}xD_{comp3}$
Compressor 4	MBE: $\dot{m}_{32} = \dot{m}_{31}$ EBE: $\dot{m}_{32} \times h_{32} + \dot{W}_{comp4} = \dot{m}_{31} \times h_{31}$ EnBE: $\dot{m}_{32} \times s_{32} + \dot{S}_{gen,comp4} = \dot{m}_{31} \times s_{31}$ ExBE: $\dot{m}_{32} \times ex_{32} + \dot{E}x_{Q_{comp4}} = \dot{m}_{31} \times ex_{31} + \dot{E}xD_{comp4}$
Turbine 1	MBE: $\dot{m}_{19} = \dot{m}_{20}$ EBE: $\dot{m}_{19} \times h_{19} = \dot{m}_{20} \times h_{20} + \dot{W}_{tur1}$ EnBE: $\dot{m}_{19} \times s_{19} + \dot{S}_{gen,tur1} = \dot{m}_{20} \times s_{20}$ ExBE: $\dot{m}_{19} \times ex_{19} + \dot{E}x_{Q_{tur1}} = \dot{m}_{20} \times ex_{20} + \dot{E}xD_{tur1}$
Pump 1	MBE: $\dot{m}_{17} = \dot{m}_{18}$ EBE: $\dot{m}_{17} \times h_{17} + \dot{W}_{Pump1} = \dot{m}_{18} \times h_{18}$ EnBE: $\dot{m}_{17} \times s_{17} + \dot{S}_{gen,Pump1} = \dot{m}_{18} \times s_{18}$ ExBE: $\dot{m}_{17} \times ex_{17} + \dot{W}_{Pump1} = \dot{m}_{18} \times ex_{18} + \dot{E}xD_{Pump1}$
Pump 2	MBE: $\dot{m}_{41} = \dot{m}_{34}$ EBE: $\dot{m}_{41} \times h_{41} + \dot{W}_{Pump2} = \dot{m}_{34} \times h_{34}$ EnBE: $\dot{m}_{41} \times s_{41} + \dot{S}_{gen,Pump2} = \dot{m}_{34} \times s_{34}$ ExBE: $\dot{m}_{41} \times ex_{41} + \dot{W}_{Pump1} = \dot{m}_{34} \times ex_{34} + \dot{E}xD_{Pump2}$
Pump 3	MBE: $\dot{m}_{14} = \dot{m}_{15}$ EBE: $\dot{m}_{14} \times h_{14} + \dot{W}_{Pump3} = \dot{m}_{15} \times h_{15}$ EnBE: $\dot{m}_{14} \times s_{14} + \dot{S}_{gen,Pump3} = \dot{m}_{15} \times s_{15}$ ExBE: $\dot{m}_{14} \times ex_{14} + \dot{W}_{Pump1} = \dot{m}_{15} \times ex_{15} + \dot{E}xD_{Pump3}$
Pump 4	MBE: $\dot{m}_{37} = \dot{m}_{38}$ EBE: $\dot{m}_{37} \times h_{37} + \dot{W}_{Pump4} = \dot{m}_{38} \times h_{38}$ EnBE: $\dot{m}_{37} \times s_{37} + \dot{S}_{gen,Pump4} = \dot{m}_{38} \times s_{38}$ ExBE: $\dot{m}_{37} \times ex_{37} + \dot{W}_{Pump1} = \dot{m}_{38} \times ex_{38} + \dot{E}xD_{Pump4}$
Expansion Valve	MBE: $\dot{m}_{30} = \dot{m}_{33}$ EBE: $\dot{m}_{30} \times h_{30} = \dot{m}_{33} \times h_{33}$ EnBE: $\dot{m}_{30} \times s_{30} + \dot{S}_{gen,exp} = \dot{m}_{33} \times s_{33}$ ExBE: $\dot{m}_{30} \times ex_{30} = \dot{m}_{33} \times ex_{33} + \dot{E}xD_{exp}$

4.5 Thermochemical Cycle Simulations

This study has two different thermochemical cycles in the systems studied as Mg-Cl and Cu-Cl cycles. The Aspen One chemical simulation software is used for simulations of these cycles. Aspen Plus is a software to be used for chemical modeling and simulating chemical processes [44]. This software has very wide usage especially for the optimization processes in the industry. In this way, the performance of the processes can be increased, the energy consumption of plants can be

reduced as well as initial installation and operating costs can be reduced. Thanks to its optimization tool, which offers economical and technical optimization opportunities, processes can be optimized for the most efficient results in factors such as environmental conditions and substances so on. Due to these options and wide usage areas, Aspen Plus has been chosen as a simulation tool for thermochemical processes. It is possible to explain the processes performed in the Aspen implementation in two main headings as *Property specifications*, *Simulation specifications.*

4.5.1 Property Specifications

Aspen Plus has its database containing pure substances and phase information. Aspen plus allows the addition of the desired component with the option of large databases in the implementation of any chemical process. For any component that is not available in the database, Aspen offers the possibility to add it manually by stating its chemical structure and properties. As can be seen in Figure 4.3, the user in the "Properties" section can search and add components from the existing library. Another point that the user must determine before starting the simulation is the method to be used. For determining the default method to be used in the simulation, while in the "Properties" section, the "Specifications" tab must be used in the "Methods" folder (see Figure 4.4). Multiple methods can be added simultaneously in a simulation file and different methods can be assigned for particular processes. On the other hand, in the same file, the "Pure components" section allows temperature-dependent correlation coefficients (a_0, a_1, a_2,etc.) to be determined.

4.5.2 Selected Methods and Components

Two different thermochemical cycles are simulated by using Aspen Plus as the Cu-Cl cycle and Mg-Cl cycle. Some components are necessary that are common and different for both cycles have been added. Cuprous chloride (CuCl), Copper oxychloride (Cu2OCl2), water (H2O), hydrochloric acid (HCl) and oxygen (O2) are the components for Cu-Cl cycle, although magnesium chloride (MgCl2), magnesium oxide (MgO), hydrochloric acid (HCl), oxygen (O2) and water (H2O).

Table 4.13 Cu-Cl cycle specifications

(a) Cu-Cl Cycle	
Specifications	**Description**
Step Number	4
Simulation Software	Aspen-Plus
Method	IDEAL
Electrolysis Temperature	70
Hydrolysis Temperature	400
Thermolysis Temperature	500

Table 4.14 Mg-Cl cycle specifications

(b) Mg-Cl Cycle	
Specifications	**Description**
Step Number	3
Simulation Software	Aspen-Plus
Method	ELECNRTL
Electrolysis Temperature	70
Hydrolysis Temperature	537
Chlorination Temperature	537
Steam/Mg Ratio	17:1

After determining the components, the method selection is essential for each simulation. The method selection varies according to the processes and fluids which are used in simulation and has great importance. The Mg-Cl cycle has three different phases of the assigned components. Then, the ELECNRTL method which is an extended version of NRTL is the most feasible one among the ones that contain these three phases. This method is a member of "Activity Coefficient Property Methods" and can be found with this filter in the component finder section [45].

For the Cu-Cl cycle, the IDEAL method corresponding to the ideal gas state has been added according to the selected components.

4.5.3 Flowsheet of Simulation

After adding the required components and determining the global conditions for overall simulations from the "Properties" section, the user should pass to the "Simulation" section. The software gives an error notification if the required definitions are not completed in the "Properties" section.

The flowsheet is constructed with the system components selected from the "Model Palette" tab in the "Simulation" section. The same tab can be used to add streams that are related to the system. The specifications should be determined from the "Blocks" folder for each component such as heat exchanger, pumps, turbines, reactors, separators so on and "Streams" folder for each stream.

At this stage, the required specifications required for each flowsheet block must be defined to Aspen Plus by the user. Temperature and fraction information is requested by the system for each block outlets. Otherwise, the user receives an "Input Incomplete" warning. Lastly, if more than one global method is defined to the system, suitable methods must be assigned for each block.

For both two system, the Cu-Cl cycle and the Mg-Cl cycle, Aspen flowsheets are created. Heat recovery heat exchangers, separators and mixers are the common components for both systems. Major chemical reactions of decomposition (thermolysis), electrolysis, hydrolysis for Cu-Cl cycle, chlorination for the Mg-Cl cycle are defined with default reactor types and be specified by the user. Figure 4.10 and Figure 4.11 illustrate the Aspen flowsheets of Mg-Cl and Cu-Cl cycles respectively.

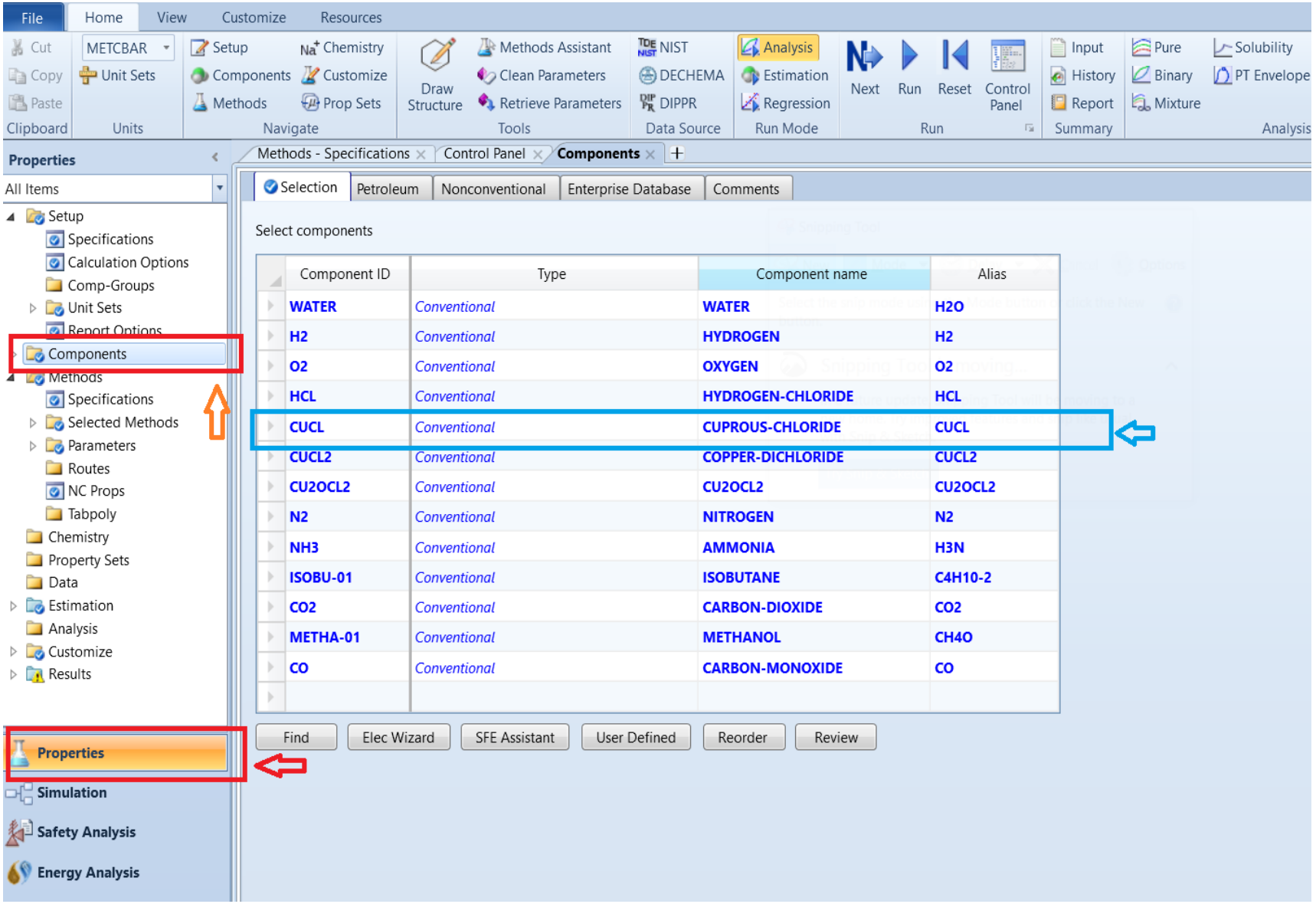

Figure 4.8 Aspen Plus, system components

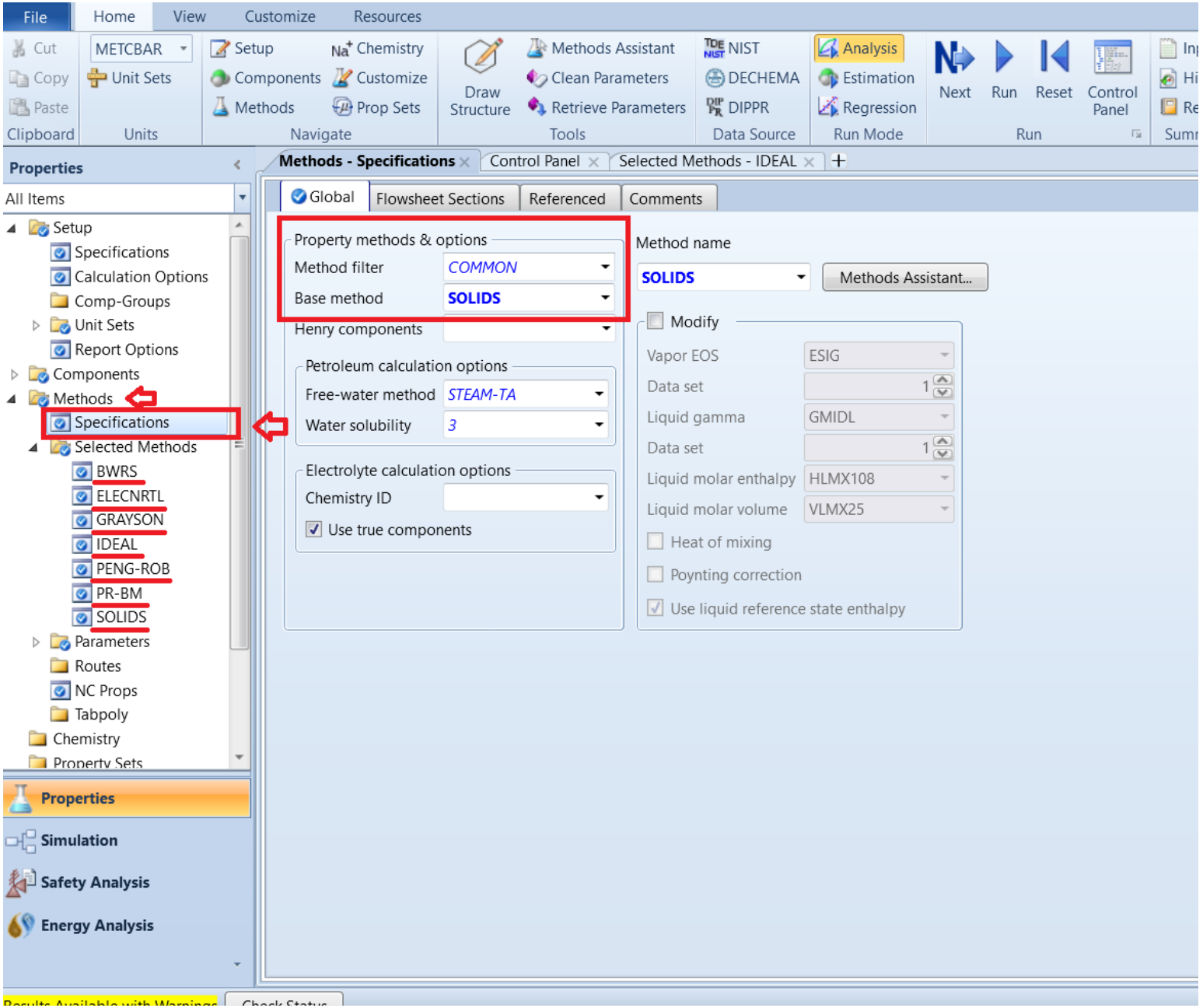

Figure 4.9 Aspen Plus, methods for simulation

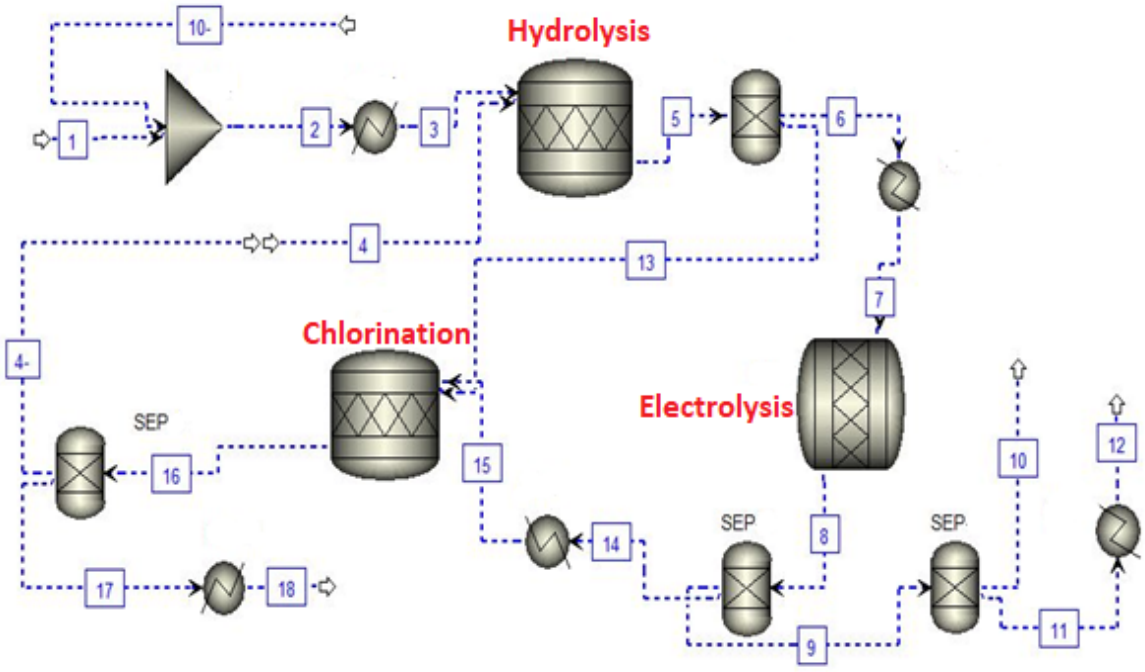

Figure 4.10 Aspen Plus flowsheet of Mg-Cl cycle components

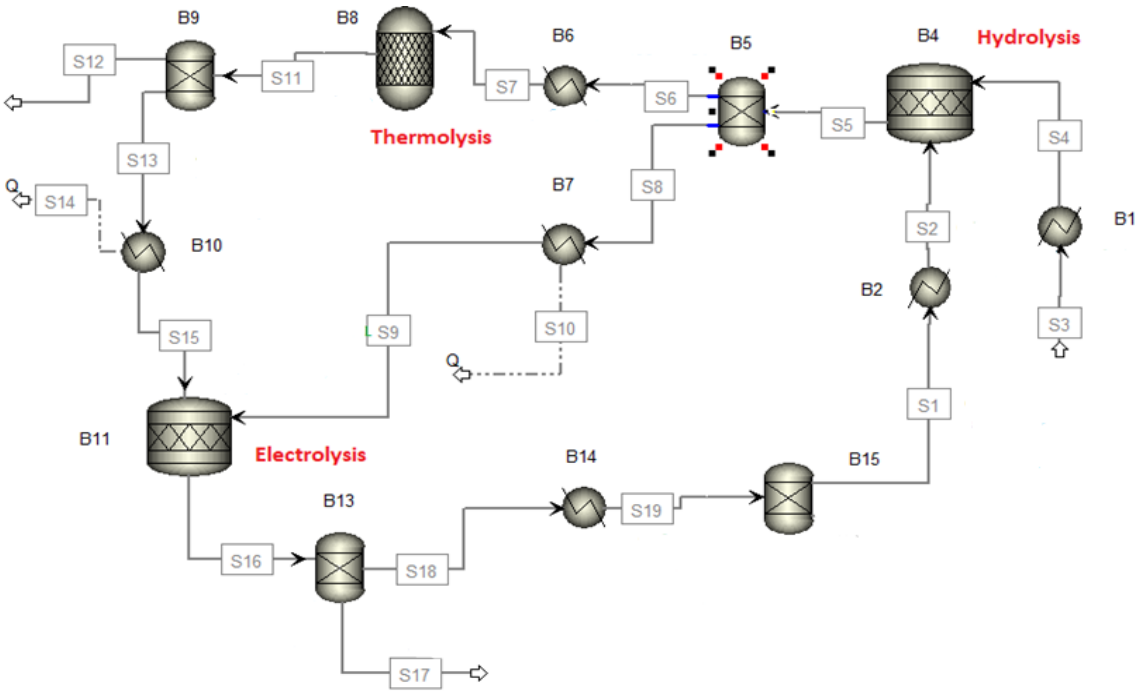

Figure 4.11 Aspen Plus flowsheet of Cu-Cl cycle components

Chapter 5 RESULTS AND DISCUSSION

The thermodynamic analysis for the three proposed integrated systems is conducted through energy and exergy approach to study their performance. Engineering Equation Solver (EES) software is used to perform thermodynamic analysis although Aspen Plus software is used to simulate thermochemical cycles that exist in four systems which are cuprous chloride cycles and magnesium chloride cycles. This chapter provides the results of the thermodynamic analysis and outputs of each system and the parametric studies on the results when environmental and working conditions vary to understand the effects of these variations on the energetic and exergetic performances. Energy and exergy efficiencies, exergy destruction rates for every major component of each system and state point thermodynamic results are obtained for each section. Finally, a comparison between the proposed systems is provided to determine the most efficient method for the production of the same commodities.

The evaluated energy and exergy efficiencies (at an ambient temperature and pressure of 25°C and 101 kPa respectively) for all the proposed integrated systems are shown in Figure 5.1. According to a comparison of the systems, the second version of system 3 has the highest energy and exergy efficiencies of 49.58% and 59.23% respectively while system 1 has the lowest values for the energy (25.38) and exergy (28.94%) efficiencies. As a result of this comparison, heat upgrade from geothermal provides better efficiencies in comparison with the integration of solar and wind energy sources. When the heat upgrading from geothermal is evaluated within itself, the version with the Mg-Cl cycle (system 3) is more efficient energetically by 8% and exergetically by 19.2%. When we evaluate the versions using heat upgrade configuration in systems using Cu-Cl and Mg-Cl cycle, we obtain better results.

In this section, each system and different versions of these systems are studied separately and results are explained. Each sub-section provides the case study results and parametric studies for each integrated system. The evaluated state point results, efficiencies and coefficient of performance (COP) are used to determine the performance of the systems.

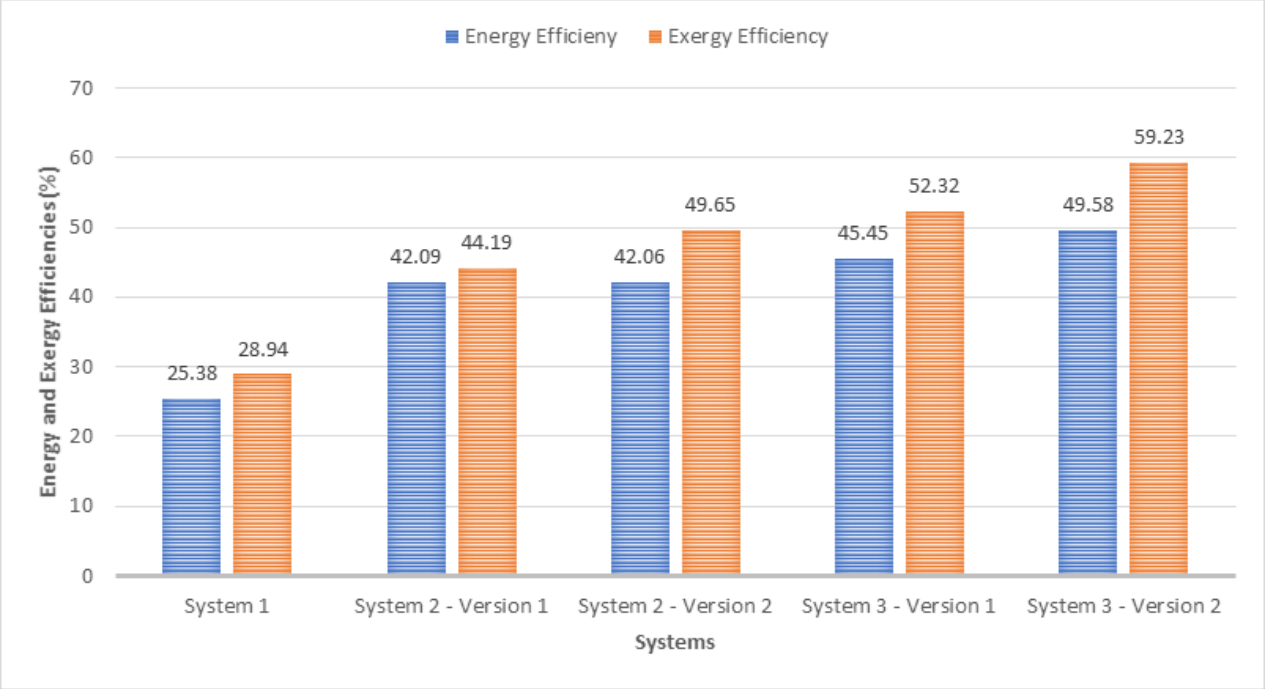

(a)

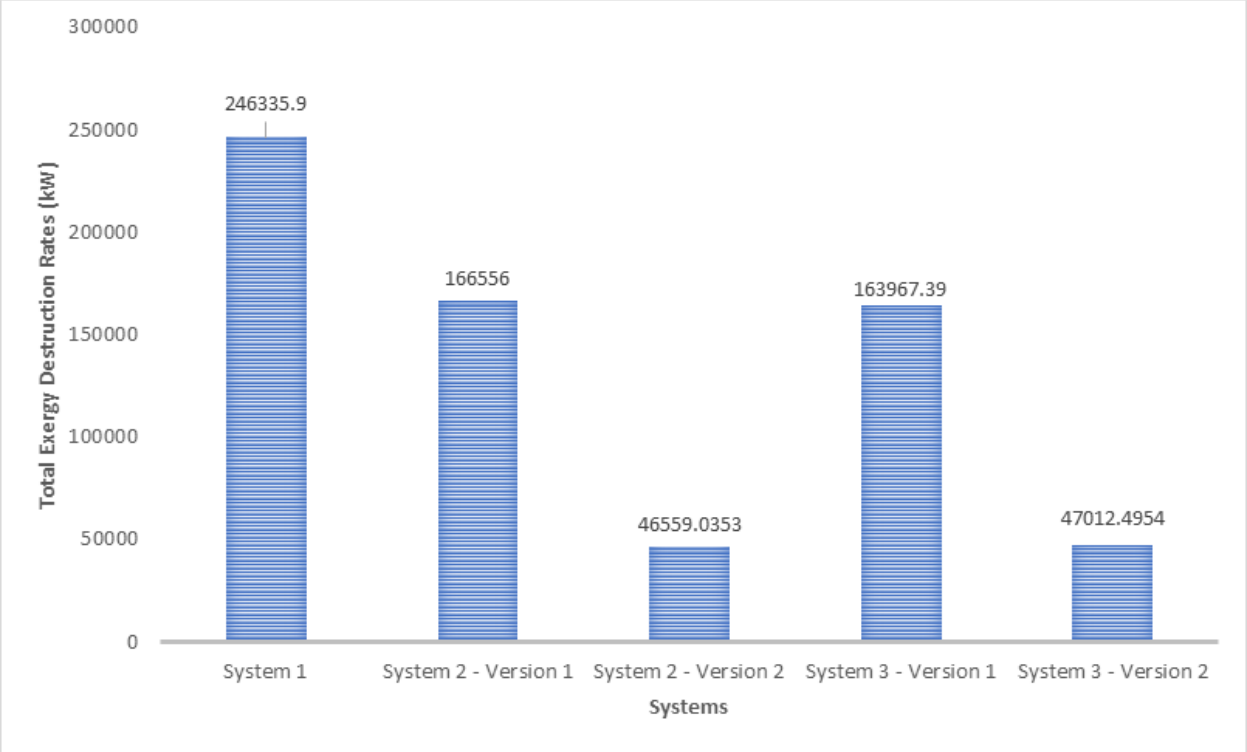

(b)

Figure 5.1 (a) Overall system energy and exergy efficiencies at 25 °C ambient temperature and 101 kPa ambient pressure, (b) total exergy destruction rates

5.1 System 1

In system 1, the solar power tower is used as an energy source besides geothermal. Due to the availability of solar energy during day time and being seasonal, thermal heat storage is used as an option to store energy. Thermodynamic properties of the system's state points and production capacities are examined in section 5.1.1 and the results of the parametric studies conducted are shown in section 5.1.2.

5.1.1 Case Study Results

Table 5.1, gives the results of the thermodynamic study of state points. Information regarding the working fluid and exergy values of state points can be found alongwith temperature, pressure, enthalpy and entropy information. Table 5.2 provide the inputs and outputs of the overall system as well as major components. Three turbines of the system are capable to produce 16828 kW electric energy after the needs of the pumps and compressors used in the system are met. The system is capable to generate 25873 kW of heat for space heating purposes. Solar power tower which is integrated into the system has the 93323 kW solar energy to be received although 10 wind power towers are capable to produce 12088 kW electric energy. Figure 5.2 and Table 5.3 shows the exergy destruction rates and exergetic efficiencies respectively in order to examine the working performances of the major system components of system 1. The detailed exergy destruction rate calculations are given in Chapter 4. As can be seen in Figure 5.2, the highest exergy destruction rate is detected at the compressor with 6935 kW. Solar power tower exergy destruction rate follows this with 4949 kW. The lowest exergy destruction is evaluated for the wind power tower with the 259.69 kW. On the other hand, the highest exergetic efficiency is obtained for Turbine 2 with a value of 99.25%. Turbine 1 has the second highest exergy efficiency of 97.44% where the lowest exergetic efficiency value is obtained for space heating with 57.65%.

Table 5.1 State points thermodynamic properties

State Points	Fluid	Mass Flow Rate (kg/s)	Temperature (°C)	Pressure (kPa)	Specific Enthalpy (kJ/kg)	Specific Entropy (kJ/kg K)	Specific Exergy (kJ/kg)
1	Molten Salt	400	1176	1900	711.2	0.0.6606	518.9
2	Molten Salt	400	1126	1300	647.8	0.616	468.7
3	Water	400	700	1000	39243924	8.275	1462
4	Water	400	600	700	3701	8.197	1262
5	Water	300	445	550	3366	7.887	1020

6	Water	300	475	700	3428	7.861	1090
7	CO2	300	310	1000	272.8	0.2036	216.7
8	CO2	300	195	300	155.6	0.2066	98.54
9	CO2	300	145	350	106.4	0.06649	91.11
10	CO2	300	210	700	3924	0.07592	151.11
11	R134a	200	110	122	334.6	1.266	-38.29
12	R134a	200	200	137	448.7	1.531	-2.921
13	R134a	200	85	125	329.8	1.251	-38.54
14	R134a	400	150	137	394.5	1.41	-21.06
15	R134a	400	85	125	329.8	1.251	-38.54
16	R134a	200	140	137	384.1	1.385	-24.06
17	R134a	200	80	87	325.6	1.268	-47.93
18	R134a	200	20	90	272.2	1.1	-51.19
19	R134a	200	85	125	329.8	1.251	-38.54
20	R134a	80	140	137	384.2	1.389	-25.29
21	R134a	80	95	130	339.3	1.274	-35.9
22	Water	300	260	960	2966	6988	888.2
23	Water	300	190	940	2807	6.677	821.8
24	Water	300	105	920	440.2	1.361	39.15
25	CO2	300	185	220	146	0.2442	77.69
26	CO2	300	150	160	112.1	0.2273	48.86
27	CO2	300	25	150	1.52	0.07781	26.17
28	CO2	300	30	220	2.129	0.1374	47.57
29	SeaWater	116.23	21	100	87.56	0.3086	0.1123
30	Fresh Water	40	21	100	87.56	0.3086	0.1123
31	Fresh Water	0.4825	21	100	87.56	0.3086	0.1123
32	Fresh Water	0.4825	600	300	3704	8.591	1148
36	Brine Water	40	21	5	87.47	0.3086	0.01703
37	Molten Salt	400	910	1280	431.7	0.4476	302.8
38	Molten Salt	400	920	1900	442.3	0.4562	310.8
39	Molten Salt	300	910	1000	431.6	0.4476	302.7
40	Molten Salt	300	750	1000	262.9	0.4942	179.7
41	Molten Salt	300	650	1000	157.9	0.1862	107
42	R134a	200	70	100	316.1	1.23	-45.94
43	Water	150	25	100	104.3	0.3651	-0.001003
44	Water	150	60	100	250.6	0.8294	7.795

Table 5.2 Input/Output of major system components, system 1

Component	Value
Output Work of Turbine 1 (kW)	**13035**
Output Work of Turbine 2 (kW)	**35177**
Output Work of Turbine 3 (kW)	**25380**
Input Power of Compressor	**11714**
Input Power of Pump 1 (kW)	**1095**
Input Power of Pump 2 (kW)	**22822**
Input Power of Pump 3 (kW)	**18848**
Input Power of Pump 4 (kW)	**4227**
Net Power Output (kW)	**16828**
Heating Condenser (kW)	**25873**
Hot Water (kW)	**21949**
Solar Power Tower Output (kW)	**93323**
Wind Power Towers Output	**12088**
Fresh-water production (kg/s)	**48.23**
Methanol production (kg/s)	**1.326**

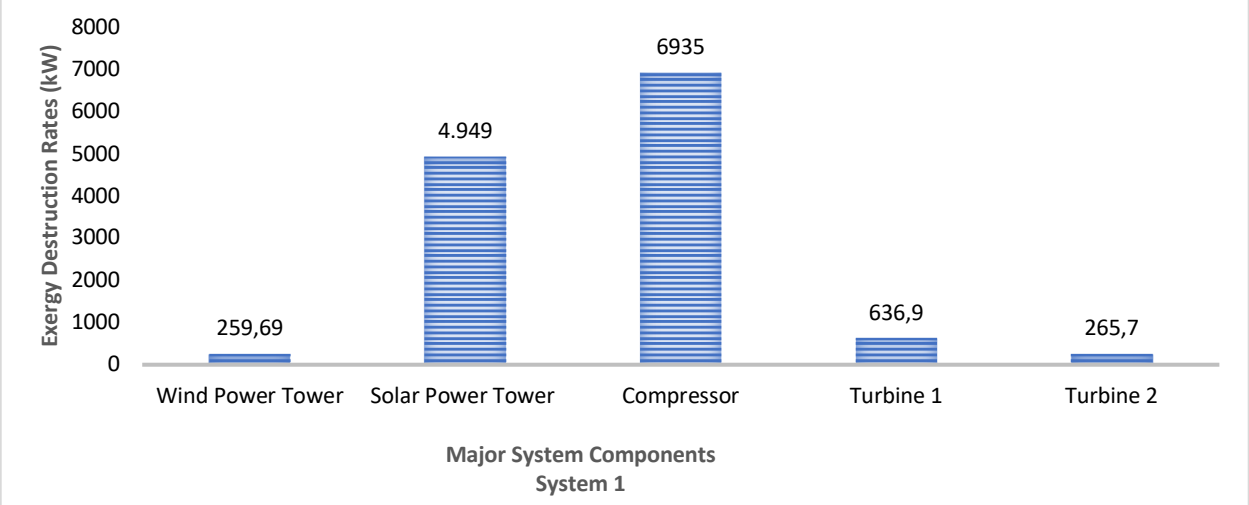

Figure 5.2 Exergy destruction rates for major system 1 components

Table 5.3 Exergetic efficiency for system major components

Component	Exergetic Efficiency (%)
Condenser	85.67
Compressor	45.41
Turbine 2	99.25
Turbine 1	94.77
Heat Exchanger 5	93.88
Heat Exchanger 1	61.06
Space Heater	57.65

5.1.2 Parametric Results

Some parametric studies are conducted for the system's performance analysis. Parameters such as ambient temperature, working output and so on are have been varied and their effects have been studied on the system performance. The first parametric study has been conducted to analyze the effect of ambient temperature on general system efficiencies. Figure 5.3 shows the changes in the system energetic and exergetic efficiencies by gradually increasing ambient temperature from 5 °C to 35 °C. In this context, we see that there is no change in energy efficiency, but as the ambient temperature rises, there is a decrease in the exergetic efficiency. At the low ambient temperatures, it is possible to say that the highest exergetic efficiency is obtained. Exergetic efficiency we received in the case study 25°C degree as 28.84%, increases to 29.34% at 5 °C degree ambient temperature.

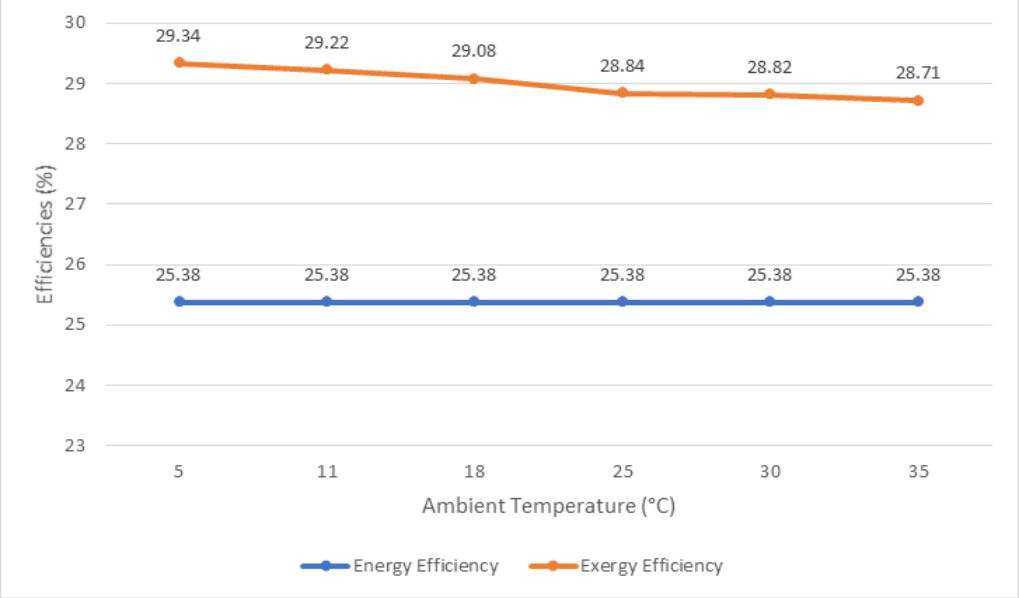

Figure 5.3 Overall system parametric energy and exergy efficiency results when ambient temperature varies at 101 kPa ambient pressure

Figure 5.4 shows the effect of the ambient temperature on the exergy destruction rates of the major system components. The ambient temperature is gradually varied between 5 °C and 35 °C. Although there is no significant change in Turbine 1, Turbine 2 and wind power tower, the exergy destruction of solar power tower is increased by 52.52% from the one at 5 °C to the one 35 °C. On the other hand, an almost 800 kW increase has been observed in the exergy destruction of the compressor.

Exergy efficiency is another parameter that is considered as a tool for performance analysis. Section 5.1.1 gives information about the exergetic efficiencies of the components for 25 °C ambient temperature. Figure 5.5 shows the influence of the ambient temperature on the exergy efficiency of some major system compoenents. The biggest loss in exergetic performance is experienced in the space heater with 15%. In contrast to the exergy losses of the components, organic Rankine cycle 1 and organic Rankine cycle 2 gained in terms of exergetic efficiency. These increases are about 8% and 3%, respectively, for the organic Rankine cycle 1 and organic Rankine cycle 2.

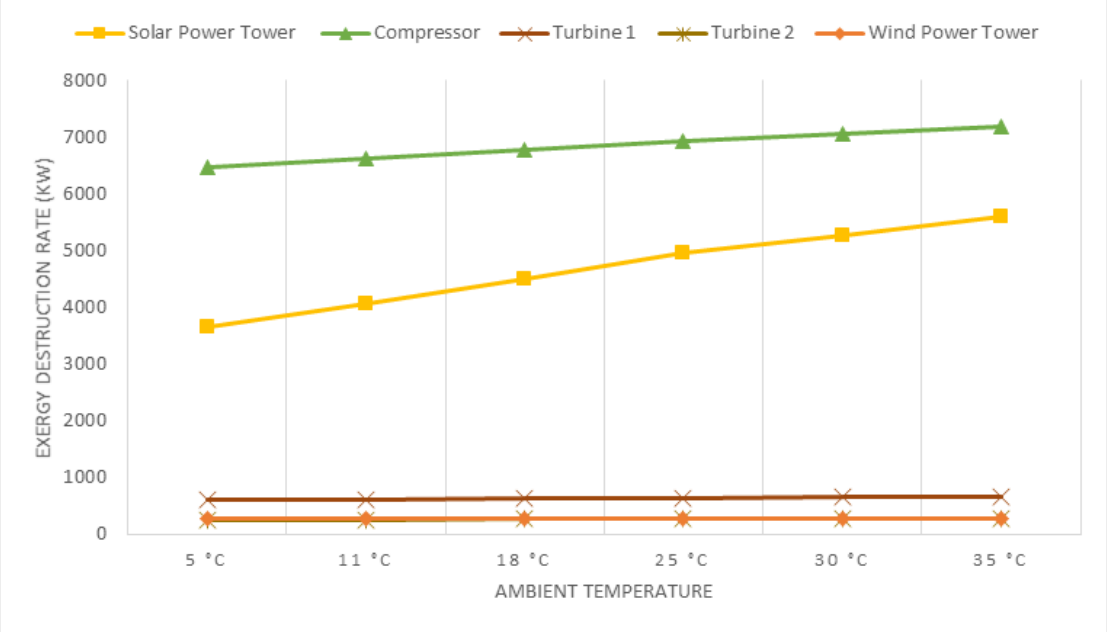

Figure 5.4 Parametric exergy destruction rates for major system 1 components when ambient temperature varies

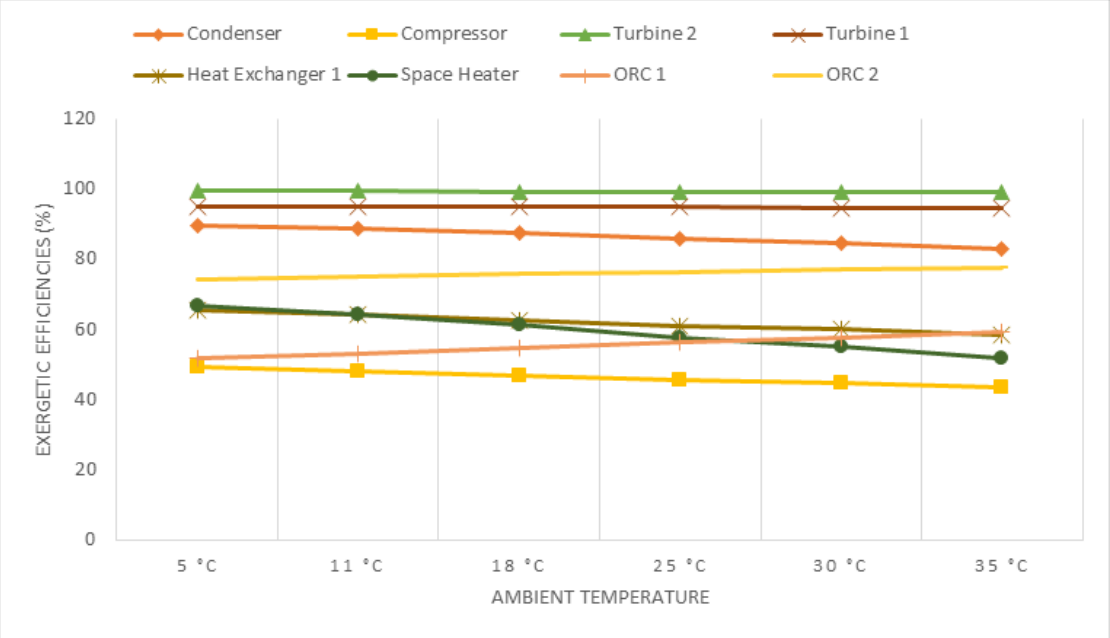

Figure 5.5 Parametric energetic efficiency results for major system 1 components and ORCs when ambient temperature varies

Organic Rankine cycle 2, transfers the heat stored at molten salt thermal heat storage to the R134a working fluid to be used at space heating. At that point, Turbine 2 is used to produce electricity. A parametric study is conducted to observe the effect of the pressure at state point 7. Figure 5.6 shows the effect of the pressure at state 7 on the efficiency of the organic Rankine cycle and the overall efficiency of the system. In the case study, the pressure at state 7 is 1000 kPa and Turbine 2 can produce 35180 kW electric energy. The pressure level is increased from the 800 kPa to 1700 kPa gradually and the corresponding change in the efficiencies is observed. The increase in energy and exergy efficiency has been observed as 22.92% and 28.92% respectively. Although the increase at overall efficiency is lower when compared to the cycle.

On the other hand, Figure 5.7 shows the importance of the effect of the electricity production capacity of the Rankine cycle on overall system efficiency. Produced electricity by the ORC 2 in the case study conditions is 35183 kW. The electrical energy produced by the Turbine 2 when the state 7 pressure is raised to 1700 kPa, reaches 44486 kPa. System 1 is capable to desalinate the seawater to produce freshwater in order to meet the freshwater demand of the community. For this purpose, a multi-stage desalination unit is preferred due to its advantages such as lower energy consumption and higher efficiencies than conventional ones. Figure 5.8 shows the produced freshwater amount in terms of kg per second when the number of stages which is used in the desalination unit varies.

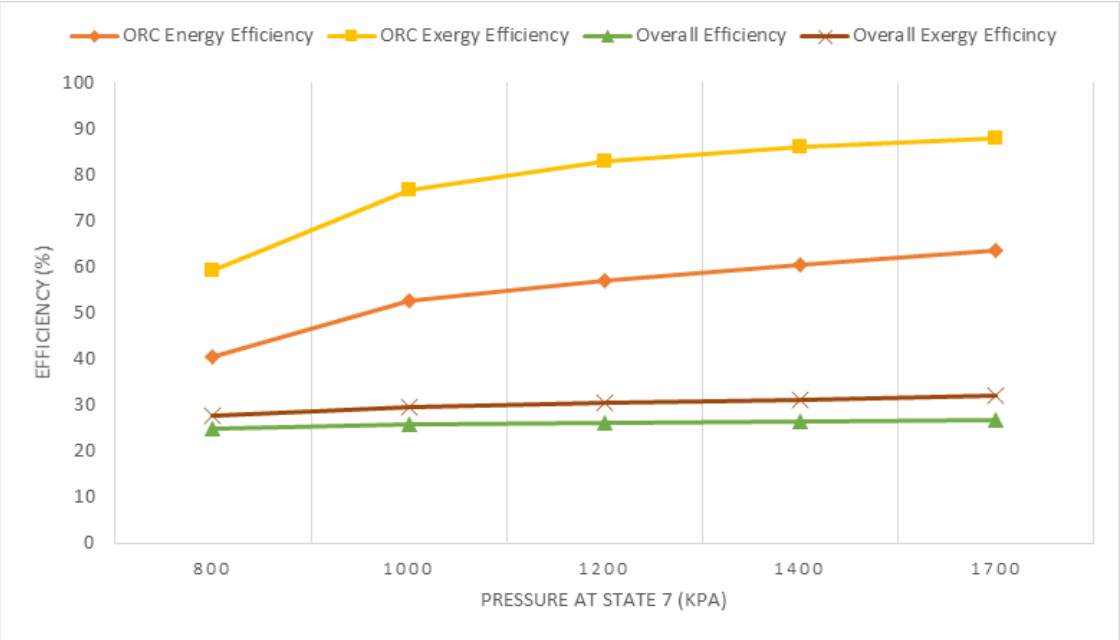

Figure 5.6 Parametric energy and exergy efficiencies for ORC and overall system when the pressure at state 7 varies

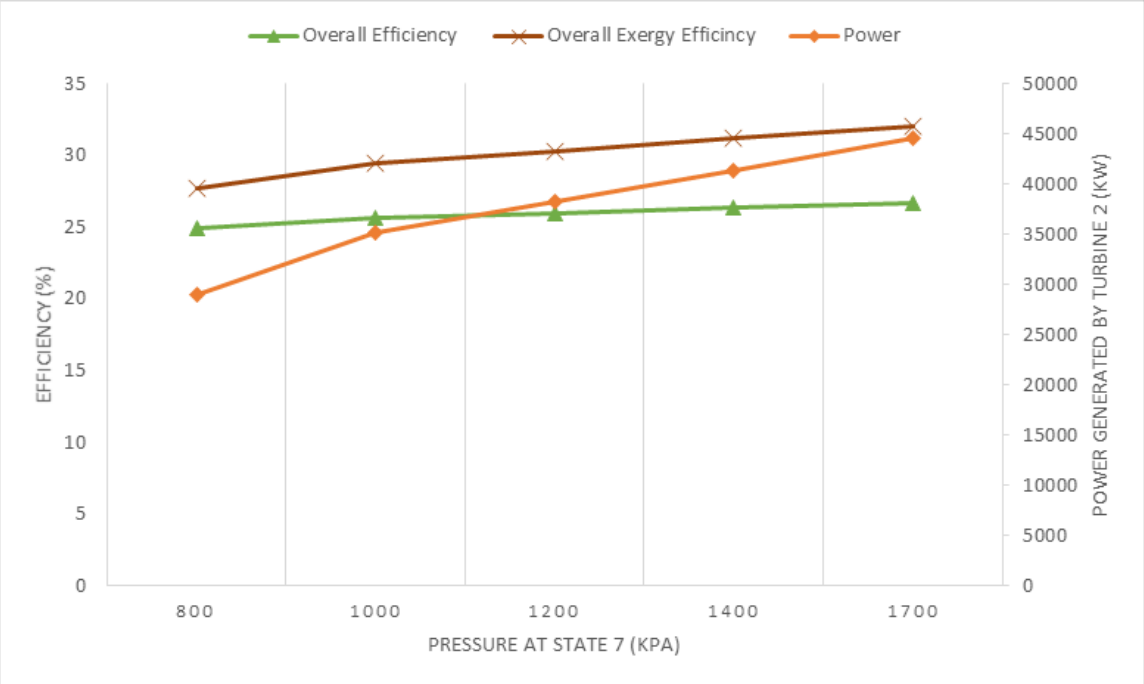

Figure 5.7 Power generated by turbine 2 and overall system energy and exergy efficiencies

The number of stages of the desalination unit is three as mentioned in chapter 3. The relation of the produced freshwater amount with the stage number is explained in section 4.4.3. The number of stages is gradually increased, to 5 from 1 and the variation on the produced freshwater is observed in Figure 5.8.

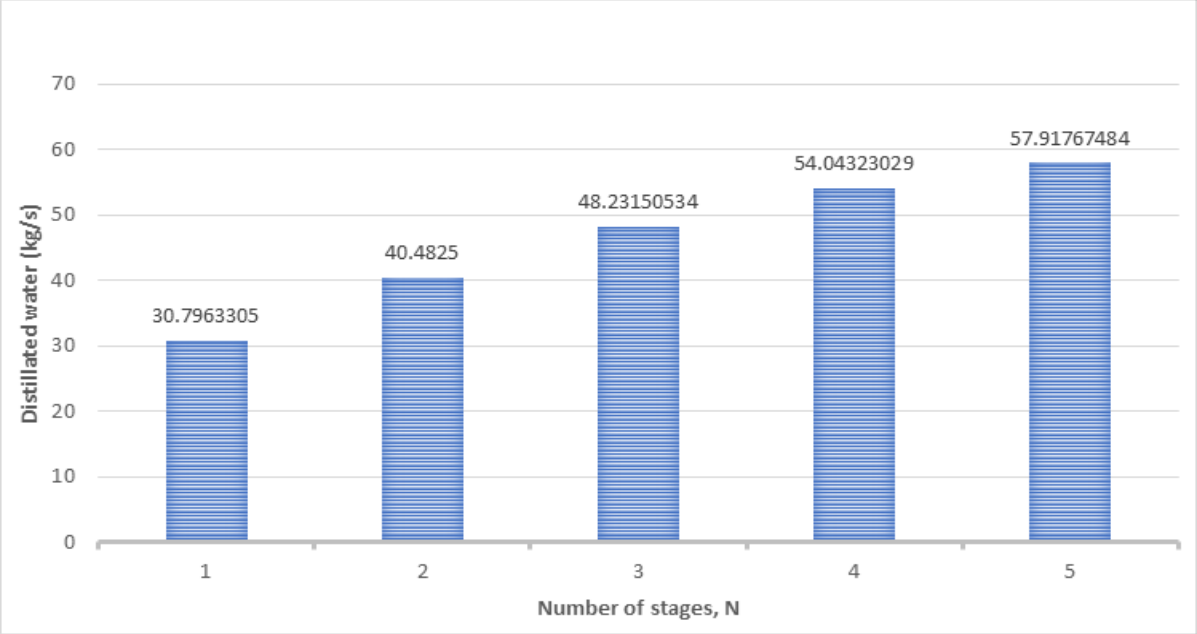

Figure 5.8 Parametric distilled water ratios when the stage number of the desalination unit varies

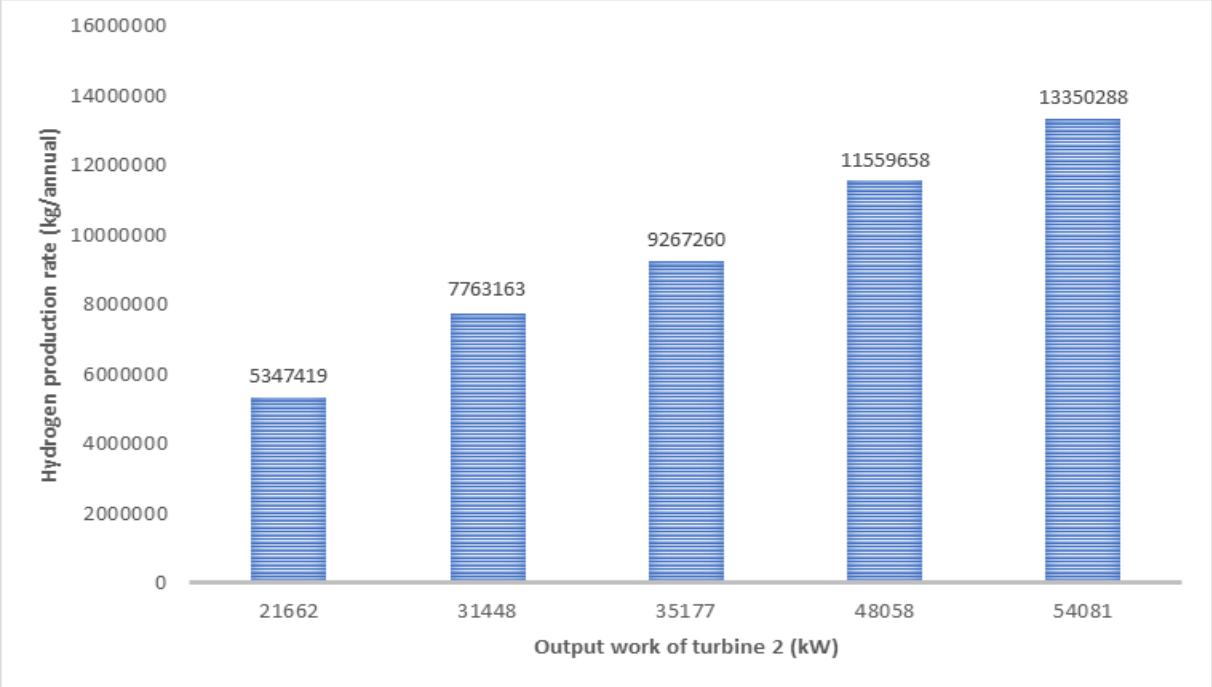

Figure 5.9 Parametric hydrogen production rates when electricity consumption rate varies

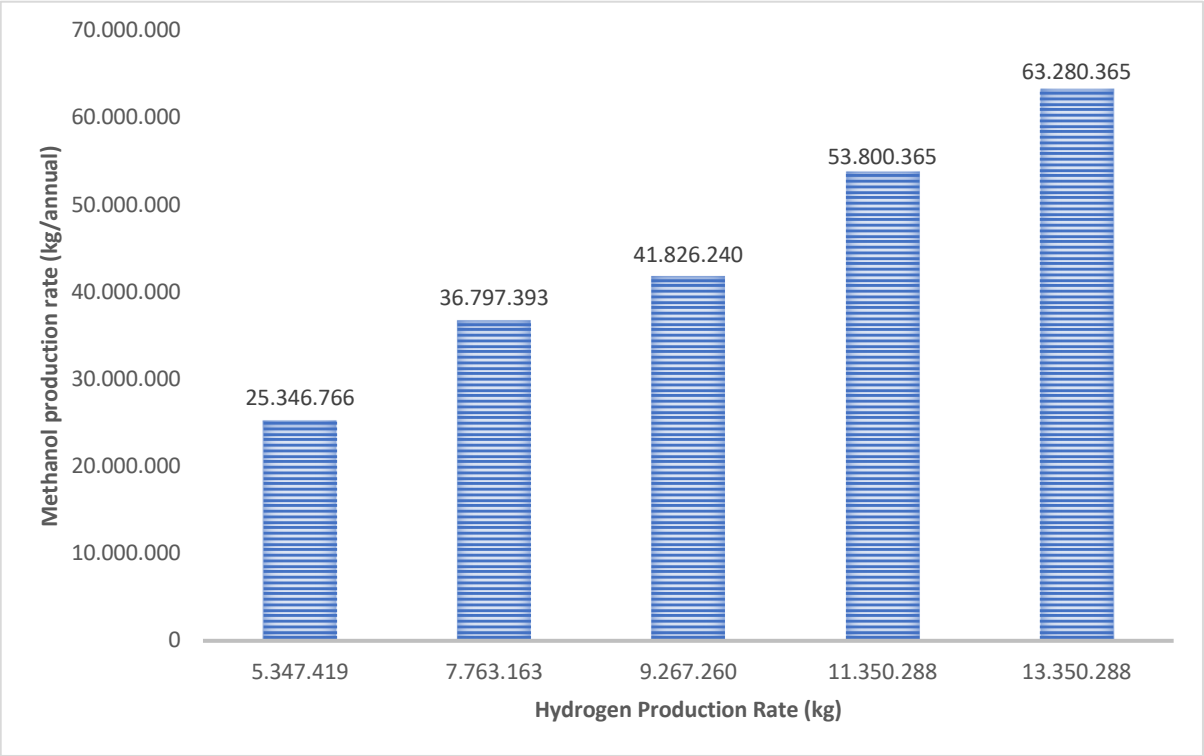

Figure 5.10 Methanol production rate by methanol synthesis reactor when hydrogen consumption rate varies

System 1 is capable to produce methanol by using methanol synthesis reactor. The thermodynamic properties and reactor specifications are given in chapter 3. Methanol synthesis reactor is fed with hydrogen produced by a high-temperature electrolyzer. A high-temperature electrolyzer requires electricity to produce hydrogen. This requirement is met with electricity produced by Turbine 2. Figure 5.9 shows the hydrogen production capacity of the high-temperature electrolyzer when the generated power by Turbine 2 varies. In this context, when the generated electricity is increased to 54081 kW from the 21662 kW the produced hydrogen amount is also increased to 13,350,288 kg per annual from 5,347,419 kg per annual. This increases effects the of methanol production directly. Figure 5.10 shows the increase of methanol production respect hydrogen production.

5.2 System 2

System 2 has two different versions which are separated according to the energy sources used. In this system, the wind energy tower is not used as energy sources in both versions. The main feature that distinguishes system 2 from the system 3 is that it uses the Cu-Cl cycle in both versions as the thermochemical cycle.

5.2.1 Version 1 of the System 2

In the first version of the second system, solar power tower and geothermal are used as energy sources. As in the first system, molten salt storage is used for storing the thermal energy obtained from the solar power tower. The thermochemical cycle that used for the production of hydrogen which is one of the useful outputs. Section 5.2.1 has two parts that discuss the case study and the effects of the different parameters of system performance.

5.2.1.1 Case Study Results

This section discusses the results of the thermodynamic study on system performance and gives the capacity of production. Table 5.4 shows the thermodynamic properties of the Cu-Cl thermochemical cycle which is used to produce hydrogen. This state point information is valid for both versions of the system 2. Table 5.5 provides the thermodynamic properties at the various state points for version 1 of the systems 2 and 3.

Table 5.4 State points thermodynamic properties of Cu-Cl cycle, system 2

State Points	Fluid	Mass Flow Rate (kg/hr)	Temperature (°C)	Pressure (kPa)	Specific Enthalpy (kJ/kg)	Specific Entropy (kJ/kg K)
S1	CUCL2	968.05	80	100	358.625	5.20646
S2	CUCL2	968.05	400	100	684.115	8.16871
S3	Water	64.855	25	100	-15864.3	-9.05
S4	Water	64.855	400	100	-12690.9	-0.88
S5	HCL - CU2OCL2	1032.92	400	100	-1901.41	4.6565
S6	CU2OCL2	770.4	400	100	-1789.51	5.92543
S7	CU2OCL2	770.4	500	100	-1791.51	5.9227
S8	HCL	262.517	400	100	-2229.89	0.93268
S9	HCL	262.517	25	100	-2531.77	2.4214
S11	O2 - CUCL	770.388	500	100	519.517	23.723
S12	O2	57.5978	500	100	466.493	7.09864
S13	CUCL	712.791	500	100	523.22	1.178
S15	CUCL	712.791	430	100	475.885	1.17808
S16	H2 - CUCL2	975.307	25	100	306.132	4.092
S17	H2	7.25717	25	100	1.84E-13	0.054
S18	CUCL2	968.05	25	100	306.519	4.116
S19	CUCL2	968.05	80	100	358.625	5.206

Table 5.5 State points thermodynamic properties of version 1 of the system 2 and 3

State Points	Fluid	Mass Flow Rate (kg/s)	Temperature (°C)	Pressure (kPa)	Specific Enthalpy (kJ/kg)	Specific Entropy (kJ/kg K)	Specific Exergy (kJ/kg)
2	Molten Salt	400	1176	1300	711	0.6606	519.6
5	Water	300	400	550	3271	7.75	1018
6	Water	300	500	700	3482	7.931	1176
7	CarbonDioxide	300	370	1000	725.2	0.7943	493
8	CarbonDioxide	300	250	300	545	0.821	304.9
9	CarbonDioxide	300	180	350	140.5	0.1448	101.9
10	CarbonDioxide	300	210	700	169.2	0.07592	151.1
11	R134a	200	110	122	415.8	1.468	-17.2
12	R134a	200	200	137	448.7	1.531	-2.921
13	R134a	200	85	125	271.6	1.531	-43.38
14	R134a	400	150	137	394.5	1.41	-21.06
15	R134a	400	85	125	271.6	1.072	-43.38
16	R134a	200	140	137	334.5	1.257	-35.54
17	R134a	200	80	87	298.2	1.188	-51.16
18	R134a	200	20	90	271.4	1.098	-51.17
19	R134a	200	120	125	271.6	1.072	-43.38
20	Water	300	200	900	2834	6.753	825.8
21	Water	300	260	920	2968	7.01	883.1
22	Water	300	190	920	2808	6.689	819.5
23	Water	300	105	900	440.2	1.361	39.13
24	CarbonDioxide	300	137	265	99.16	0.1012	73.49
25	CarbonDioxide	300	98	160	63.17	0.104	36.69
26	CarbonDioxide	300	60	150	28.93	0.018	27.84
27	CarbonDioxide	300	90	220	55.48	0.023	53.09
28 – Sys 2	SeaWater	115.38	21	100	87.56	0.308	0.1123
28 – Sys 3	SeaWater	115.73	21	100	87.56	0.308	0.1123
29	Fresh Water	40	21	100	87.56	0.3086	0.1123
30 – Sys 2	Fresh Water	0.186	21	100	87.56	0.3086	0.1123
30 – Sys 3	Fresh Water	0.306	21	100	87.56	0.3086	0.1123
31	Brine Water	40	21	5	87.47	0.308	0.01703
37	Molten Salt	400	920	1300	441.7	0.4562	310.2
38	Molten Salt	400	940	1350	462.3	0.4734	325.8
39	Molten Salt	300	910	800	431.4	0.4476	302.5
40	Molten Salt	300	820	780	336.4	0.364	232.4
41	Molten Salt	300	600	760	105.2	0.1277	71.69
41-1	Molten Salt	300	660	790	168.2	0.1975	113.9
42	Water	300	690	370	3905	8.713	1313
43-System 2	Water	300	600	250	3704	8.676	1123

44-System 2	Water	300	600	250	3704	8.676	1123
45-System 2	Water	300	580	250	3660	8.625	1904
46	Water	300	600	370	3703	8.494	1177
47	Water	200	70	100	316.1	1.23	-45.97
48	Water	150	25	100	104.3	0.3651	-0.001703
49	Water	150	50	100	250.6	0.8294	7.975

Table 5.6 gives the input and output information for major system components. Three turbines of the system are capable to produce 4180 kW electric energy after the needs of the pumps and compressors used in the system are met. The system is capable to generate 25873 kW of heat for space heating purposes. Solar power tower which is integrated into the system has the 93323 kW solar energy to be received. The system can produce 7.2517 kg of hydrogen per hour. For the major system components, exergy destruction rates are given in Figure 5.11. The highest exergy destruction rate is in the solar power tower with 11020 kW. The compressor comes after with 6935 kW exergy destruction rate. The lowest exergy destruction rate belongs to Turbine 1.

Table 5.6 Input/Output of major system components, version 1 of the system 2

Component	**Value**
Output Work of Turbine 1 (kW)	**7197**
Output Work of Turbine 2 (kW)	**38049**
Output Work of Turbine 4 (kW)	**60187**
Input Power of Compressor (kW)	**11714**
Input Power of Pump 1 (kW)	**5395**
Input Power of Pump 2 (kW)	**22822**
Input Power of Pump 3 (kW)	**35803**
Electrolysis (HCl electrolysis of Cu-Cl)	**173.3**
Net Power Output (kW)	**4182**
Heating Condenser (kW)	**25873**
Solar Power Tower Output (kW)	**93323**
Fresh-water production (kg/s)	**47.887**
Hydrogen output by Cu-Cl cycle (kg/hr)	**7.2517**

Exergetic efficiency values are chosen as one of the parameters showing components' operating performance. Table 5.7 shows the evaluated exergy efficiencies for each system component and two organic Rankine Cycle which is used in the system. The highest exergy efficiency values are achieved as 97.79% and 97.94% for Turbines 1 and 2 respectively. On the other hand the heat exchanger 1 is the component with the lowest exergetic efficiency. Table 5.8 shows the exergy destruction data for the components of Cu-Cl thermochemical cycle process.

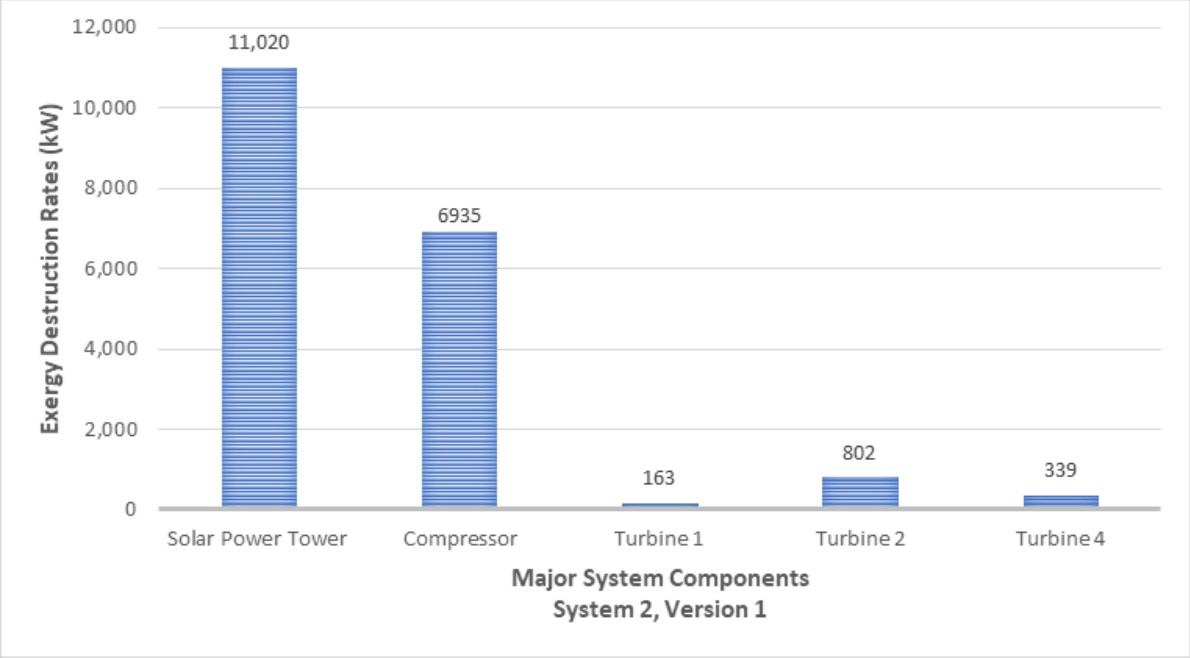

Figure 5.11 Exergy destruction rates for major system 2 and system 3 version, 1 components

Table 5.7 Exergtic efficiencies for system major components for system 2 and system 3, version1

Component	**Exergetic Efficiency (%)**
Heat Exchanger 1	43.8
Heat Exchanger 5	63.25
Solar Tower	87.5
Space Heater	57.65
Turbine 1	97.79
Turbine 2	97.94
Condenser	59.34
ORC 1	70.13
ORC 2	65.28

Table 5.8 Exergy destruction rates for Cu-Cl cycle components

Component	Exergy Destruction Rate (kW)
Electrolyser	208.2
Hydrolysis	249.1
Thermolysis	641

5.2.1.2 Parametric Results

Some parametric studies have been conducted on the system to determine the system operation performance and the effects of operating conditions on the results. The first parametric study on the first version of the system 2, is conducted to observe the effect of the ambient temperature on the energy and exergy efficiencies. Ambient temperature is gradually increased to 35 °C from 5 °C. As mentioned in the previous sections, the ambient temperature is considered as 25 °C for the case study where the energy and exergy efficiencies are 42.09% and 44.19% respectively.

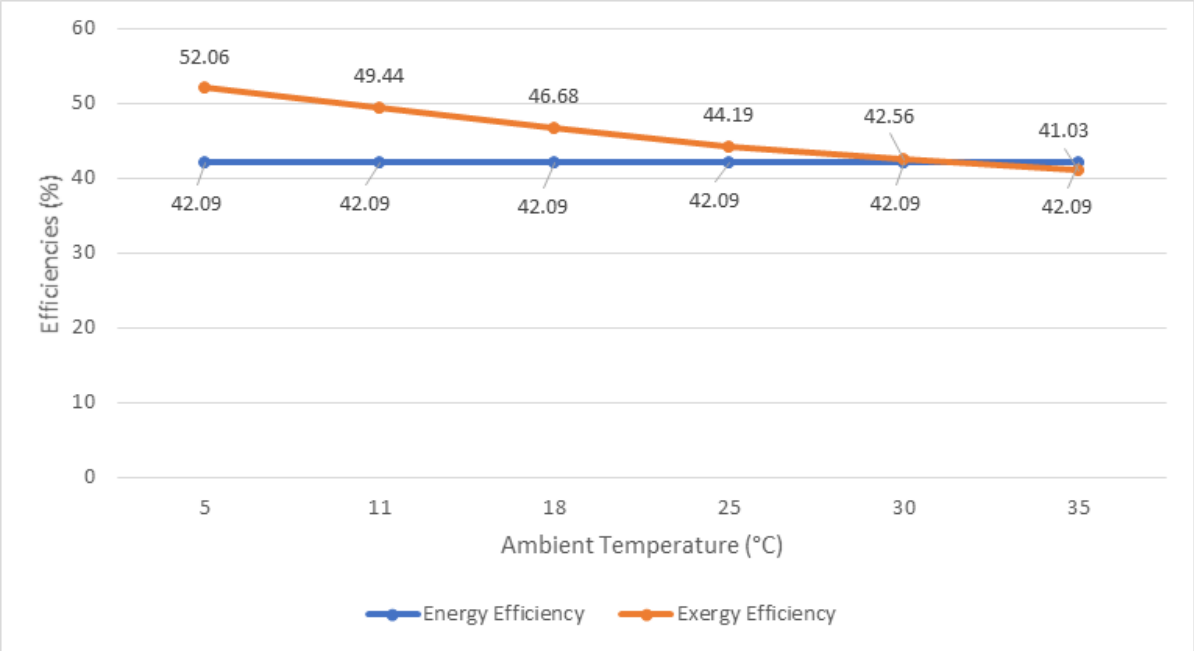

Figure 5.12 Overall system energy and exergy efficiency results when ambient temperature varies

As can be seen in Figure 5.12, the energy efficiency is not affected by the change in ambient temperature however, the exergy efficiency is observed to decrease. Beyond an ambient temperature of 30°C, the exergy efficiency drops below the energy efficiency.

Another parametric study is conducted to observe the impact of the ambient temperature on the exergy destruction rates of the system components. The exergy destruction rates for the system components for the case study are given in section 5.2.1.1 where the ambient temperature is 25 °C. In Figure 5.13, the ambient temperature is gradually increased from 5 °C to 35 °C to observe the effect on exergy destruction. Although there is no significant change in system turbines, exergy destruction rates are increased with the ambient temperature. This increment is shown in the solar power tower with 17% where the compressor follows it with 10.78%.

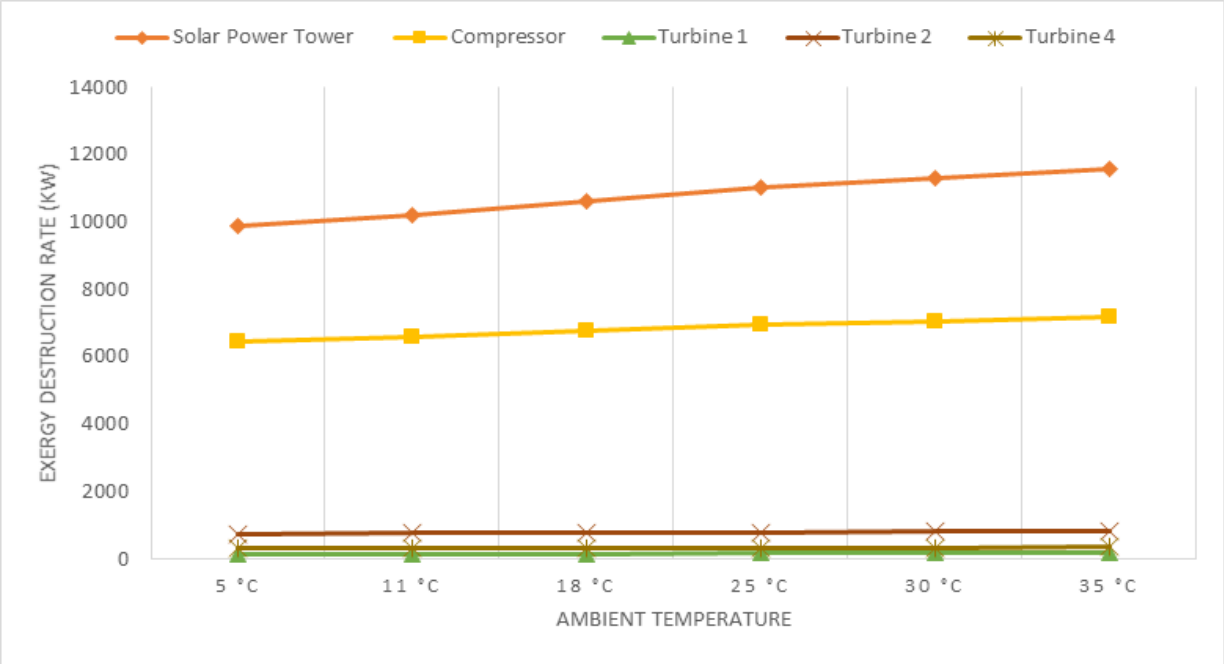

Figure 5.13 Parametric exergy destruction rate results for system 2 version 1 when ambient temperature varies

The pressure at state point 7 is changed to observe its effect on system efficiency. As mentioned in section 5.2.1.1, the power generated by Turbine 2 of the organic Rankine cycle is 38049 kW where the pressure at the state point 7 is 1000 kPa. The pressure of the state point 7 is increased gradually to 1700 kPa and the overall energy and exergy efficiencies are observed with the increased power. With the state point 7 pressure change, the turbine power output increases to 51086 kW from 31568 kW which results in increment in overall energy and exergy efficiency by 2.37% and 3.44% respectively. As a result of the pressure state point 7, there is also a change in organic Rankine cycle energy and exergy efficiency as well as overall efficiencies. This increment in the energy and exergy efficiency of the organic Rankine cycle is observed as 28.35% and 14.8533% when the pressure is increased to 1700 kPa from 800 kPa. Another and the last

parametric study is conducted for the desalination unit in the system to produce fresh water. As mentioned in previous sections, the operation principle and production.

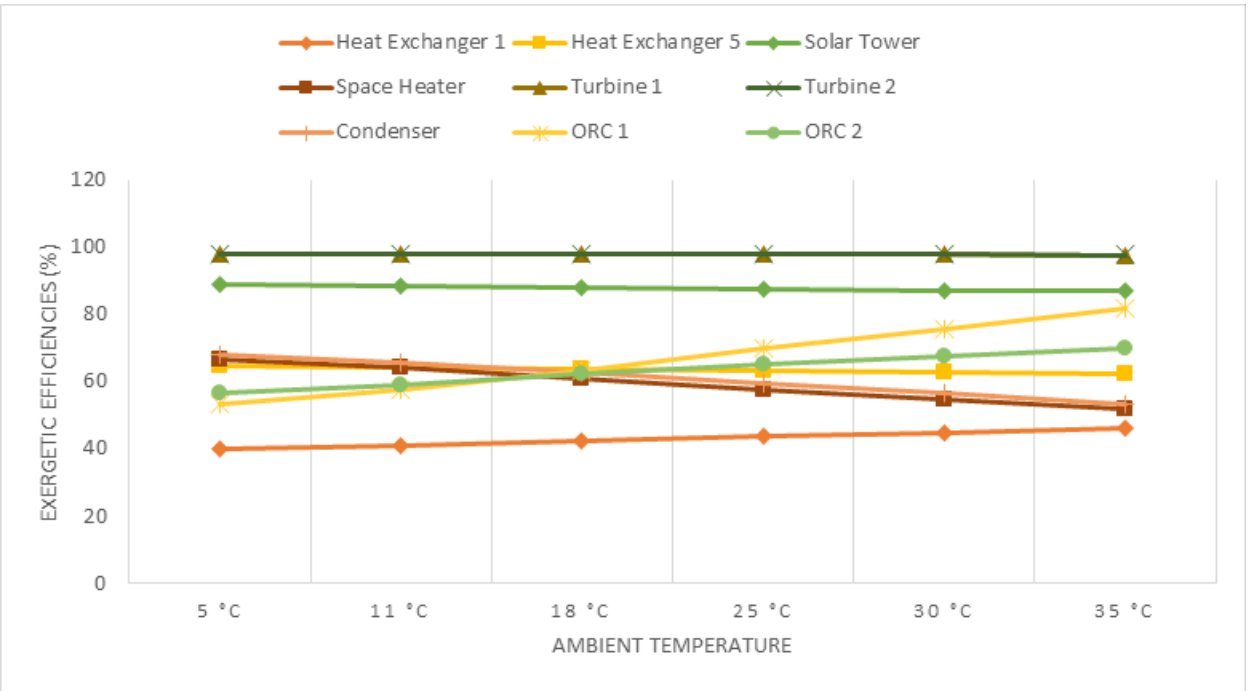

Figure 5.14 Parametric exergetic efficiency result for system 2 version 1 when ambient temperature varies

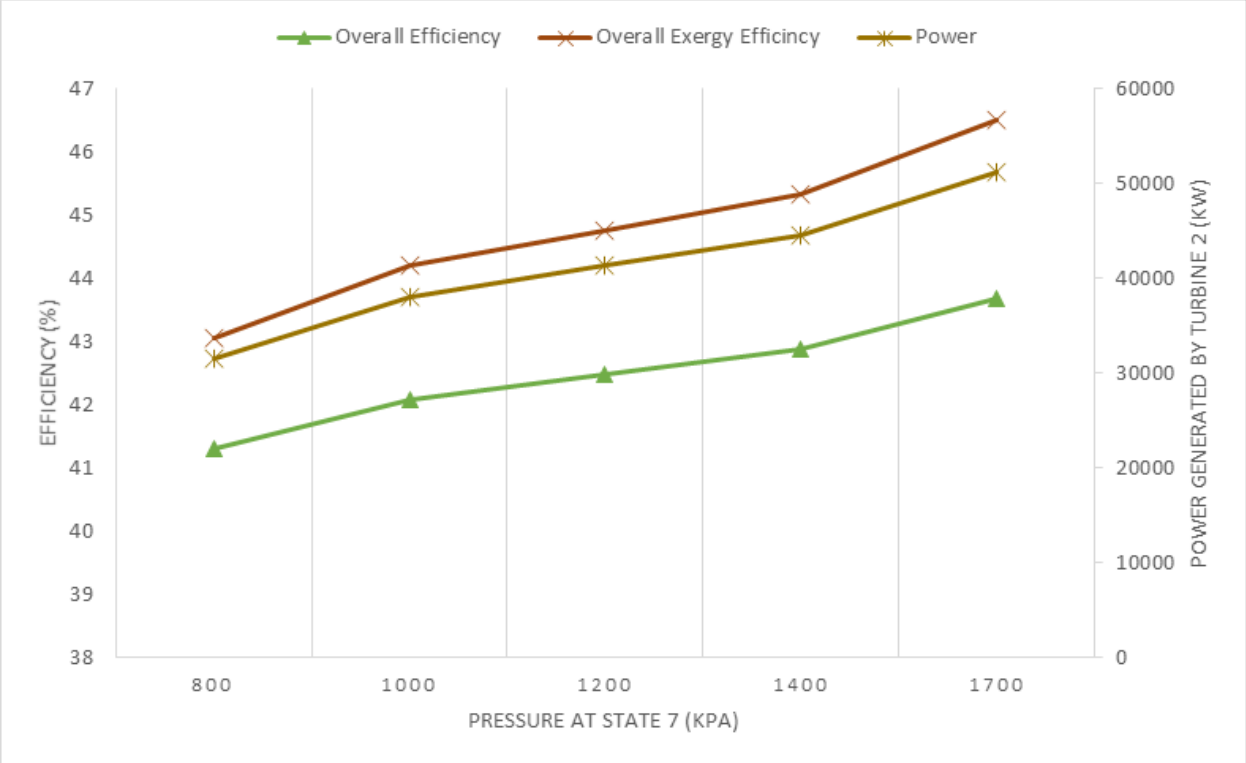

Figure 5.15 Power generated by turbine 2 and overall system energy and exergy efficiencies

calculations are explained in section 4.4.3. when the number of stages is increased from one to five the produced freshwater amount per second is increased to 57.4934 kg from 30.5707 kg.

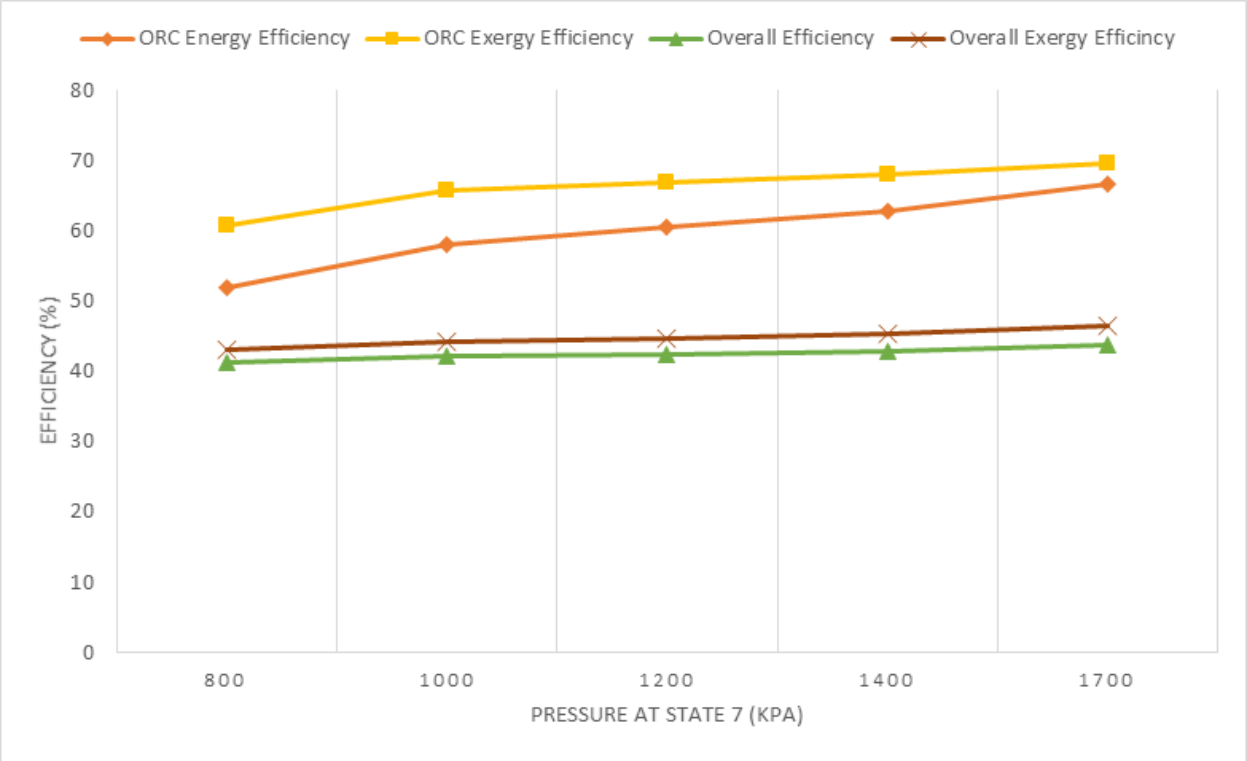

Figure 5.16 Parametric energy and exergy efficiencies for ORC and overall system when the pressure at state 7 varies

5.2.2 Version 2 of the System 2

In the second version of the system 2, the most important change which distinguishes the system from the first version is using only geothermal as energy sources. In order to reach the required temperature levels for the thermochemical cycle, which is the Cu-Cl cycle for the system 2, cascades heat pump configuration is used.

5.2.2.1 Case Study Results

This section of the chapter gives some information about the thermodynamical properties of this version of the system 2 as a case study. Table 5.9 is can be used to find required thermodynamical information about the state points such as specific enthalpy, specific entropy, specific exergy as well as working fluid type or state temperature and pressure status.

Table 5.10 gives the input and output information of major system components. One turbine of the system is capable to produce 8277 kW electric energy after the needs of the pumps and

compressors used in the system are met. The system has the capacity to generate 8080 kW of heat for space heating purposes. The system can produce 7.2517 kg per the second hydrogen.

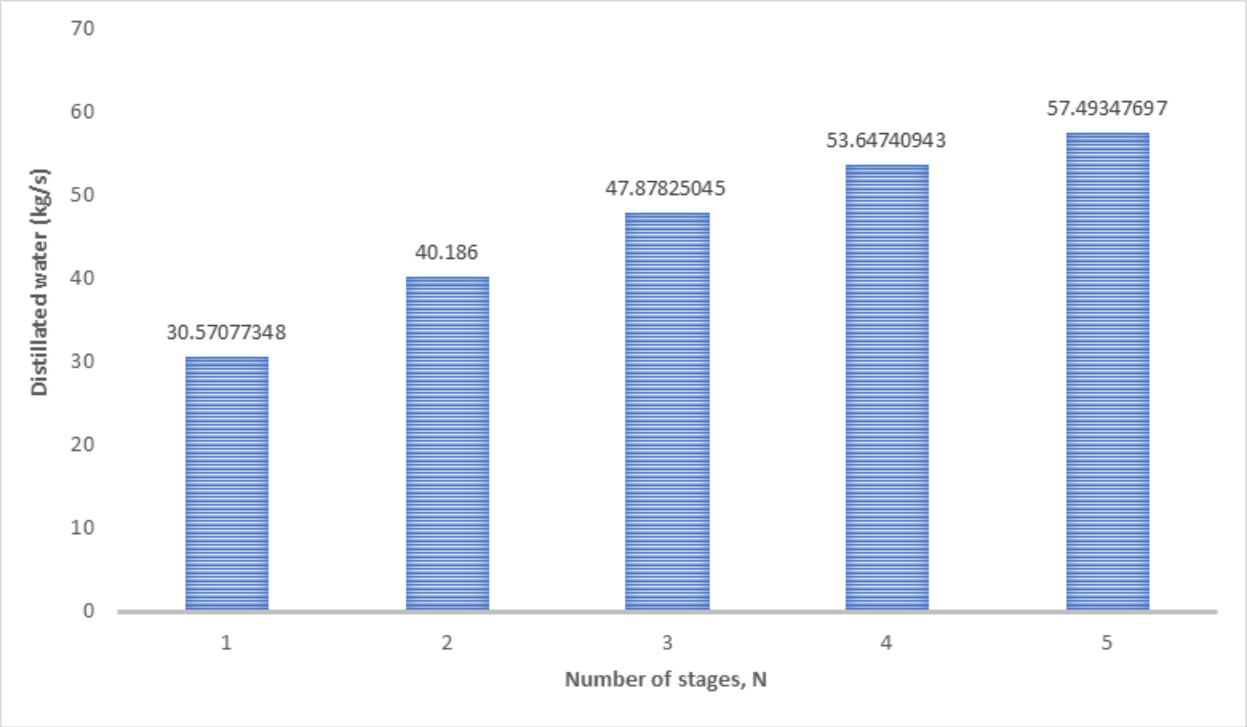

Figure 5.17 Parametric distilled water ratios when the stage number of the desalination unit varies

The exergy destruction rates for the major system components of the second version of the system 2 is given in Figure 5.18. The highest destruction rate is for compressor M1 with 40.32 kW which is 43.42% higher than the second-highest exergy destruction rate of compressor 1. Exergy efficiencies of the major system components are given in Table 5.11. The turbine 1 and compressor 4 have the highest exergy efficiencies while the condenser and space heater results in the lowest exergy efficiencies. The system has the heat upgrading configuration to reach the required temperature levels for the thermodynamic cycle to produce hydrogen energy. This heat upgrading system consists of two cycles which are Mercury heat pump at the bottom and Cu-Cl heat pump at the top. Coefficients of performance (COP) is calculated to understand the performance of this heat pump configuration. Figure 5.19 shows the COP value of the CuCl-Mercury cascaded heat pump and the stand-alone Cu-Cl heat pump. The calculation principle of the COP for this heat pump configuration is explained in section 4.4.6.

Table 5.9 State points thermodynamic properties of version 2 of the system 2 and the system 3

State Points	Fluid	Mass Flow Rate (kg/s)	Temperature (°C)	Pressure (kPa)	Specific Enthalpy (kJ/kg)	Specific Entropy (kJ/kg K)	Specific Exergy (kJ/kg)
0			25	101			
3	CuCl	19.08	576	102	1125	2.782	300.1
4	CuCl	1.58	576	102	1125	2.782	300.1
5	CuCl	0.39	576	102	1125	2.782	300.1
6	CuCl	17.11	576	102	1125	2.782	300.1
7	CuCl	0.39	480.993	0.03	1089	3.227	131.7
7-1	CuCl	0.39	480.993	0.03	1089	3.227	131.7
7-2	CuCl	0.39	480.993	0.03	1089	3.227	131.7
7-3	CuCl	0.39	480.993	0.03	1089	3.227	131.7
7-4	CuCl	0.39	480.993	0.03	1089	3.227	131.7
8	CuCl	0.39	480.993	0.03	1089	3.227	131.7
9	CuCl	0.39	1275.78	0.44	1392	3.469	362.4
10	CuCl	0.39	676.26	0.44	1163	3.282	189.2
11	CuCl	0.39	853.75	0.81	1223	3.289	247
12	CuCl	0.39	676.26	0.81	1163	3.231	204.5
13	CuCl	0.39	779.17	1.03	1202	3.25	238
14	CuCl	17.5	676.26	1.03	1163	3.211	210.5
15	CuCl	17.5	676.26	102	1163	2.825	325.5
16	CuCl	17.11	576	1.05	1125	3.167	185.6
16-1	CuCl	17.11	584	1.05	1128	3.17	186.6
16-2	CuCl	17.11	587	1.05	1129	3.172	188.3
17	Carbon Dioxide	400	70	150	37.84	0.04513	28.89
18	Carbon Dioxide	400	85	220	50.92	0.01047	52.3
19	Carbon Dioxide	400	135	265	97.25	0.09659	72.97
20	Carbon Dioxide	400	95	160	60.42	0.09653	36.16
21-Mercury	Mercury (Hg)	0.916	296.86	30	40.6	0.1009	15.03
22-Mercury	Mercury (Hg)	0.916	1292.89	290	188.2	0.2486	118.6
23-Mercury	Mercury (Hg)	0.916	485.89	290	66.43	0.14	29.22
24-Mercury	Mercury (Hg)	0.916	748.1	565	104.2	0.1827	54.22
25-Mercury	Mercury (Hg)	0.916	485.89	565	66.45	0.14	29.24
26-Mercury	Mercury (Hg)	0.916	638.43	818	88.03	0.1659	43.09
27-Mercury	Mercury (Hg)	0.916	485.89	818	66.47	0.14	29.26
28-Mercury	Mercury (Hg)	0.916	296.86	30	39.65	0.09919	14.6
29	Water	300	200	960	2830	6.712	833.9
30	R134a	150	80	125	325.1	1.238	-39.3
31	R134a	150	135	137	379	1.372	-25.45
32	R134a	150	125	102	369.1	1.372	-35.15
33	R134a	150	70	102	316.1	1.228	-45.47

34	Water	300	325	960	3106	7.235	954
35	Water	300	320	960	3095	7.217	948.7
36	Water	300	300	960	3052	7.144	927.9
37	SeaWater	115.38	21	100	87.56	0.308	0.1123
38	Fresh Water	40	21	100	87.56	0.3086	0.1123
39	Fresh Water	0.186	21	100	87.56	0.3086	0.1123
40	Brine Water	40	21	5	87.47	0.308	0.01703
41	Water	300	320	940	3095	7.228	946.1
42	Water	300	145	920	610.3	1.789	81.8
43	R134a	150	80	100	325.4	1.257	-44.61
44	Water	100	25	100	104.3	0.3651	-0.001003
45	Water	100	50	100	208.8	0.7018	4.152

Table 5.10 Input/Output of major system components, version 2 of the system 2

Component	**Value**
Input Power of Compressor 1 (kW)	**118.1**
Input Power of Compressor 2 (kW)	**23.37**
Input Power of Compressor 3 (kW)	**15.26**
Input Power of Compressor 4 (kW)	**1480**
Input Power of Compressor M1 (kW)	**135.2**
Input Power of Compressor M2 (kW)	**34.57**
Input Power of Compressor M3 (kW)	**19.77**
Output Work of Turbine 1 (kW)	**14733**
Input Power of Pump 1 (kW)	**2616**
Input Power of Pump 2 (kW)	**3048**
Net Power Output (kW)	**8277**
Electrolysis (HCl electrolysis of Cu-Cl)	**173.3**
Heating Condenser (kW)	**8080**
Hot Water (kW)	**10450**
Fresh-water production (kg/s)	**47.887**
Hydrogen output by Cu-Cl cycle (kg/hr)	**7.2517**

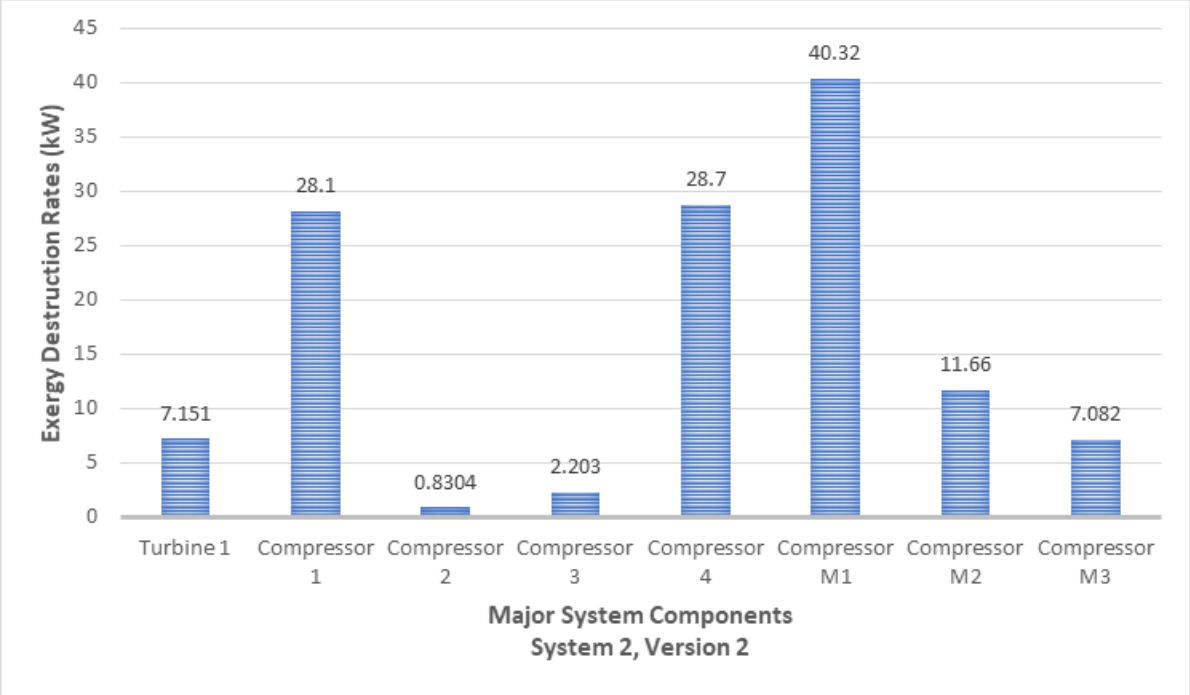

Figure 5.18 Exergy destruction rates for major system 2, version 2 components

Table 5.11 Exergetic efficiencies for system major components

Component	Exergetic Efficiency (%)
Compressor 1	76.2
Compressor 2	96.45
Compressor 3	85.56
Compressor 4	98.06
Compressor M1	70.18
Compressor M2	66.27
Compressor M3	64.17
Condenser	50.28
Space Heater	51.02
Turbine 1	99
Rankine 1	65.07

As can be seen in Figure 5.19, the COP values calculated for the stand-alone CuCl heat pump are 120.93% higher for the energetic COP and 81.71% higher for the exergetic COP in comparison with the cascaded configuration. For the cascaded Mercury-CuCl heat pump which is used in this version of the system has 1.557 energetic COP and 1.1279 exergetic COP.

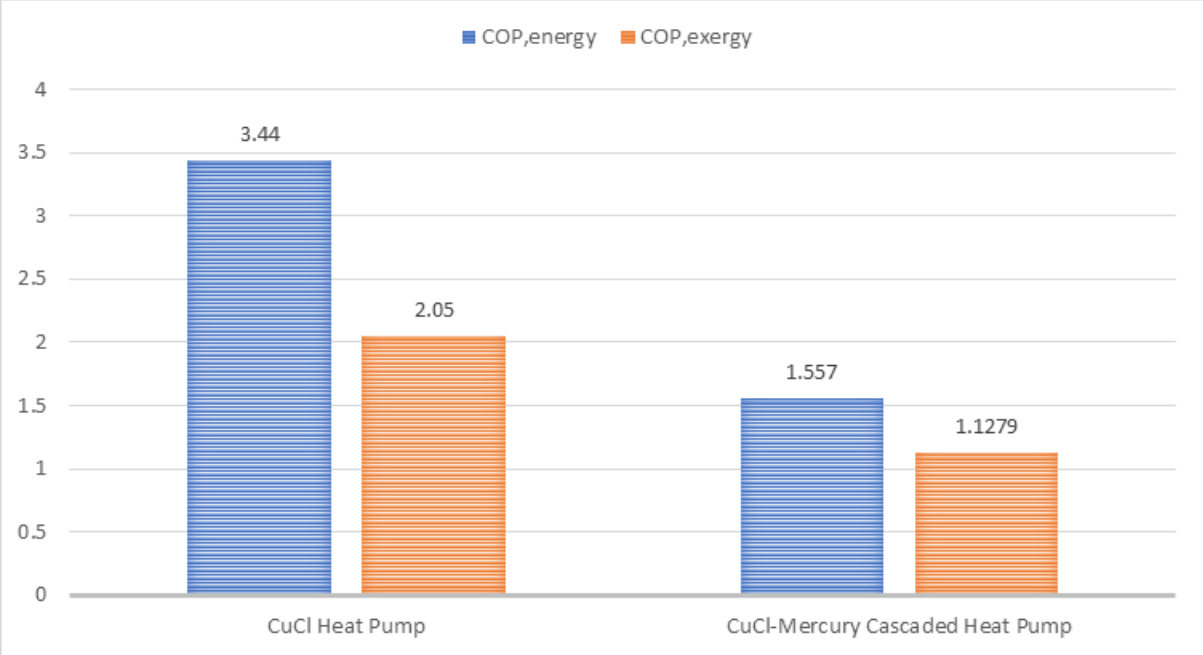

Figure 5.19 Comparison of energetic and exergetic coefficient of performance results for CuCl-Mercury cascaded heat pump

5.2.2.2 Parametric Results

Some parametric studies have also been conducted for the second version of the system 2 to analyze the system performance. The first parametric study is conducted to observe the effect of the ambient temperature on the system performance as can be seen in Figure 5.20. The ambient temperature is increased gradually from 5 °C to 35 °C. Similar to the parametric studies presented in the previous sub-sections, the variation of ambient temperature does not affect the energetic efficiency. However, the exergetic efficiency of the system, which was evaluated to be 49.65% at an ambient temperature value of 25 °C for the reference case, decreases from 59.97% to 45.67% at 5 °C and 35 °C respectively.

A parametric study has been conducted to observe the effect of the ambient temperature on the exergetic efficiency of the major system components which can be seen in Figure 5.21. The highest energetic changes are observed in the space heater and condenser. Space heater and condenser have shown the highest change with 11.77% and 14.07% decrease. Besides these components, the organic Rankine cycle has a curve of increment with 24.48%.

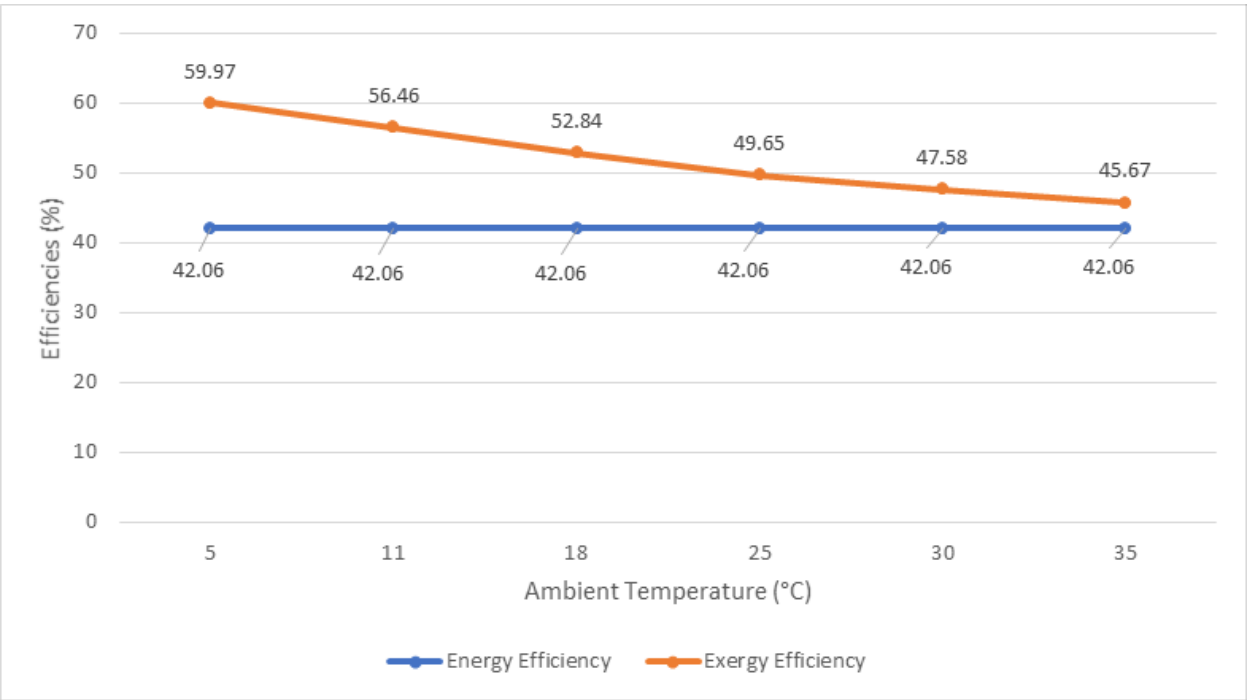

Figure 5.20 Parametric energy and exergy efficiency results for system 2 version 2 when ambient temperature varies

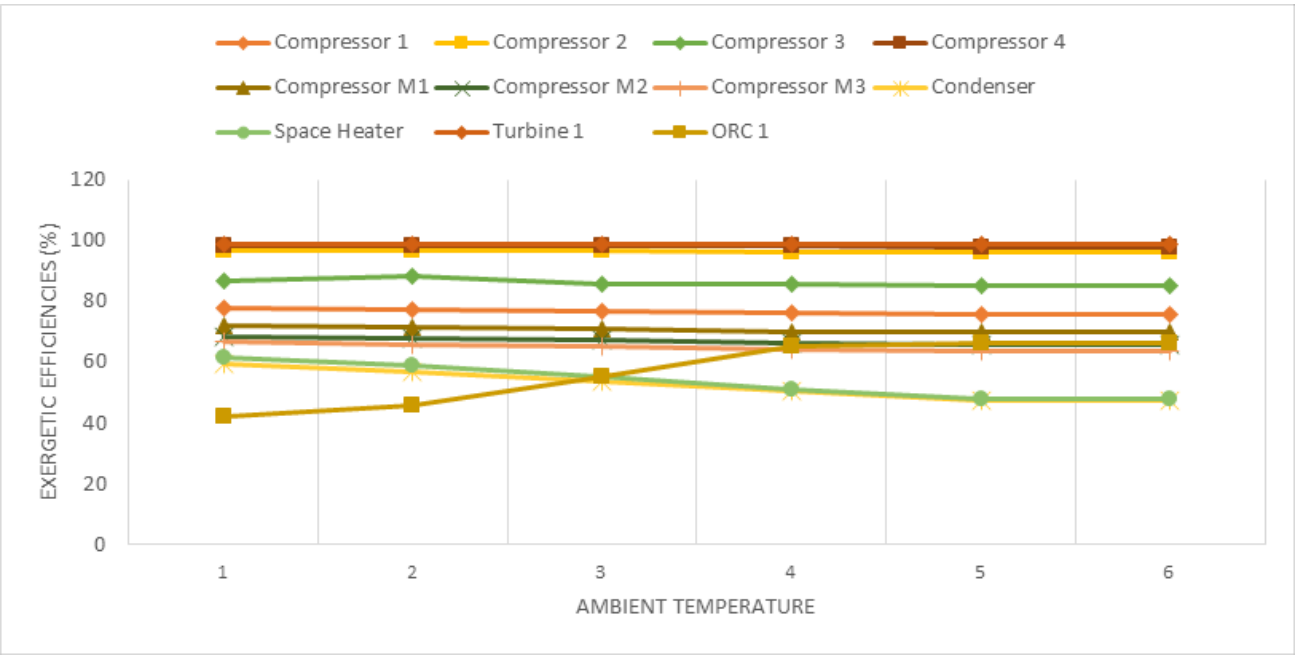

Figure 5.21 Parametric exergetic efficiency results for the system 2 version 2 when ambient temperature varies

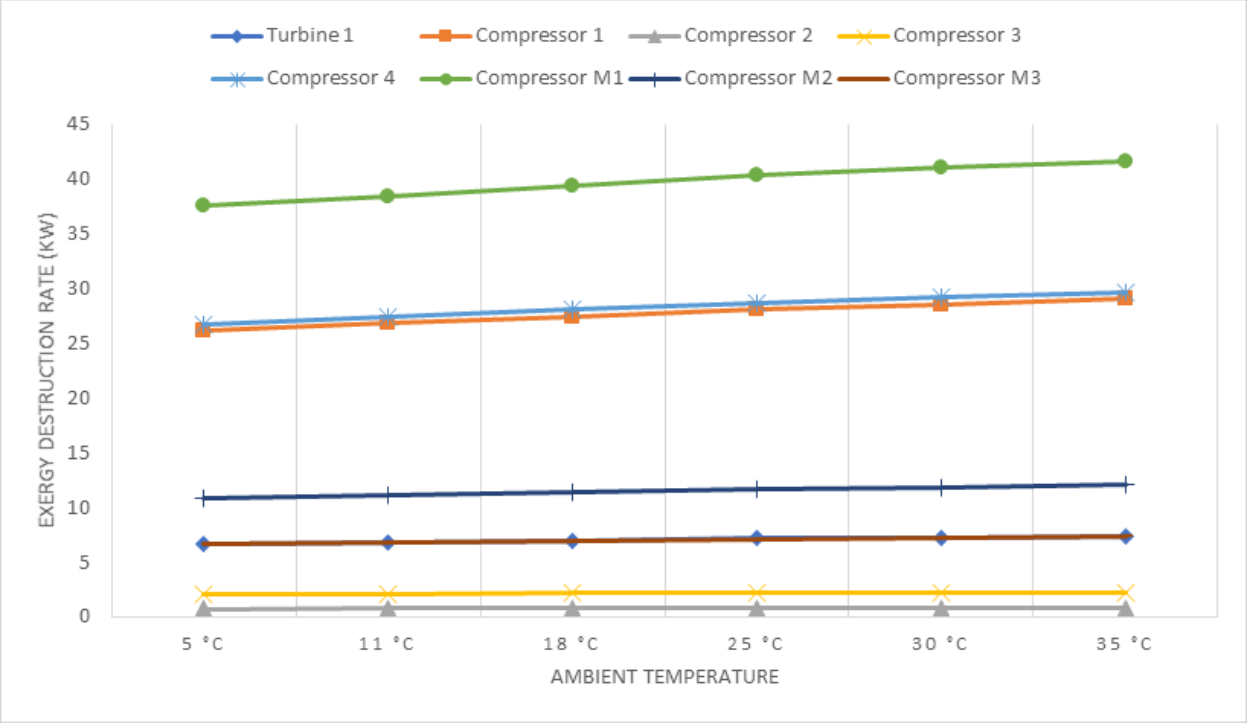

Figure 5.22 Parametric exergy destruction rates the system 2 version 2 when ambient temperature varies

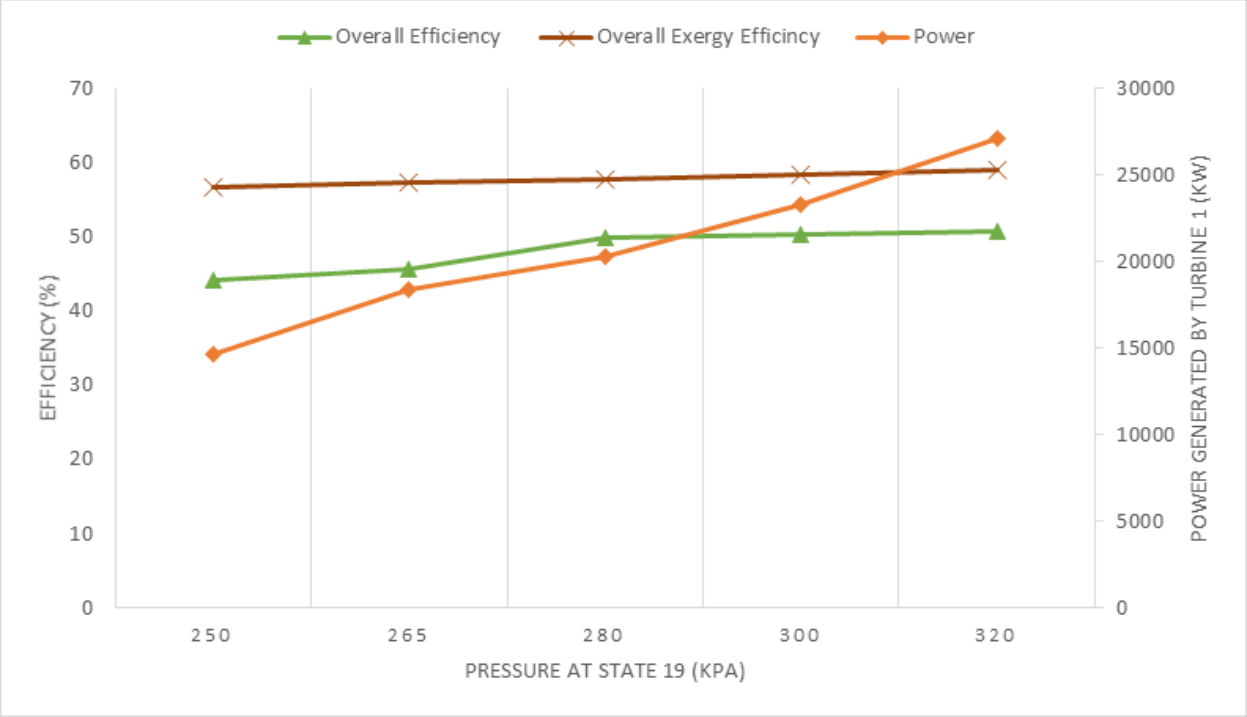

Figure 5.23 Power generated by turbine 1 and overall system energy and exergy efficiencies

Another parametric study is conducted for exergy destruction rates of the system components when ambient temperature varies. For this parametric study ambient temperature gradually increased from 5 °C to 35 °C. The increment trend in the exergy destruction rates is close to each other and approximately 10.80% for each component as can be seen in Figure 5.22.

The pressure at state point 19 is varied to observe its effect on system efficiency as shown in Figure 5.23. As mentioned in section 5.2.2.1, the power generated by Turbine 2 of the organic Rankine cycle is 18383 kW where the pressure at state point 19 is 265 kPa. The pressure of the state point 19 is increased gradually to 320 kPa and the overall energy and exergy efficiencies are observed with the increased power. With the state point 19 pressure change, the turbine power output increases to 27128 kW from 14620 kW which results in increment in overall energy and exergy efficiency by 6.65% and 2.4% respectively. As a result of the pressure state point 19, there is also a change in organic Rankine cycle energy and exergy efficiency as well as overall efficiencies. This increment in the energy and exergy efficiency of the organic Rankine cycle is observed as 16.71% and 13.43% when the pressure is increased to 320 kPa from 250 kPa as can be seen in Figure 5.24.

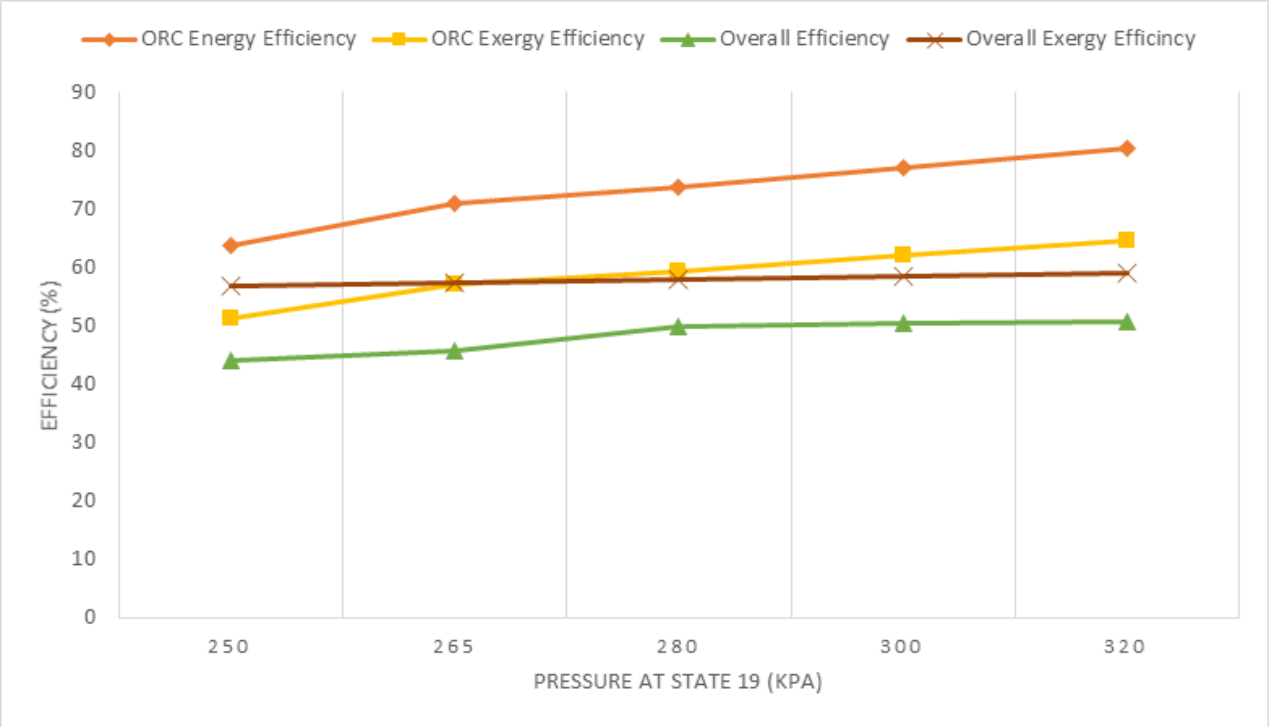

Figure 5.24 Parametric energy and exergy efficiencies for ORC and overall system when the pressure at state 19 varies

5.3 System 3

The system 3 is distinguished from the system 2 such that the thermochemical cycle used in this system is the Mg-Cl cycle. The system has two different versions that are distinguished from each other with the energy sources they use.

5.3.1 Version 1 of the System 3

The first version of the third system is similar to the first version of the second system. The version has a solar power tower and a geothermal energy source. The only difference is with regards to the thermochemical cycle which is the Mg-Cl cycle for hydrogen production in this system.

5.3.1.1 Case Study Results

Table 5.5, Figure 5.11 and Table 5.7 provides information regarding the state points of the thermochemical Mg-Cl cycle such as the specific enthalpy, entropy and exergy values as well as the working fluid, temperature or pressure information; exergy destruction rates for the major system components; exergetic efficiency for the system components respectively.

Table 5.12 State points thermodynamic properties of Mg-Cl Cycle, system 3

State Points	Fluid	Mass Flow Rate (kg/hr)	Temperature (°C)	Pressure (kPa)	Specific Enthalpy (kJ/kg)	Specific Entropy (kJ/kg K)
S1	Water	64.855008	25	100	-15865.5743	-9.055741367
S2	Water	1102.535136	70	100	-15688.74486	-8.501185197
S3	Water	1102.535136	537	100	-12402.51794	-0.487413256
S4	MGCL2	411.308928	537	100	-6313.566755	-0.930011497
S5	MGO - HCL - Water	1513.844064	537	100	-10485.01189	-0.144444725
S6	HCL - Water	1339.729056	537	100	-9983.915211	0.041068924
S7	HCL - Water	1339.729056	70	100	-12466.64704	-6.039887464
S8	Water - H2 - CL2	1339.729056	70	100	-11884.31854	-6.101133293
S9	Water - H2	1033.417728	70	100	-15459.86964	-8.133203515
S10	Water	1024.709126	70	100	-15677.69302	-8.468853518
S11	H2	8.7086016	70	100	645.8007672	2.069080884
S12	H2	8.7086016	25	100	0.490040095	0.053458234
S13	MGO	174.115008	537	100	-14340.70349	-1.571880697
S14	CL2	306.311328	70	100	20.93665031	0.068011815
S15	CL2	306.311328	537	100	260.5330778	0.50683882
S16	O2	480.426336	537	100	-5332.539741	-0.655520252
S17	O2	69.117408	537	100	505.4275873	0.977942332
S18	O2	69.117408	25	100	-0.248676265	0.002780747

Table 5.13 shows the system specifications for the first version of the system 3. The system can produce 8.7 kg/h of hydrogen. Table 5.14 shows the exergy destruction rates for the various components of the Mg-Cl thermochemical cycle.

5.3.1.2 Parametric Results

A parametric study has been conducted on the system to observe system operating performance. The first parametric study is conducted to observe the effect of the ambient temperature on the system. With the gradual increase of the ambient temperature from 5 °C to 35 °C, changes in energy and exergy efficiencies are observed as shown in Figure 5.25. The energy efficiency of the system is not affected by temperature changes although the exergy efficiency of the system is decreased by 25.40% which is 52.32% in the case study.

Table 5.13 Input/Output of major system components, version 1 of the system 3

Component	**Value**
Output Work of Turbine 1 (kW)	**7197**
Output Work of Turbine 2 (kW)	**38049**
Output Work of Turbine 4 (kW)	**60187**
Input Power of Compressor (kW)	**11714**
Input Power of Pump 1 (kW)	**5395**
Input Power of Pump 2 (kW)	**22822**
Input Power of Pump 3 (kW)	**35803**
Input Power of Pump 4 (kW)	**8262**
Electrolysis (HCl electrolysis of Mg-Cl)	**261.7**
Net Power Output (kW)	**8519**
Heating Condenser (kW)	**25873**
Solar Power Tower Output (kW)	**93323**
Fresh-water Production (kg/s)	**48.0212**
Hydrogen output by Mg-Cl cycle (kg/hr)	**8.70880**

As can be seen in Figure 5.27, state point 7 pressure level is changed to observe its effect on system efficiency. The power generated by Turbine 2 of the organic Rankine cycle is 38049 kW where the pressure at state point 7 is 1000 kPa. The pressure of the state point 7 is increased gradually to 1700 kPa and the overall energy and exergy efficiencies are observed with the increased power.

With the state point 7 pressure change, the turbine power output increases to 47779 kW from 34856 kW which results in increment in overall energy and exergy efficiency by 1.54% and 2.24% respectively.

Table 5.14 Exergy destruction rates for Mg-Cl cycle components

Component	**Exergy Destruction Rate (kW)**
Electrolyser	50.06
Hydrolysis	49.51
Chlorination	24.02

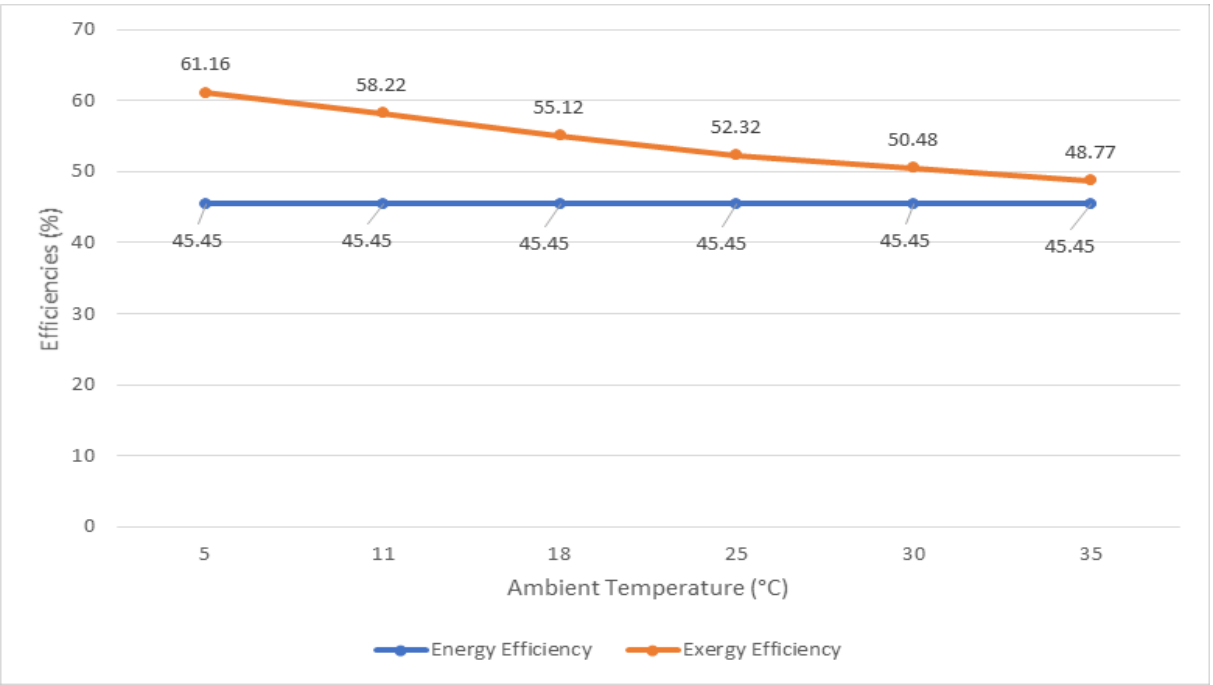

Figure 5.25 Parametric overall energy and exergy efficiency results for the system 3 version 1 when ambient temperature varies

As a result of the pressure state point 7, there is also a change in organic Rankine cycle energy and exergy efficiency as well as overall efficiencies. This increment in the energy and exergy efficiency of the organic Rankine cycle is observed as 17.32% and 16.91% when the pressure is increased to 1700 kPa from 800 kPa.

Figure 5.28 shows the effect of number of stages of the desalination unit on fresh-water production. In the case study, the stage number is considered as three and 48.02 kg/s of fresh-water is produced.

In this parametric study, stage number is increased gradually from one to five and freshwater produced is increased to 57.6651 kg/s from 30.6620 kg/s.

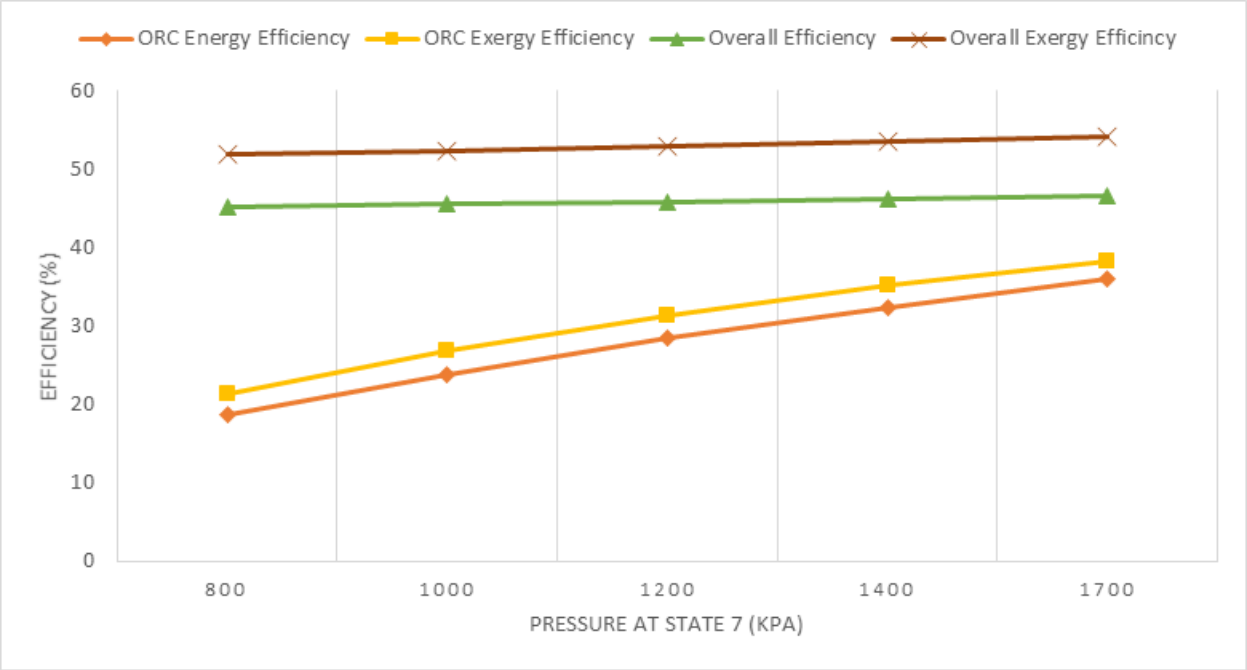

Figure 5.26 Parametric energy and exergy efficiencies for ORC and overall system when the pressure at state 7 varies

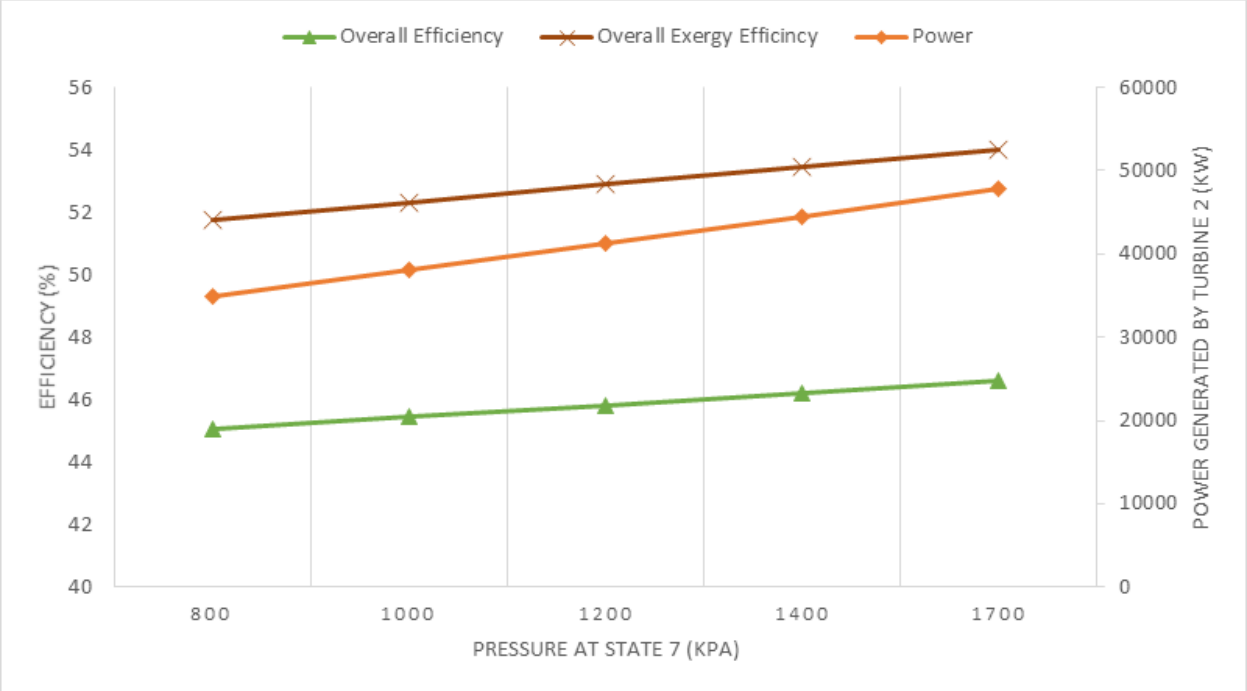

Figure 5.27 Power generated by turbine 2 and overall system energy and exergy efficiencies

5.3.2 Version 2 of the System 3

Version 2 of the system 3 is distinguished from the first version of the system with the energy sources they use. In this version of the system, the only geothermal energy source is used and a heat upgrading configuration is used to reach required temperature levels.

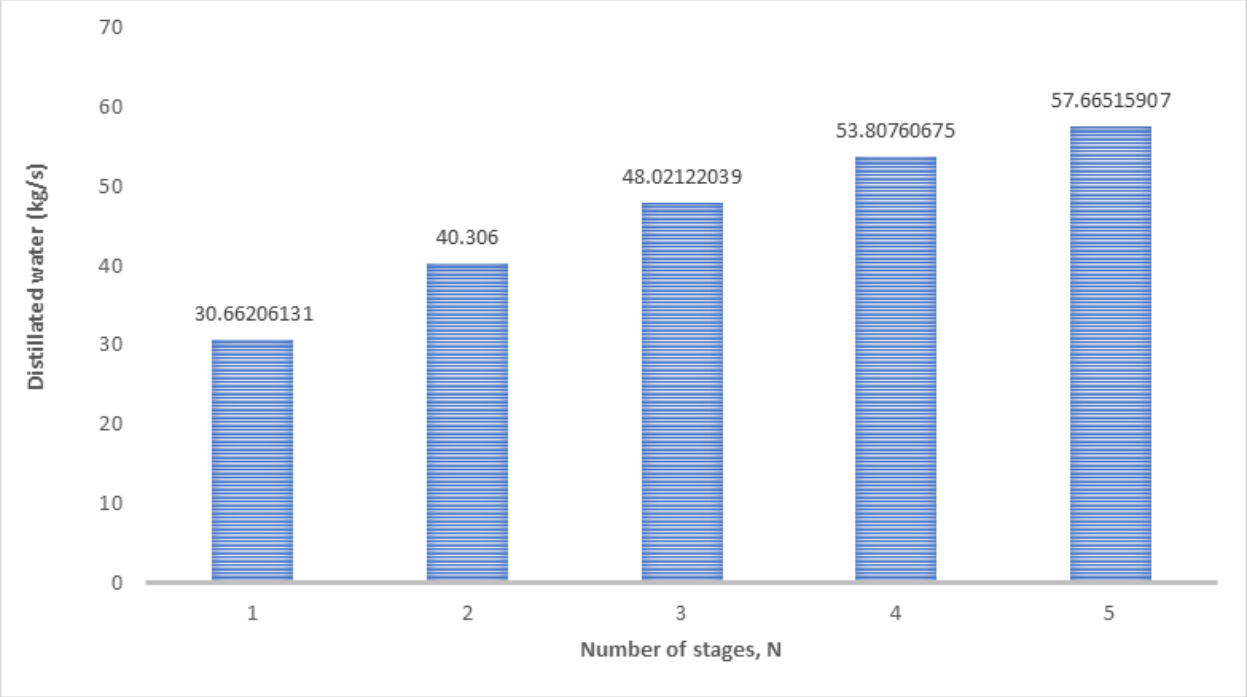

Figure 5.28 Parametric distilled water ratios when the stage number of the desalination unit varies

5.3.2.1 Case Study Results

Table 5.8 gives the required thermodynamic information of the state points such as specific enthalpy, specific entropy and specific exergy as well as state working fluid, temperature and pressure levels.

Table 5.15 shows the system input and output capacities for the major system components. Figure 5.29 shows the COP value of the MgCl-Mercury cascaded heat pump and the stand-alone Cu-Cl heat pump. Section 4.4.6 denotes the calculation principle of the COP fo this heat pump configuration. As can be seen in Figure 5.29, the COP values calculated for the stand-alone CuCl heat pump 120.92% higher for energetic COP and 120.94% higher for exergetic COP. For the cascaded Mercury-CuCl heat pump which is used in this version of the system has 2.972 energetic COP and 1.771 exergetic COP.

Table 5.15 Input/Output of major system components, version 2 of the system 3

Component	Value
Input Power of Compressor 1 (kW)	**118.1**
Input Power of Compressor 2 (kW)	**23.37**
Input Power of Compressor 3 (kW)	**15.26**
Input Power of Compressor 4 (kW)	**1480**
Input Power of Compressor M1 (kW)	**135.2**
Input Power of Compressor M2 (kW)	**34.57**
Input Power of Compressor M3 (kW)	**19.77**
Output Work of Turbine 1 (kW)	**14733**
Input Power of Pump 1 (kW)	**2616**
Input Power of Pump 2 (kW)	**3048**
Net Power Output (kW)	**16096**
Electrolysis (HCl electrolysis of Mg-Cl)	**261.7**
Heating Condenser (kW)	**8080**
Hot Water (kW)	**10450**
Fresh-water Production (kg/s)	**48.0212**
Hydrogen output by Mg-Cl cycle (kg/hr)	**8.70880**

5.3.2.2 Parametric Results

A parametric study has been conducted to observe the effect of ambient temperature on energy and exergy efficiencies of the system. The ambient temperature is increased to 35 °C degrees from 5 °C gradually. A decrease is observed for the exergy efficiency of the system due to the change of ambient temperature while the energy efficiency remains the same as can be seen in Figure 5.30.

The pressure at state point 19 is changed to observe its effect on system efficiency. As mentioned in section 5.3.2.1, the power generated by Turbine 2 of the organic Rankine cycle is 14733 kW where the pressure at state point 19 is 265 kPa. The pressure of the state point 19 is increased gradually to 320 kPa and the overall energy and exergy efficiencies are observed with the increased power.

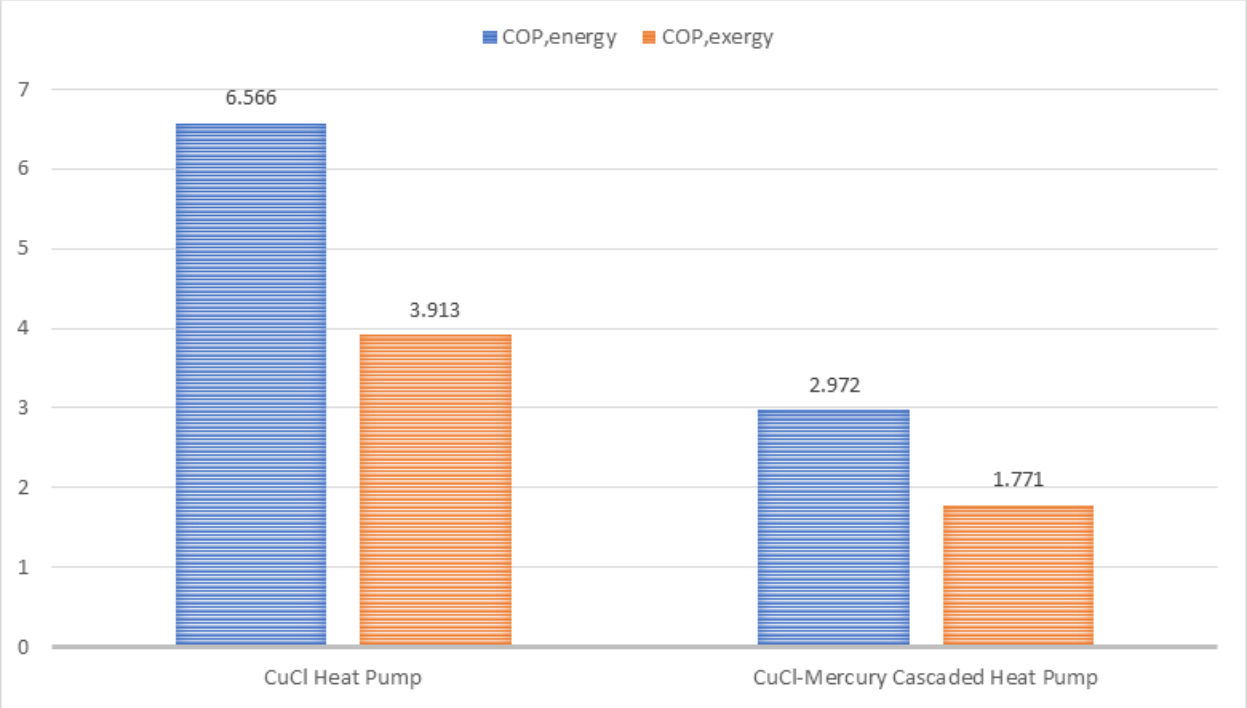

Figure 5.29 Comparison of energetic and exergetic coefficient of performance results for MgCl-Mercury cascaded heat pump

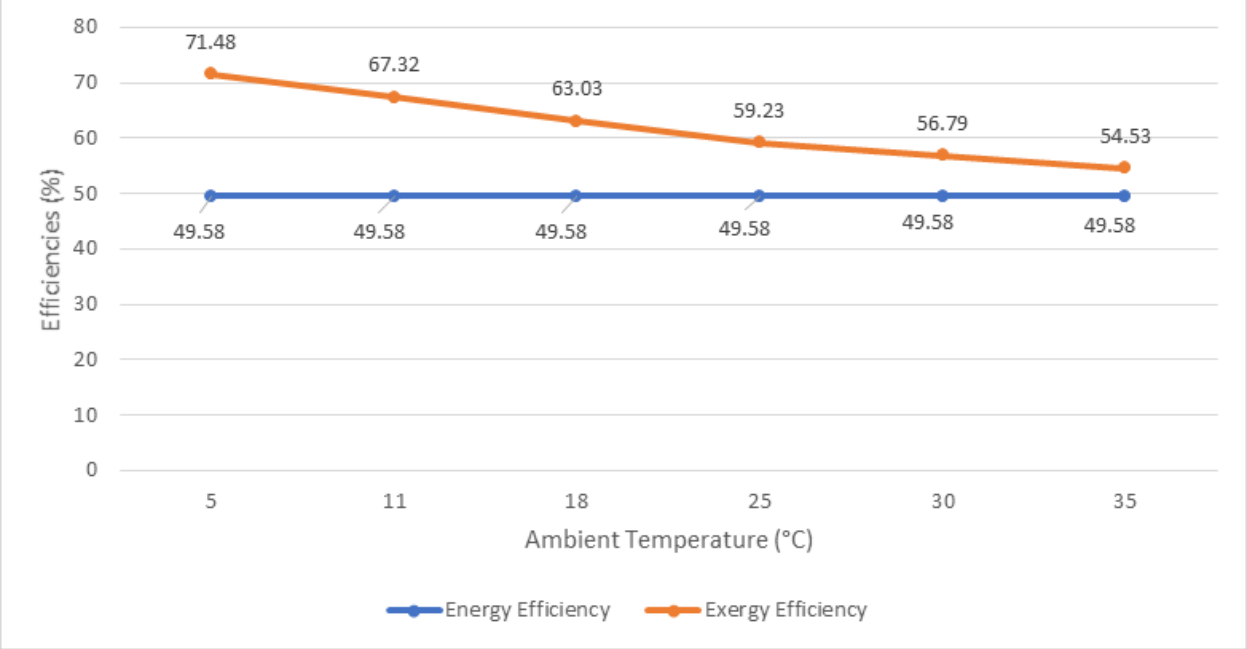

Figure 5.30 Parametric overall energy and exergy efficiency results for the system 3 version 2 when ambient temperature varies

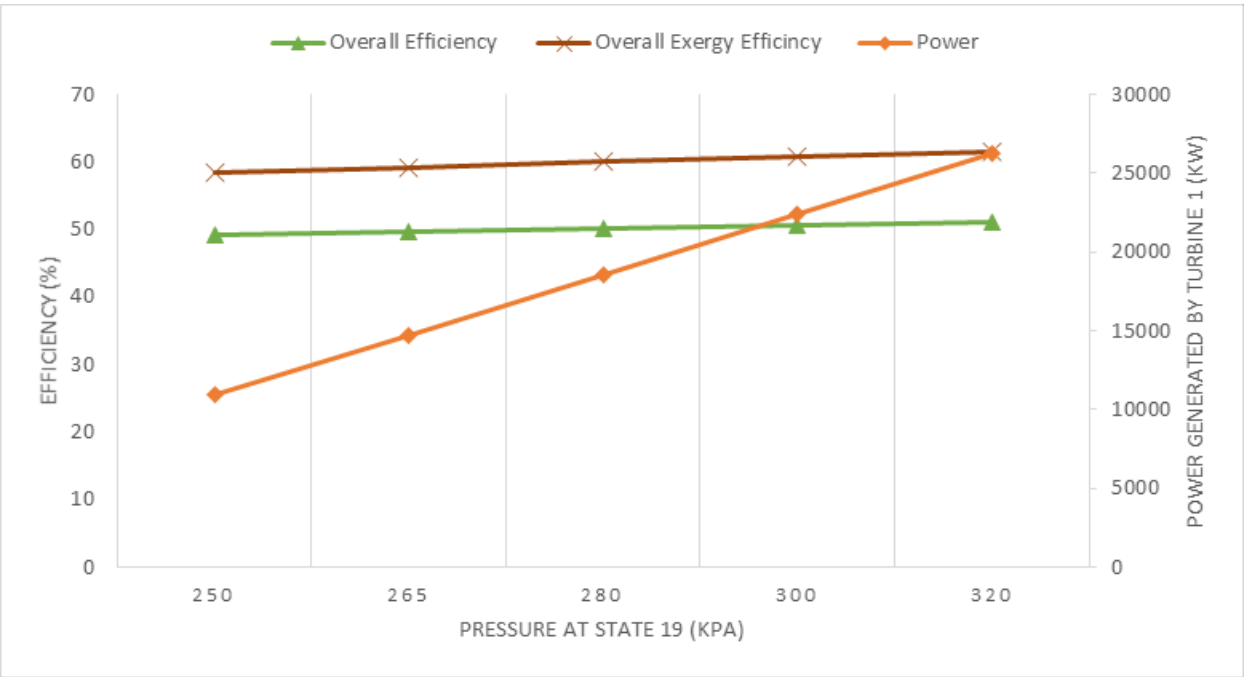

Figure 5.31 Power generated by turbine 1 and overall system energy and exergy efficiencies

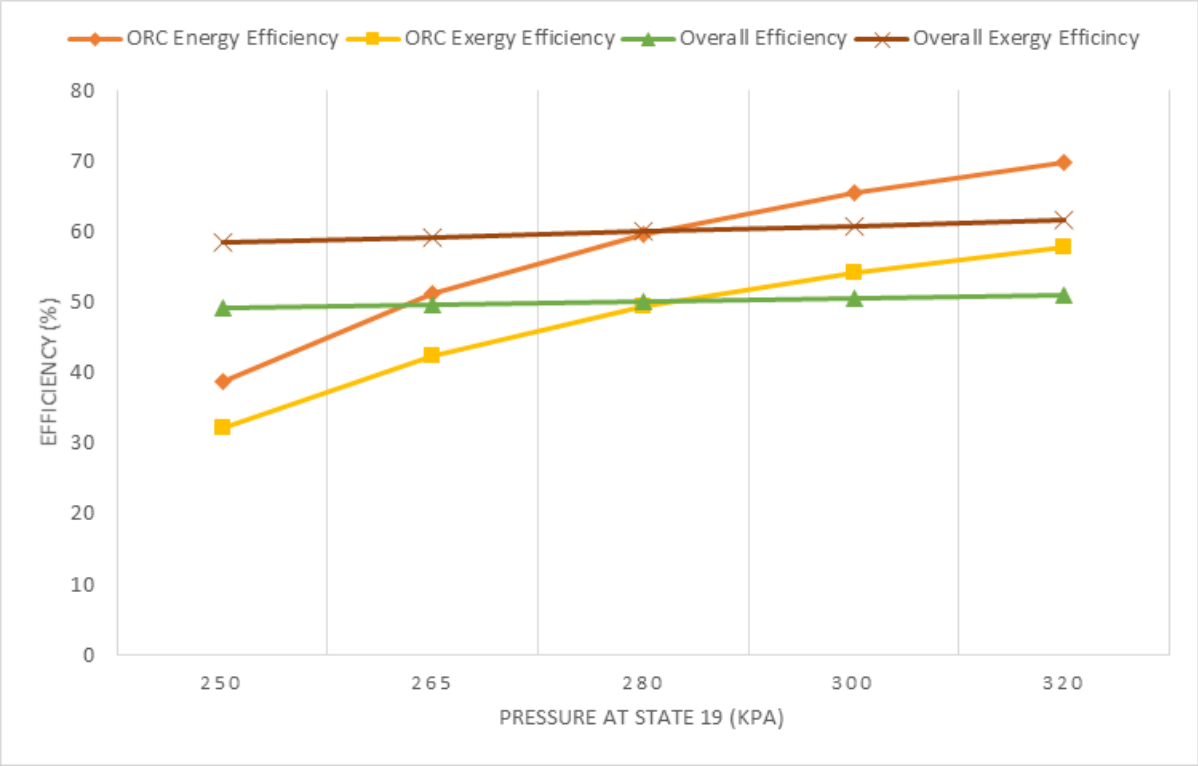

Figure 5.32 Parametric energy and exergy efficiencies for ORC and overall system when the pressure at state 19 varies

With the state point 19 pressure change, the turbine power output increases from 10970 kW to 26203 kW which results in increment in overall energy and exergy efficiency by 2.01% and 3.05% respectively as can be seen in Figure 5.31.

As a result of the pressure at state point 19, there is also a change in the organic Rankine cycle energy and exergy efficiency values as well as overall efficiencies. This increment in the energy and exergy efficiency of the organic Rankine cycle is observed as 31.05% and 25.72% respectively when the pressure is increased from 250 kPa to 320 kPa as can be seen in Figure 5.32.

Chapter 6 CONCLUSIONS AND RECOMMENDATIONS

This thesis proposes and examines three different integrated systems aiming to enable more efficient and sustainable hydrogen production with green and renewable resources. A reference case for each study and a sensitivity analysis has been conducted for each system and their versions in terms of energy and exergy approaches. The main points that this study focusses on are the energy and exergy efficiencies to investigate the system operating performances. With this method, it is possible to compare the operating performance of each system with each other. This chapter discusses and presents the main findings as a result of the thermodynamic analysis of the systems and their variants. Some suggestions for the potential improvements with regards to the processes and future research directions are also provided in this chapter.

6.1 Conclusions

Geothermal based multigenerational system which is integrated with a solar tower and desalination unit where hydrogen production is achieved by thermochemical cycles and high-temperature electrolyzers are proposed. Vancouver, Canada is considered to be the proposed location for these three integrated systems. PEM type high-temperature electrolyzer is considered as the hydrogen production method in the first proposed system. Moreover, the Cu-Cl and the Mg-Cl thermochemical cycles are preferred as the hydrogen production methods in the second and third systems respectively. For the first system and both versions of the second and third systems, thermal energy recovered by solar tower met the high-temperature requirements of the hydrogen production processes. The first system offers a methanol synthesis option to capture the carbon dioxide released from the industry in order to help mitigate its environmental impact. Additional configuration which is seen as CuCl-Mercury cascaded heat pump technology in the second versions of the second and third systems are used to upgrade heat recovered from geothermal source to meet the high-temperature requirement of the thermochemical cycles. Higher energy and exergy efficiencies are observed in the systems which use only geothermal as an energy source when compared with the systems integrated with solar and wind power.

Major energy sources meet the high-temperature requirements of hydrogen production units primarily, thereafter, excess energy and other energy sources are utilized to achieve commodities such as electricity, space heating, hot water, freshwater and hydrogen which is used to produce methanol synthesis in the first system.

The brine disposal method for the multistage desalination unit will be dictated by geography. The current system proposes direct discharge into oceans, surface water or sewage, deep well injection and brine evaporation ponds. However, brine disposal is a real environmental problem. New methods should be developed to prevent this situation. Salt disposed of desalination can be used in various processes. Chlorine can be manufactured by the electrolysis of a sodium chloride solution which is known as the Chloralkali process.

The main findings which are acquired from the thermodynamic analysis of the five integrated systems through energy and exergy approach are listed as follows:

- Using the heat upgrading from geothermal source as the only heat source in version 2 of the system 3 has shown the best performance with an overall energy efficiency of 49.58% and an overall exergy efficiency of 59.23% amongst the five different integrated systems considered. It is also clearly observed to be the most advantageous of the heat upgrading configurations by comparing the first and second versions of the system 2 which results in the same energy overall efficiency but 5.44 % more exergy efficiency.
- In the second versions of the systems 2 and 3, the required temperature levels for the thermochemical cycle have been achieved with cascaded heat pump configurations. With Mercury-CuCl cascaded heat pump configuration, the energetic COP (COP_{en}) of 1.6 and the exergetic COP (COP_{ex}) of 1.1 are obtained for the Cu-Cl thermochemical cycle (System 2, Version 2). For the Mg-Cl thermochemical cycle (System 3, Version 2), the energetic COP (COP_{en}) of 2.9 and the exergetic COP (COP_{ex}) of 1.8 are obtained.
- The second version of system 3 has the capacity to produce 16049 kW while the first system can generate electric power at a rate of 16828 kW after the energy needs of the electrolyzer, system pumps and compressors are met.
- Systems 1, 2 and 3 are capable of producing fresh-water at flow rates of 48.2 kg/s, 47.8 kg/s and 48.0 kg/s respectively.
- The sensitivity analysis results have shown that an increase in the number of stages in the multi-effect desalination unit results in a corresponding increase in the amount of the fresh-water produced. Although, the space heating capacity of the first system and the first versions of systems 2 and 3 is 25873 kW, this amount decreases to 8080 kW.

- The systems achieve hydrogen production as one of the useful outputs by thermochemical cycles. Both versions of system 2 produce 7.25 kg/h of hydrogen whereas both variants of system 3 generate hydrogen at a capacity of 8.7 kg/h.
- When the total exergy destruction rates are compared, the heat upgrading options of the systems result in lower values with 257% less exergy destruction rate for system 2 and 248% less exergy destruction rate for system 3 compared to their first versions.
- The lowest total exergy destruction rate is achieved as 46559.03 kW in the second version of the system 2 although it has 7.52% less energy and 9.58% less exergy efficiency than the second version of system 3 which has 47012.49 kW total exergy destruction rate.

6.2 Recommendations

- The performance of the Cu-Cl and Mg-Cl thermochemical cycles should be investigated by lab-scale experiments. The experiments should be conducted for each step to investigate high and mid-temperature reaction performances.
- Further studies should be performed for the Cu-Cl and Mg-Cl reactors to maintain the process which requires less energy consumption for the high-temperature reactors such as chlorination, hydrolysis and thermolysis steps.
- It should be studied to expand the cascaded heat pump configuration used to meet the heat requirement from geothermal, with one or more heat pump cycle if needed, to obtain higher COP values.
- Multi-objective optimization based on the thermoeconomic and thermodynamic analysis should be performed for the overall system to help reduce the GHG emissions and costs while simultaneously increasing the process efficiencies.
- Dynamic analysis in addition to the steady-state analysis is important for more information about the operation.
- A detailed study should be carried out on storage and transportation methods of hydrogen and methanol produced in the systems.
- A life cycle assessment is a prior requirement to integrate one of these systems in real life to estimate the environmental impact and total operating costs.

REFERENCES

[1] I. Dincer, “Green methods for hydrogen production,” *Int. J. Hydrogen Energy*, vol. 37, no. 2, pp. 1954–1971, 2012, doi: 10.1016/j.ijhydene.2011.03.173.

[2] A. S. F. Farshid Zabihian, “Greenhouse gas emissions of fossil fuel-fired power plants: current status and reduction potentials, case study of Iran and Canada,” *Int. J. Glob. Warm.*, vol. 2, no. 2, 2010.

[3] U. Z. Tahir Abdul Hussain Ratlamwala, Ammar Ahmed Raja, Subhan Raza Jaffry, “Geothermal and solar energy amalgamated multigeneration system escorting diverse needs of a district,” *Int. J. Exergy*, vol. 29, no. 2–4, 2019, doi: https://doi.org/10.1504/IJEX.2019.100369.

[4] R. M. A. Dincer I., *Exergy: Energy, Environment and Sustainable Development*. UK: Elsevier, 2007.

[5] H. Caliskan, I. Dincer, and A. Hepbasli, “Exergoeconomic and environmental impact analyses of a renewable energy based hydrogen production system,” *Int. J. Hydrogen Energy*, vol. 38, no. 14, pp. 6104–6111, 2013, doi: 10.1016/j.ijhydene.2013.01.069.

[6] Natural Resources Canada, “Canada – A Global Leader in Renewable Energy Enhancing Collaboration on Renewable Energy Technologies,” *Energy Mines Minist. Conf.*, no. August, p. 14, 2013, doi: 10.1016/j.bbr.2010.04.014.

[7] Treasury Board of Canada Secretariat, “Government of Canada sets ambitious GHG reduction targers for federal operations,” 2017. [Online]. Available: https://www.canada.ca/en/treasury-board-secretariat/news/2017/12/government_of_canadasetsambitiousghgreductiontargetsforfederalop.html.

[8] M. Calderón, A. J. Calderón, A. Ramiro, and J. F. González, “Automatic management of energy flows of a stand-alone renewable energy supply with hydrogen support,” *Int. J. Hydrogen Energy*, vol. 35, no. 6, pp. 2226–2235, 2010, doi: 10.1016/j.ijhydene.2009.12.028.

[9] T. I. Sigfusson, “Pathways to hydrogen as an energy carrier,” *Philos. Trans. R. Soc. A Math. Phys. Eng. Sci.*, vol. 365, no. 1853, pp. 1025–1042, 2007, doi: 10.1098/rsta.2006.1960.

[10] A. Bakenne, W. Nuttall, and N. Kazantzis, “Sankey-Diagram-based insights into the hydrogen economy of today,” *Int. J. Hydrogen Energy*, vol. 41, no. 19, pp. 7744–7753, 2016, doi: 10.1016/j.ijhydene.2015.12.216.

[11] A. Ozbilen, I. Dincer, and M. A. Rosen, “A comparative life cycle analysis of hydrogen production via thermochemical water splitting using a Cu-Cl cycle,” *Int. J. Hydrogen Energy*, vol. 36, no. 17, pp. 11321–11327, 2011, doi: 10.1016/j.ijhydene.2010.12.035.

[12] A. S. Joshi, I. Dincer, and B. V. Reddy, “Solar hydrogen production: A comparative performance assessment,” *Int. J. Hydrogen Energy*, vol. 36, no. 17, pp. 11246–11257, 2011, doi: 10.1016/j.ijhydene.2010.11.122.

[13] I. Dincer and C. Acar, “Review and evaluation of hydrogen production methods for better sustainability,” *Int. J. Hydrogen Energy*, vol. 40, no. 34, pp. 11094–11111, 2014, doi: 10.1016/j.ijhydene.2014.12.035.

[14] W. C. Lattin and V. P. Utgikar, “Global warming potential of the sulfur-iodine process using life cycle assessment methodology,” *Int. J. Hydrogen Energy*, vol. 34, no. 2, pp. 737–744, 2009, doi: 10.1016/j.ijhydene.2008.10.059.

[15] G. Naterer *et al.*, “Recent Canadian advances in nuclear-based hydrogen production and the thermochemical Cu-Cl cycle,” *Int. J. Hydrogen Energy*, vol. 34, no. 7, pp. 2901–2917, 2009, doi: 10.1016/j.ijhydene.2009.01.090.

[16] M. F. Orhan, I. Dinçer, and M. A. Rosen, “Efficiency comparison of various design schemes for copper-chlorine (Cu-Cl) hydrogen production processes using Aspen Plus software,” *Energy Convers. Manag.*, vol. 63, pp. 70–86, 2012, doi: 10.1016/j.enconman.2012.01.029.

[17] C. Zamfirescu, G. F. Naterer, and I. Dincer, “Vapor compression CuCl heat pump integrated with a thermochemical water splitting cycle,” *Thermochim. Acta*, vol. 512, no. 1–2, pp. 40–48, 2011, doi: 10.1016/j.tca.2010.08.020.

[18] T. A. H. Ratlamwala and I. Dincer, “Energy and exergy analyses of a Cu-Cl cycle based integrated system for hydrogen production,” *Chem. Eng. Sci.*, vol. 84, pp. 564–573, 2012, doi: 10.1016/j.ces.2012.08.052.

[19] S. Aghahosseini, I. Dincer, and G. F. Naterer, “Integrated gasification and Cu-Cl cycle for trigeneration of hydrogen, steam and electricity,” *Int. J. Hydrogen Energy*, vol. 36, no. 4, pp. 2845–2854, 2011, doi: 10.1016/j.ijhydene.2010.11.078.

[20] G. F. Naterer *et al.*, “Clean hydrogen production with the Cu-Cl cycle-Progress of international consortium, I: Experimental unit operations,” *Int. J. Hydrogen Energy*, vol. 36, no. 24, pp. 15472–15485, 2011, doi: 10.1016/j.ijhydene.2011.08.012.

[21] S. Aghahosseini, I. Dincer, and G. F. Naterer, “Process integration of hydrolysis and electrolysis processes in the Cu-Cl cycle of hydrogen production,” *Int. J. Hydrogen Energy*, vol. 38, no. 23, pp. 9633–9643, 2013, doi: 10.1016/j.ijhydene.2013.05.108.

[22] K. Gabriel, L. Finney, and P. Dolloso, “Preliminary results of the integrated hydrolysis reactor in the Cu-Cl hydrogen production cycle,” *Int. J. Hydrogen Energy*, vol. 44, no. 20, pp. 9743–9752, 2019, doi: 10.1016/j.ijhydene.2018.12.150.

[23] H. Ozcan and I. Dincer, “Thermodynamic modeling of a nuclear energy based integrated system for hydrogen production and liquefaction,” *Comput. Chem. Eng.*, vol. 90, pp. 234–246, 2016, doi: 10.1016/j.compchemeng.2016.04.015.

[24] M. T. Balta, I. Dincer, and A. Hepbasli, “Performance assessment of solar-driven integrated Mg-Cl cycle for hydrogen production,” *Int. J. Hydrogen Energy*, vol. 39, no. 35, pp. 20652–20661, 2014, doi: 10.1016/j.ijhydene.2014.06.133.

[25] A. Patyk, T. M. Bachmann, and A. Brisse, “Life cycle assessment of H2 generation with high temperature electrolysis,” *Int. J. Hydrogen Energy*, vol. 38, no. 10, pp. 3865–3880, 2013, doi: 10.1016/j.ijhydene.2013.01.063.

[26] C. Zamfirescu and I. Dincer, “Performance investigation of high-temperature heat pumps with various BZT working fluids,” *Thermochim. Acta*, vol. 488, no. 1–2, pp. 66–77, 2009, doi: 10.1016/j.tca.2009.01.028.

[27] C. Zamfirescu, I. Dincer, and G. Naterer, “Performance evaluation of organic and titanium based working fluids for high-temperature heat pumps,” *Thermochim. Acta*, vol. 496, no. 1–2, pp. 18–25, 2009, doi: 10.1016/j.tca.2009.06.021.

[28] J. G. Powles, “Is molten cuprous chloride a molecular liquid?,” *J. Phys. C Solid State Phys.*, vol. 8, no. 7, 1975.

[29] W. Wongsuwan, S. Kumar, P. Neveu, and F. Meunier, *A review of chemical heat pump technology and applications*, vol. 21, no. 15. 2001.

[30] A. Odukoya and G. F. Naterer, “Upgrading waste heat from a cement plant for thermochemical hydrogen production,” *Int. J. Hydrogen Energy*, vol. 39, no. 36, pp. 20898–20906, 2014, doi: 10.1016/j.ijhydene.2014.10.096.

[31] A. Odukoya and G. F. Naterer, “Calcium oxide/steam chemical heat pump for upgrading waste heat in thermochemical hydrogen production,” *Int. J. Hydrogen Energy*, vol. 40, no. 35, pp. 11392–11398, 2015, doi: 10.1016/j.ijhydene.2015.03.086.

[32] M. Almahdi, “Integrated Heat Pump Options for Heat Upgrading in Cu-Cl Cycle for Hydrogen Production,” no. April, 2016.

[33] K. Wang and Y. L. He, “Thermodynamic analysis and optimization of a molten salt solar power tower integrated with a recompression supercritical CO2 Brayton cycle based on integrated modeling,” *Energy Convers. Manag.*, vol. 135, pp. 336–350, 2017, doi: 10.1016/j.enconman.2016.12.085.

[34] F. Sorgulu and I. Dincer, “Design and analysis of a solar tower power plant integrated with thermal energy storage system for cogeneration,” *Int. J. Energy Res.*, vol. 43, no. 12, pp. 6151–6160, 2019, doi: 10.1002/er.4233.

[35] A. A. Kiss, J. J. Pragt, H. J. Vos, G. Bargeman, and M. T. de Groot, “Novel efficient process for methanol synthesis by CO2 hydrogenation,” *Chem. Eng. J.*, vol. 284, pp. 260–269, 2016, doi: 10.1016/j.cej.2015.08.101.

[36] T. M. Sugao SUGAWARA, Takashi SATO, “On the Equation of State of Mercury Vapour,” *Bullettin JSME*, vol. 5, no. 20, pp. 711–718, 1962.

[37] WHO, “Mercury in health care: Policy paper,” p. 2, 1991.

[38] M. Gutstein, E. R. Furman, and G. M. Kaplan, “FOR STATIONARY POWER,” no. August 1975, 2020.

[39] “Meteo Blue.” [Online]. Available: https://www.meteoblue.com/en/weather/week/arizona_honduras_3615069.

[40] Meteo Blue, “Meteo Blue, Weather History for Vancouver,” 2020. [Online]. Available: https://www.meteoblue.com/en/weather/archive/export/vancouver_canada_6173331.

[41] R. E. Wilson and R. W. Thresher, “Electrical Energy From the Wind.,” *Mech. Eng.*, vol. 106, no. 1, pp. 60–69, 1984.

[42] M. O. Hansen, *Aerodynamics of wind turbines. Routledge*. 2015.

[43] Z. Z. R.Matz, “Low-temperature vapour compression and multi-effect distillation of seawater. Effects of design on operation and economics,” *Desalination*, vol. 52, no. 2, 1985, doi: https://doi.org/10.1016/0011-9164(85)85009-8.

[44] Aspen Tech., “Aspen Plus.” [Online]. Available: www.aspentech.com.

[45] A. T. Inc, “Aspen Physical Property System: Physical Property Methods,” *Methods*, pp. 1–234, 2009.

APPENDIX A: Example EES Code For System 1 Version 1

```
"Mass Flow Rates"
"kg/s"
m_dot_2=400
m_dot_5=300
m_dot_6=300
m_dot_7=300
m_dot_8=300
m_dot_9=300
m_dot_10=300
m_dot_11=200
m_dot_12=200
m_dot_13=200
m_dot_14=400
m_dot_15=400
m_dot_16=200
m_dot_17=200
m_dot_18=200
m_dot_19=200
m_dot_20=300
m_dot_21=300
m_dot_22=300
m_dot_23=300
m_dot_24=200
m_dot_25=200
m_dot_26=200
m_dot_27=200
m_dot_28=120
m_dot_29=40
m_dot_30=40
m_dot_31=40
m_dot_37=400
m_dot_38=400
m_dot_39=300
m_dot_40=300
m_dot_41=300
m_dot_411=300
m_dot_42=300
m_dot_43=300
m_dot_44=300
m_dot_45=300
m_dot_46=300
m_dot_s6=770.4/3600
m_dot_s7=770.4/3600
m_dot_47=200
m_dot_48=150
m_dot_49=150
"Temperatures"
T_hx8=650+273
T_hx9=500+273
T_0=25+273              "Kelvin"


T_2=1176+273
T_5=400+273
```

```
T_6=500+273
T_7=370+273
T_8=250+273
T_9=180+273
T_10=210+273
T_11=110+253
T_12=200+273
T_13=85+273
T_14=150+273
T_15=85+273
T_16=140+273
T_17=80+273
T_18=20+273
T_19=120+273
T_20=200+273
T_21=260+273
T_22=190+273
T_23=105+273
T_24=137+273
T_25=98+273
T_26=60+273
T_27=90+273
T_28=21+273
T_29=21+273
T_30=21+273
T_31=21+273
T_37=920+273
T_38=940+273
T_39=910+273
T_40=820+273
T_41=600+273
T_411=660+273
T_42=690+273
T_43=600+273
T_44=600+273
T_45=580+273
T_46=600+273
T_s6=400+273
T_s7=500+273
T_47=70+273
T_48=25+273
T_49=60+273
 "Pressures"
P_0=101                 "kPa"
P_2=1300
P_5=550
P_6=700
P_7=1000
P_8=300
P_9=350
P_10=700
P_11=122
P_12=137
P_13=125
P_14=137
P_15=125
```

```
P_16=137
P_17=87
P_18=90
P_19=125
P_20=900
P_21=920
P_22=920
P_23=900
P_24=265
P_25=160
P_26=150
P_27=150
P_28=100
P_29=100
P_30=100
P_31=5
P_37=1300
P_38=1350
P_39=800
P_40=780
P_41=760
P_411=790
P_42=370
P_43=250
P_44=250
P_45=250
P_46=370
P_s6=100
P_s7=100
P_47=100
P_48=100
P_49=100
"Enthalpy Values"
h_0=enthalpy(Water,T=T_0,P=P_0 )
h_2=enthalpy('Salt(58KF_42ZrF4)',T=T_2,P=P_2)
h_5=enthalpy(Water,T=T_5,P=P_5)
h_6=enthalpy(Water,T=T_6,P=P_6)
h_7=enthalpy(CarbonDioxide,T=T_7,P=P_7)
h_8=enthalpy(CarbonDioxide,T=T_8,P=P_8)
h_9=enthalpy(CarbonDioxide,T=T_9,P=P_9)
h_10=enthalpy(CarbonDioxide,T=T_10,P=P_10)
h_11=enthalpy(R134a,T=T_11,P=P_11)
h_12=enthalpy(R134a,T=T_12,P=P_12)
h_13=enthalpy(R134a,T=T_13,P=P_13)
h_14=enthalpy(R134a,T=T_14,P=P_14)
h_15=enthalpy(R134a,T=T_15,P=P_15)
h_16=enthalpy(R134a,T=T_16,P=P_16)
h_17=enthalpy(R134a,T=T_17,P=P_17)
h_18=enthalpy(R134a,T=T_18,P=P_18)
h_19=enthalpy(R134a,T=T_19,P=P_19)
h_20=enthalpy(Water,T=T_20,P=P_20)
h_21=enthalpy(Water,T=T_21,P=P_21)
h_22=enthalpy(Water,T=T_22,P=P_22)
h_23=enthalpy(Water,T=T_23,P=P_23)
h_24=enthalpy(CarbonDioxide,T=T_24,P=P_24)
h_25=enthalpy(CarbonDioxide,T=T_25,P=P_25)
```

```
h_26=enthalpy(CarbonDioxide,T=T_26,P=P_26)
h_27=enthalpy(CarbonDioxide,T=T_27,P=P_27)
h_28=enthalpy(Water,T=T_28,P=P_28)
h_29=enthalpy(Water,T=T_29,P=P_29)
h_30=enthalpy(Water,T=T_30,P=P_30)
h_31=enthalpy(Water,T=T_31,P=P_31)
h_37=enthalpy('Salt(58KF_42ZrF4)',T=T_37,P=P_42)
h_38=enthalpy('Salt(58KF_42ZrF4)',T=T_38,P=P_42)
h_39=enthalpy('Salt(58KF_42ZrF4)',T=T_39,P=P_42)
h_40=enthalpy('Salt(58KF_42ZrF4)',T=T_40,P=P_42)
h_41=enthalpy('Salt(58KF_42ZrF4)',T=T_41,P=P_42)
h_411=enthalpy('Salt(58KF_42ZrF4)',T=T_411,P=P_42)
h_42=enthalpy(Water,T=T_42,P=P_42)
h_43=enthalpy(Water,T=T_43,P=P_43)
h_44=enthalpy(Water,T=T_44,P=P_44)
h_45=enthalpy(Water,T=T_45,P=P_45)
h_46=enthalpy(Water,T=T_46,P=P_46)
h_s6=-1789.5
h_s7=-1791.5
h_47=enthalpy(R134a,T=T_47,P=P_47)
h_48=enthalpy(Water,T=T_48,P=P_48)
h_49=enthalpy(Water,T=T_49,P=P_49)
"Entropy Values"
s_0=entropy(Water,T=T_0,P=P_0)
s_2=entropy('Salt(58KF_42ZrF4)',T=T_2)
s_5=entropy(Water,T=T_5,P=P_5)
s_6=entropy(Water,T=T_6,P=P_6)
s_7=entropy(CarbonDioxide,T=T_7,P=P_7)
s_8=entropy(CarbonDioxide,T=T_8,P=P_8)
s_9=entropy(CarbonDioxide,T=T_9,P=P_9)
s_10=entropy(CarbonDioxide,T=T_10,P=P_10)
s_11=entropy(R134a,T=T_11,P=P_11)
s_12=entropy(R134a,T=T_12,P=P_12)
s_13=entropy(R134a,T=T_13,P=P_13)
s_14=entropy(R134a,T=T_14,P=P_14)
s_15=entropy(R134a,T=T_15,P=P_15)
s_16=entropy(R134a,T=T_16,P=P_16)
s_17=entropy(R134a,T=T_17,P=P_17)
s_18=entropy(R134a,T=T_18,P=P_18)
s_19=entropy(R134a,T=T_19,P=P_19)
s_20=entropy(Water,T=T_20,P=P_20)
s_21=entropy(Water,T=T_21,P=P_21)
s_22=entropy(Water,T=T_22,P=P_22)
s_23=entropy(Water,T=T_23,P=P_23)
s_24=entropy(CarbonDioxide,T=T_24,P=P_24)
s_25=entropy(CarbonDioxide,T=T_25,P=P_25)
s_26=entropy(CarbonDioxide,T=T_26,P=P_26)
s_27=entropy(CarbonDioxide,T=T_27,P=P_27)
s_28=entropy(CarbonDioxide,T=T_28,P=P_28)
s_29=entropy(Water,T=T_29,P=P_29)
s_30=entropy(Water,T=T_30,P=P_30)
s_31=entropy(Water,T=T_31,P=P_31)
s_37=entropy('Salt(58KF_42ZrF4)',T=T_37)
s_38=entropy('Salt(58KF_42ZrF4)',T=T_38)
s_39=entropy('Salt(58KF_42ZrF4)',T=T_39)
s_40=entropy('Salt(58KF_42ZrF4)',T=T_40)
```

```
s_41=entropy('Salt(58KF_42ZrF4)',T=T_41)
s_411=entropy('Salt(58KF_42ZrF4)',T=T_411)
s_42=entropy(Water,T=T_42,P=P_42)
s_43=entropy(Water,T=T_43,P=P_43)
s_44=entropy(Water,T=T_44,P=P_44)
s_45=entropy(Water,T=T_45,P=P_45)
s_46=entropy(Water,T=T_46,P=P_46)
s_s6=5.9254
s_s7=5.9227
s_47=entropy(R134a,T=T_47,P=P_47)
s_48=entropy(Water,T=T_48,P=P_48)
s_49=entropy(Water,T=T_49,P=P_49)
 "Spesific Exergies"
ex_dot_2=(h_2-h_0)-(T_0*(s_2-s_0))
ex_dot_5=(h_5-h_0)-(T_0*(s_5-s_0))
ex_dot_6=(h_6-h_0)-(T_0*(s_6-s_0))
ex_dot_7=(h_7-h_0)-(T_0*(s_7-s_0))
ex_dot_8=(h_8-h_0)-(T_0*(s_8-s_0))
ex_dot_9=(h_9-h_0)-(T_0*(s_9-s_0))
ex_dot_10=(h_10-h_0)-(T_0*(s_10-s_0))
ex_dot_11=(h_11-h_0)-(T_0*(s_11-s_0))
ex_dot_12=(h_12-h_0)-(T_0*(s_12-s_0))
ex_dot_13=(h_13-h_0)-(T_0*(s_13-s_0))
ex_dot_14=(h_14-h_0)-(T_0*(s_14-s_0))
ex_dot_15=(h_15-h_0)-(T_0*(s_15-s_0))
ex_dot_16=(h_16-h_0)-(T_0*(s_16-s_0))
ex_dot_17=(h_17-h_0)-(T_0*(s_17-s_0))
ex_dot_18=(h_18-h_0)-(T_0*(s_18-s_0))
ex_dot_19=(h_19-h_0)-(T_0*(s_19-s_0))
ex_dot_20=(h_20-h_0)-(T_0*(s_20-s_0))
ex_dot_21=(h_21-h_0)-(T_0*(s_21-s_0))
ex_dot_22=(h_22-h_0)-(T_0*(s_22-s_0))
ex_dot_23=(h_23-h_0)-(T_0*(s_23-s_0))
ex_dot_24=(h_24-h_0)-(T_0*(s_24-s_0))
ex_dot_25=(h_25-h_0)-(T_0*(s_25-s_0))
ex_dot_26=(h_26-h_0)-(T_0*(s_26-s_0))
ex_dot_27=(h_27-h_0)-(T_0*(s_27-s_0))
ex_dot_28=(h_28-h_0)-(T_0*(s_28-s_0))
ex_dot_29=(h_29-h_0)-(T_0*(s_29-s_0))
ex_dot_30=(h_30-h_0)-(T_0*(s_30-s_0))
ex_dot_31=(h_31-h_0)-(T_0*(s_31-s_0))
ex_dot_37=(h_37-h_0)-(T_0*(s_37-s_0))
ex_dot_38=(h_38-h_0)-(T_0*(s_38-s_0))
ex_dot_39=(h_39-h_0)-(T_0*(s_39-s_0))
ex_dot_40=(h_40-h_0)-(T_0*(s_40-s_0))
ex_dot_41=(h_41-h_0)-(T_0*(s_41-s_0))
ex_dot_411=(h_411-h_0)-(T_0*(s_411-s_0))
ex_dot_42=(h_42-h_0)-(T_0*(s_42-s_0))
ex_dot_43=(h_43-h_0)-(T_0*(s_43-s_0))
ex_dot_44=(h_44-h_0)-(T_0*(s_44-s_0))
ex_dot_45=(h_45-h_0)-(T_0*(s_45-s_0))
ex_dot_46=(h_46-h_0)-(T_0*(s_46-s_0))
ex_dot_s6=(h_s6-h_0)-(T_0*(s_s6-s_0))
ex_dot_s7=(h_s7-h_0)-(T_0*(s_s7-s_0))
ex_dot_47=(h_47-h_0)-(T_0*(s_47-s_0))
ex_dot_48=(h_48-h_0)-(T_0*(s_48-s_0))
```

```
ex_dot_49=(h_49-h_0)-(T_0*(s_49-s_0))
"Heat Exchanger 1"
"m_dot_21+m_dot_27=m_dot_24+m_dot_22"
"m_dot_21*h_21+m_dot_27*h_27=m_dot_24*h_24+m_dot_22*h_22"
m_dot_21*s_21+m_dot_27*s_27+S_dot_gen_hx1=m_dot_24*s_24+m_dot_22*s_22
m_dot_21*ex_dot_21+m_dot_27*ex_dot_27=m_dot_24*ex_dot_24+m_dot_22*ex_dot_22+ExD_dot_hx1

ExHeatExc1=(m_dot_24*ex_dot_24-m_dot_27*ex_dot_27)/(m_dot_21*ex_dot_21-m_dot_22*ex_dot_22)

"Heat Exchanger 2"

"m_dot_22+m_dot_18=m_dot_17+m_dot_23"
"m_dot_22*h_22+m_dot_23*h_23=m_dot_17*h_17+m_dot_23*h_23"
m_dot_22*s_22+m_dot_18*s_18+S_dot_gen_hx2=m_dot_17*s_17+m_dot_23*s_23
m_dot_22*ex_dot_22+m_dot_18*ex_dot_18=m_dot_17*ex_dot_17+m_dot_23*ex_dot_23+ExD_dot_hx2
"Heat Exchanger 3"

"m_dot_8+m_dot_13=m_dot_9+m_dot_11"
"m_dot_8*h_8+m_dot_13*h_13=m_dot_9*h_9+m_dot_11*h_11"
m_dot_8*s_8+m_dot_13*s_13+S_dot_gen_hx3=m_dot_9*s_9+m_dot_11*s_11
m_dot_8*ex_dot_8+m_dot_13*ex_dot_13=m_dot_9*ex_dot_9+m_dot_11*ex_dot_11+ExD_dot_hx3
"Heat Exchanger 4"

"m_dot_46+m_dot_39=m_dot_42+m_dot_32"
"m_dot_46*h_31+m_dot_39*h_39=m_dot_42*h_42+m_dot_40*h_40"
m_dot_46*s_46+m_dot_39*s_39+S_dot_gen_hx4=m_dot_42*s_42+m_dot_40*s_40
m_dot_46*ex_dot_46+m_dot_39*ex_dot_39=m_dot_42*ex_dot_42+m_dot_40*ex_dot_40+ExD_dot_hx4
"Heat Exchanger 5"

"m_dot_10+m_dot_6=m_dot_5+m_dot_7"
"m_dot_10*h_10+m_dot_6*h_6=m_dot_5*h_5+m_dot_7*h_7"
m_dot_10*s_10+m_dot_6*s_6+S_dot_gen_hx5=m_dot_5*s_5+m_dot_7*s_7
m_dot_10*ex_dot_10+m_dot_6*ex_dot_6=m_dot_5*ex_dot_5+m_dot_7*ex_dot_7+ExD_dot_hx5

ExHeatExc5=(m_dot_7*ex_dot_7-m_dot_10*ex_dot_10)/(m_dot_6*ex_dot_6-m_dot_5*ex_dot_5)
"Heat Exchanger 6"

"m_dot_40+m_dot_5=m_dot_6+m_dot_41"
"m_dot_40*h_40+m_dot_5*h_5=m_dot_6*h_6+m_dot_41*h_41"
m_dot_40*s_40+m_dot_5*s_5+S_dot_gen_hx6=m_dot_6*s_6+m_dot_41*s_41
m_dot_40*ex_dot_40+m_dot_5*ex_dot_5=m_dot_6*ex_dot_6+m_dot_41*ex_dot_41+ExD_dot_hx6
"Heat Exchanger 7"

"m_dot_411+m_dot_2=m_dot_39+m_dot_37"
"m_dot_411*h_411+m_dot_2*h_2=m_dot_39*h_39+m_dot_37*h_37"
m_dot_411*s_411+m_dot_2*s_2+S_dot_gen_hx7=m_dot_39*s_39+m_dot_37*s_37
m_dot_411*ex_dot_411+m_dot_2*ex_dot_2=m_dot_39*ex_dot_39+m_dot_37*ex_dot_37+ExD_dot_hx7
"Heat Exchanger 8"

"Ex_dot_Qhx8=(1-(T_0/T_hx8))*Q_dot_hx8 "

"m_dot_43=m_dot_44"
"m_dot_43*h_43=m_dot_44*h_44+Q_dot_hx8
m_dot_43*s_43+S_dot_gen_hx8=m_dot_44*s_44+(Q_dot_hx8/T_hx8)
m_dot_43*ex_dot_43=m_dot_44*ex_dot_44+Ex_dot_Qhx8+ExD_dot_hx8"
"Heat Exchanger 9"
```

"m_dot_44=m_dot_45"
"m_dot_44*h_44=m_dot_45*h_45"
m_dot_44*s_44+m_dot_s6*s_s6+S_dot_gen_hx9=m_dot_45*s_45+m_dot_s7*s_s7
m_dot_44*ex_dot_44+m_dot_s6*ex_dot_s6=m_dot_45*ex_dot_45+m_dot_s7*ex_dot_s7+ExD_dot_hx9
"Turbine 1"

"m_dot_24=m_dot_25"
m_dot_24*h_24=m_dot_25*h_25+W_dot_tur1
m_dot_24*s_24+S_dot_gen_tur1=m_dot_25*s_25
m_dot_24*ex_dot_24=m_dot_25*ex_dot_25+W_dot_tur1+ExD_dot_tur1

ExTUR1=W_dot_tur1/(m_dot_24*ex_dot_24-m_dot_25*ex_dot_25)

"Turbine 2"

"m_dot_7=m_dot_8"
m_dot_7*h_7=m_dot_8*h_8+W_dot_tur2
m_dot_7*s_7+S_dot_gen_tur2=m_dot_8*s_8
m_dot_7*ex_dot_7=m_dot_8*ex_dot_8+W_dot_tur2+ExD_dot_tur2

ExTUR2=W_dot_tur2/(m_dot_7*ex_dot_7-m_dot_8*ex_dot_8)

"Turbine 4"

"m_dot_42=m_dot_43"
m_dot_42*h_42=m_dot_43*h_43+W_dot_tur4
m_dot_42*s_42+S_dot_gen_tur4=m_dot_43*s_43
m_dot_42*ex_dot_42=m_dot_43*ex_dot_43+W_dot_tur4+ExD_dot_tur4
"Compressor"

"m_dot_17=m_dot_16"
m_dot_17*h_17+W_dot_comp=m_dot_16*h_16
m_dot_17*s_17+S_dot_gen_comp=m_dot_16*s_16
m_dot_17*ex_dot_17+W_dot_comp=m_dot_16*ex_dot_16+ExD_dot_comp

ExCOMP=(m_dot_16*ex_dot_16-m_dot_17*ex_dot_17)/W_dot_comp

"Expansion Valve"

"m_dot_19=m_dot_18"
"m_dot_19*h_19=m_dot_18*h_18"
m_dot_19*s_19+S_dot_gen_exp=m_dot_18*s_18
m_dot_19*ex_dot_19=m_dot_18*ex_dot_18+ExD_dot_exp
"Pump 1"

"m_dot_26=m_dot_27 "
m_dot_26*h_26+W_dot_PUMP1=m_dot_27*h_27
m_dot_26*s_26+S_genPUMP1=m_dot_27*s_27
m_dot_26*ex_dot_26+W_dot_PUMP1=m_dot_27*ex_dot_27+Ex_dot_Dpump1
"Pump 2"

"m_dot_11=m_dot_12 "
m_dot_11*h_11+W_dot_PUMP2=m_dot_12*h_12
m_dot_11*s_11+S_genPUMP2=m_dot_12*s_12
m_dot_11*ex_dot_11+W_dot_PUMP2=m_dot_12*ex_dot_12+Ex_dot_Dpump2
"Pump 3"

```
"m_dot_20=m_dot_21 "
m_dot_20*h_20+W_dot_PUMP3=m_dot_21*h_21
m_dot_20*s_20+S_genPUMP3=m_dot_21*s_21
m_dot_20*ex_dot_20+W_dot_PUMP3=m_dot_21*ex_dot_21+Ex_dot_Dpump3
"Pump R3"

m_dot_9*h_9+W_dot_PUMPR3=m_dot_10*h_10
m_dot_9*s_9+S_genPUMPR3=m_dot_10*s_10
m_dot_9*ex_dot_9+W_dot_PUMPR3=m_dot_10*ex_dot_10+Ex_dot_DpumpR3

"Pump 4"

"m_dot_37=m_dot_38 "
m_dot_37*h_37+W_dot_PUMP4=m_dot_38*h_38
m_dot_37*s_37+S_genPUMP4=m_dot_38*s_38
m_dot_37*ex_dot_37+W_dot_PUMP4=m_dot_38*ex_dot_38+Ex_dot_Dpump4
"Pump 5"

"m_dot_45=m_dot_46"
m_dot_45*h_45+W_dot_PUMP5=m_dot_46*h_46
m_dot_45*s_45+S_genPUMP5=m_dot_46*s_46
m_dot_45*ex_dot_45+W_dot_PUMP5=m_dot_46*ex_dot_46+Ex_dot_Dpump5
"Pump 6"

"m_dot_9=m_dot_10"
m_dot_9*h_9+W_dot_PUMP6=m_dot_10*h_10
m_dot_9*s_9+S_genPUMP6=m_dot_10*s_10
m_dot_9*ex_dot_9+W_dot_PUMP6=m_dot_10*ex_dot_10+Ex_dot_Dpump6
"Condenser"
T_con=(T_25+T_26)/2
Ex_dot_Qcon=(1-(T_0/T_con))*Q_dot_con

"m_dot_25=m_dot_26"
m_dot_25*h_25=m_dot_26*h_26+Q_dot_con
m_dot_25*s_25+S_dot_gen_con=m_dot_26*s_26+(Q_dot_con/T_con)
m_dot_25*ex_dot_25=m_dot_26*ex_dot_26+Ex_dot_Qcon+ExD_dot_con

ExCondenser=(Ex_dot_Qcon)/(m_dot_25*ex_dot_25-m_dot_26*ex_dot_26)

"Space Heating"

m_dot_14*h_14=m_dot_15*h_15+Q_dot_SpaceH

Ex_dot_QSpaceH=(1-(T_0/T_SpaceH))*Q_dot_SpaceH

T_SpaceH=80+273

ExSpaceHeating=Ex_dot_QSpaceH/(m_dot_14*ex_dot_14-m_dot_15*ex_dot_15)

"Geothermal Qin"

Geo_Qin=m_dot_20*(h_20-h_23)

Ex_dot_QGEO=((T_0/T_GEO)-1)*Geo_Qin
```

T_Geo=180
"Solar Tower Qin"

Solar_Qin=93323
Ex_dot_QSolar=(1-(T_0/T_Solar))*Solar_Qin

T_Solar=5400

m_dot_38*ex_dot_38+Ex_dot_QSolar=m_dot_2*ex_dot_2+ExD_dot_QSolar

ExSolarTower=(m_dot_2*ex_dot_2-m_dot_38*ex_dot_38)/Ex_dot_QSolar

"Hot Water Qin"

HW_Q=m_dot_48*(h_49-h_48)

Ex_dot_QHW=(1-(T_0/T_HW))*HW_Q

T_HW=(T_48+T_49)/2

"System Efficiency"

W_dot_net=(W_dot_tur1+W_dot_tur2+W_dot_tur4)-
(W_dot_PUMP1+W_dot_PUMP2+W_dot_PUMP3+W_dot_PUMP4+W_dot_PUMP5+W_dot_comp)

Eff=(Q_dot_SpaceH+W_dot_net+283566+4160+HW_Q+Q_dot_con)/(Geo_Qin+Solar_Qin+11999.83)

"241333Hydrogen-4150FreshWater-11999.83Seawater"

ExEff=(W_dot_net+Ex_dot_QSpaceH+237311+2886+Ex_dot_QHW+Ex_dot_Qcon)/(Ex_dot_QGEO+Ex_
dot_QSolar+8324.88)

"237311Hydrogen-2886FreshWater-8324.88Seawater"
"Rankine 2"

WnetR2=W_dot_tur2-W_dot_PUMPR3

QHX5=m_dot_7*(h_7-h_10)
Ex_dot_QHX5=QHX5*((T_R1/T_0)-1)
T_R1=(T_7+T_10)/2
"+Ex_dot_Qcon"

Eff_EXR2=(WnetR2)/Ex_dot_QHX5

"Rankine 1"

WnetR1=W_dot_tur1-W_dot_PUMP1
QHX1=m_dot_24*(h_24-h_27)
Ex_dot_QHX1=QHX1*((T_R2/T_0)-1)
T_R2=(T_24+T_27)/2

"+Ex_dot_QCHX1"
Eff_EXR1=(WnetR1)/Ex_dot_QHX1